

2010-04-28

# Hot Tearing in Cast Aluminum Alloys: Measures and Effects of Process Variables

Shimin Li

*Worcester Polytechnic Institute*

Follow this and additional works at: <https://digitalcommons.wpi.edu/etd-dissertations>

---

## Repository Citation

Li, S. (2010). *Hot Tearing in Cast Aluminum Alloys: Measures and Effects of Process Variables*. Retrieved from <https://digitalcommons.wpi.edu/etd-dissertations/203>

This dissertation is brought to you for free and open access by Digital WPI. It has been accepted for inclusion in Doctoral Dissertations (All Dissertations, All Years) by an authorized administrator of Digital WPI. For more information, please contact [wpi-etd@wpi.edu](mailto:wpi-etd@wpi.edu).

**Hot Tearing in Cast Aluminum Alloys:**  
Measures and Effects of Process Variables

by

**Shimin Li**

A Dissertation

Submitted to the Faculty

of the

WORCESTER POLYTECHNIC INSTITUTE

*In partial fulfillment of the requirements of the*

Degree of Doctor of Philosophy

in

Materials Science and Engineering

April 2010

APPROVED:

---

Dr. Diran Apelian, Advisor  
Howmet Professor of Engineering

---

Dr. Richard D. Sisson Jr.  
George F. Fuller Professor  
Director of Manufacturing and Materials Engineering

## **ABSTRACT**

Hot tearing is a common and severe defect encountered in alloy castings and perhaps the pivotal issue defining an alloy's castability. Once it occurs, the casting has to be repaired or scrapped, resulting in significant loss. Over the years many theories and models have been proposed and accordingly many tests have been developed. Unfortunately many of the tests that have been proposed are qualitative in nature; meanwhile, many of the prediction models are not satisfactory as they lack quantitative information, data and knowledge base. The need exists for a reliable and robust quantitative test to evaluate/characterize hot tearing in cast alloys.

This work focused on developing an advanced test method and using it to study hot tearing in cast aluminum alloys. The objectives were to: 1) develop a reliable experimental methodology/setup to quantitatively measure and characterize hot tearing; and 2) quantify the mechanistic contributions of the process variables and investigate their effects on hot tearing tendency. The team at MPI in USA and CANMET-MTL in Canada has collaborated and developed such a testing setup. It consists mainly of a constrained rod mold and the load/displacement and temperature measuring system, which gives quantitative, simultaneous measurements of the real-time contraction force/displacement and temperature during solidification of casting. The data provide information about hot tearing formation and solidification characteristics, from which their quantitative relations are derived. Quantitative information such as tensile coherency, incipient crack refilling, crack initiation and propagation can be obtained. The method proves to be repeatable and reliable and has been used for studying the effects of various parameters (mold temperature, pouring temperature and grain refinement) on hot tearing of different cast aluminum alloys. In scientific sense this method can be used to study and reveal the nature of the hot tearing, for industry practice it provides a tool for production control. Moreover, the quantitative data and fundamental knowledge gained in this thesis can be used for validating and improving the existing hot tearing models.

## ACKNOWLEDGEMENTS

First and foremost I want to heartily thank my advisor Professor Diran Apelian for his guidance, stimulating advice, encouragement and patience during my research and study. My research life at WPI became a wonderful journey with a great mentor.

My sincere thanks go to my thesis committee members Professor Richard D. Sisson Jr., Professor Makhoul M. Makhoul and Professor Diana Lados for encouragement, critical comments and stimulus questions. I thank my class professors Professor Satya S. Shivkumar, Yiming Rong, Jianyu Liang, Isa Bar-On and Mahadevan Padmanabhan for teaching me fundamental knowledge.

I'd like to gratefully acknowledge the member companies of the Advanced Casting Research Center (ACRC) to fund this project, especially the focus group and the group co-chairs John Jorstad and Ray Donahue, for their support and input.

The support of CANMET Material Technology Laboratory is very important to this project. The hospitality of the lab during my six weeks stay there is very much appreciated. Special thanks go to Dr. Kumar Sadayappan for his guidance, valuable discussions and continuous support, as well as a member of my thesis committee. I would also like to thank Geethe Nadugala, Jim Thomson and other people involved in this project for their help with the initial trials conducted there.

My fellow MPI groupmembers, Dr. Kimon Symeonidis, Dr. Brian Dewhirst, Dr. Daniel Backman, Ning Sun, Cecelia Borgonovo and Hao Yu made this group a source of friendship as well as good advice and collaboration. I'm very grateful for their continuous encouragement and benefit a lot from those stimulating discussions and sharing ideas. Dr. Libo Wang deserves a special thank for his assistance in experiments and invaluable discussions.

I greatly appreciate our department secretary Rita Shilansky, and MPI staff Carol Garofoli, Maureen Plunkett, Carl Raatikanen, and Bradford Lynch for their help. I thank all of those who supported me in any respect during the completion of my thesis.

Finally, I owe my deepest gratitude to my family. My parents tried their best to support me in all my pursuits. My sisters and brother always give me love and encouragement. My husband Yonggang Zheng always stands beside me and encourages me. Thank you for your love and belief in me!

# TABLE OF CONTENTS

<b>ABSTRACT .....</b>	<b>I</b>
<b>ACKNOWLEDGEMENTS .....</b>	<b>II</b>
<b>TABLE OF CONTENTS .....</b>	<b>III</b>
<b>EXECUTIVE SUMMARY .....</b>	<b>1</b>
Introduction .....	1
Objectives .....	1
Methodology .....	2
Outcomes/Conclusions .....	3
<b>CHAPTER I: Hot Tearing of Aluminum Alloys – A Critical Literature Review .....</b>	<b>6</b>
<b>CHAPTER II: Characterization of Hot Tearing in Cast Al Alloys:</b>	
Methodology and Procedures .....	<b>43</b>
<b>CHAPTER III: Why Some Al Alloys Hot Tear and others do not?</b>	
– Part I: Effects of Mold Temperature and Pouring Temperature .....	<b>61</b>
<b>CHAPTER IV: Why Some Al Alloys Hot Tear and others do not?</b>	
– Part II: The Role of Grain Refinement .....	<b>87</b>
<b>APPENDICES .....</b>	<b>102</b>
APPENDIX A: Quantitative Investigation of Hot Tearing of Al-Cu Alloy (206) Cast in a Constrained Bar Permanent Mold.....	102
APPENDIX B: Castability Measures for Diecasting Alloys: Fluidity, Hot Tearing, and Die Soldering .....	110

# EXECUTIVE SUMMARY

## Introduction

Hot tearing is a common and severe defect encountered in alloy castings and perhaps the pivotal issue defining an alloy's castability. It is identified as cracks, either on the surface or inside the casting. The main tear and its numerous minor offshoots generally follow intergranular paths and the failure surface usually reveals a dendritic morphology. Once hot tearing occurs, the casting has to be repaired or scraped, resulting in significant loss. Previous work by many researchers show that hot tearing is a complex phenomenon, it lies at the intersection of heat flow, fluid flow and mass flow, and various factors have influences on its formation. These factors include alloy composition, its solidification and thermo-mechanical characteristics, melt treatment, casting and mold design, mold material, and process parameters etc. Over the years many theories and models have been proposed and accordingly many tests have been developed. Unfortunately the tests that have been proposed are generally qualitative in nature; meanwhile, many of the prediction models are not satisfactory as they lack quantitative information, data and knowledge base. The need exists for a reliable and robust quantitative test to evaluate/characterize hot tearing in cast alloys. WPI and CANMET - both members of the Light Metal Alliance - joined forces to address this need and to develop a quantitative means of measuring hot tearing. The premise is that one cannot control what one cannot measure.

## Objectives

This work focused on developing a quantitative test method and subsequently using it to study hot tearing in cast aluminum alloys. The objectives were to:

- Develop a reliable experimental methodology/setup to quantitatively measure and characterize hot tearing.
- Quantify the mechanistic contributions of process variables; investigate the effects of the variables on hot tearing tendency.

## Methodology

In order to achieve the above objectives, the following methodology and strategies were pursued:

- Conducted an extensive and critical literature review; scrutinized the proposed mechanisms and identified the major factors which control the formation of hot tears.
- **Phase I** – Developed a reliable experimental methodology/setup to quantitatively characterize hot tearing in cast aluminum alloys.
  - Established collaboration with CANMET for this project
  - Designed and manufactured the mold apparatus
  - Selected, tested, calibrated, and integrated measuring devices, load cell, LVDT, and data acquisition system etc.
  - Selected model and reference alloys to test and calibrate the system
  - Conducted trial tests to verify and fine-tune the developed measurement apparatuses/techniques
  - Run experiments using the developed setup on alloys 206, 713, and reference alloy A356 and used two molds of different materials, a copper alloy and H13 steel
  - Conducted qualitative tests using N-Tec and ring molds to verify the trends. The tested alloys included 206, 319, A356, 390, 518 and 713
  - Established standard procedure to interpret the measured data and related them to hot tearing characterization
  - Proved the system's repeatability and reliability.
- **Phase II** – Investigated the effects of important process variables on hot tearing. Performed systematic experiments with the H13 constrained rod mold to fully characterize the effects of process variables on the formation of hot tears in A356 and 206 alloys. The studied variables were:
  - Mold temperature
  - Pouring temperature
  - Grain refinement
- **Phase III** – Computer simulation
  - Conducted computer simulations on stress/strain development using casting simulation software Magma.

- Provided quantitative data and information from this work to the major casting software companies, ESI and Magma, for validating the hot tearing modulus of their software.

## Outcomes/Conclusions

The outcomes from this work have been presented in six articles that have either been published or submitted to professional journals. These are:

1. S. Li and D. Apelian, Hot Tearing of Aluminum Alloys – A Critical Literature Review, submitted to International Journal of Metalcasting (**Chapter 1**).
2. S. Li, K. Sadayappan and D. Apelian, Characterization of Hot Tearing in Al Cast Alloys: Methodology and Procedures, submitted to International Journal of Cast Metals Research (**Chapter 2**).
3. S. Li, K. Sadayappan and D. Apelian, Why Some Al Alloys Hot Tear and others do not? – Part I: Effects of Mold Temperature and Pouring Temperature, prepared to submit to <sup>Metall. Mater. Trans. A</sup>. (**Chapter 3**).
4. S. Li, K. Sadayappan and D. Apelian, Why Some Al Alloys Hot Tear and others do not? – Part II: the Role of Grain Refinement, prepared to submit to <sup>Metall. Mater. Trans. A</sup>. (**Chapter 4**).
5. S. Li, D. Apelian, K. Sadayappan. Quantitative Investigation of Hot Tearing of Al-Cu Alloy (206) Cast in a Constrained Bar Permanent Mold, Materials Science Forum, Vols. 618-619 (2009): 57-62 (presented at Fourth International Light Metals Technology Conference, Queensland, Australia. June 2009) – **Appendix A**
6. B. Dewhirst, S. Li, P. Hogan, D. Apelian. Castability Measures for Diecasting Alloys: fluidity, hot tearing, and die soldering, La metallurgia italiana, 3 (2009): 37-42 (presented at the International Conference High Tech DieCasting, Montichiari, April 2008, organized by AIM) - **Appendix B**

A synopsis of these outcomes/papers is given below:

- An extensive literature review on hot tearing was carried out. The review focused on: (i) Theories of hot tearing; (ii) Hot tearing and its affecting variables; and (iii) Test methods. A summary of hot tearing criteria/models is provided. The critical issues and areas for improvement in the hot tearing field were discussed. (**Chapter 1**)



- In **Phase I**, a reliable quantitative hot tearing test method was developed. ( *Chapter 2, Appendices A and B*)
  - An experimental setup to quantitatively characterize hot tearing behavior of Al alloys has been developed. It consists mainly of a constrained rod mold, load/displacement and temperature measuring system, which gives simultaneous measurements of the real-time contraction force/displacement and temperatures during solidification of the casting.
  - Procedure of data analysis was proposed. Based on the measured data, the load, displacement and temperature as a function of time and thus the solid fraction are obtained.
  - The data provide information about hot tearing formation and solidification characteristics, from which their quantitative relations are derived. Information such as tensile coherency, incipient crack refilling, crack initiation and propagation in the mush can be detected from the load curve, its first derivative and cooling curve. The amount of linear shrinkage can be measured.
  - The measurement results are repeatable and reliable.
  
- In **Phase II**, systematic investigation of the process variables on hot tearing was completed. Effect of mold temperature and pouring temperature (*Chapter 3*)
  - Important solidification characteristic data and critical data on hot tearing formation were determined using the developed technique. The crack area in the hot spot region for each condition was measured and used as hot tearing susceptibility index.
  - Alloy A356 has high resistance to hot tearing. No hot tearing forms under the tested conditions, while M206 shows significant hot tearing tendency under the same conditions.
  - Mold temperature has a great influence on hot tearing of alloy 206. The severity of hot tearing and the amount of linear contraction decreased significantly with increasing mold temperature because elevated mold temperature promotes uniform casting contraction and therefore alleviates stress concentration. On the other hand, the thermal gradient influences the grain morphology during solidification. Lower mold temperature results in higher thermal gradients which promotes columnar

structure. The columnar structure is detrimental when its growth direction is vertical to the tensile force, which favors the hot tearing formation.

- The severity of hot tearing in alloy M206 increases with increasing pouring temperature in the tested range. The effect is not as significant as that of mold temperature. Two factors might contribute to this increase. First, the ability of the structure to accommodate the stress buildup due to thermal contraction decreases since the grain size becomes larger with increasing pouring temperature (a lower cooling rate). On the other hand, the liquid film thickness between grains increases due to large grain size, which would tend to increase hot tearing susceptibility.
- The grain morphology and loading (contraction) rate developed in the constrained casting are important factors to hot tearing formation.

#### Effect of grain refinement (*Chapter 4*)

- Grain refinement decreases the grain size and changes the grain morphology from columnar structures for unrefined casting to equiaxed dendritic or globular structures. Grain size and grain morphology have significant effect on hot tearing susceptibility in alloy 206. It was found that a fine globular structure prevents hot tearing formation during solidification of 206.

## **2. Phase III:** Computer simulation

- The effective plastic strains accumulated during solidification have been calculated for 206 castings cast at different mold temperatures using casting simulation software. The results show that the strain in critical area is much lower at higher mold temperature, which should be associated with the lower hot tearing tendency in higher temperature mold.
- The quantitative data and information has been provided to ProCast and Magma to validate their hot tearing model. Preliminary results were generated in the trial runs.

# HOT TEARING OF ALUMINUM ALLOYS

## – A Critical Literature Review

Shimin Li and Diran Apelian  
Metal Processing Institute  
Worcester Polytechnic Institute, MA 01609

### **Abstract**

*Hot tearing is a common and severe defect in casting and it is perhaps the pivotal issue defining an alloy's castability. The subject has been extensively studied through various perspectives for decades and more recently computational models have been developed; however despite these accomplishments there is confusion in the literature. The governing mechanisms and the control of hot tearing are not totally clear. Experiments show inconsistent results and different opinions exist about what roles some processing or alloy factors play. WPI's Casting Center (ACRC) initiated a major project devoted to developing a reliable experimental apparatus/methodology to quantitatively study hot tearing and use it in studying the effects of various parameters on hot tearing. As part of this endeavor, a comprehensive literature review was conducted. The review focuses on: (i) Theories of hot tearing; (ii) Hot tearing variables; and (iii) Test methods. A summary of hot tearing criteria/models are also provided.*

**Keywords:** *Hot tearing, Aluminum alloys, Process parameters, Grain structure, Hot Tearing measurement, Hot tearing criterion and model.*

# Table of Contents

## Abstract

## 1. Introduction

## 2. Theories of Hot Tearing Formation

2.1 Theories based on stress, strain, and strain rate

2.2 Theories based on other principles

## 3. Hot Tearing Variables

3.1 Alloy factors

*3.1.1 Effects of alloy chemistry*

*3.1.2 Effects of grain, its size and morphology*

3.2 Processing parameters

*3.2.1 Superheat*

*3.2.2 Mold temperature*

## 4. Hot Tearing Measurements

## 5. Hot Tearing Criteria and Models

## 6. Concluding Comments

## 7. Acknowledgements

## 8. References

*Summary - Hot Tearing Criteria and Models*

## **1. Introduction**

Hot tearing is a common and serious defect encountered during solidification of castings. It is also referred to as hot cracking, hot shortness or hot brittleness. Irrespective of the name, it is an irreversible defect that appears as cracks, either on the surface or inside the casting. Hot tears are generally large and visible to the naked eye. Sometimes, they can also be small and only be observed using magnetic particle inspection and penetrating dyes, etc<sup>1</sup>. It generally consists of a main tear and numerous minor offshoots, which follow intergranular paths, and the failure surface reveals a dendritic morphology<sup>2</sup>. The subject of hot tearing has been extensively studied and many test techniques and computational models were developed. Reviews in the field have been done by Novikov<sup>3</sup>, Sigworth<sup>4</sup>, and Eskin<sup>5</sup> et al. The numerous studies show that hot tearing is a complex phenomenon, it lies at the intersection of heat flow, fluid flow and mass flow, and various factors have influences on its formation. The variables include alloy composition, mold properties, casting design and process parameters, etc<sup>5</sup>. A fine grain structure and a controlled casting process mitigate and limit hot tearing<sup>4,6</sup>. Over the years, much work has been devoted to understanding the mechanism of hot tearing. In general, it is accepted that hot tearing occurs due to solidification shrinkage and thermal deformation developed during solidification. However, whether thermal stress or thermal strain, or strain rate is the controlling factor is still not clear. Moreover, how hot tearing is measured (or controlled) is not standardized and a reliable predictive model is still not available.

## **2. Theories of Hot Tearing Formation**

### **2.1 Theories based on stress, strain, and strain rate**

Hot tearing has been investigated since the beginning of 20th century. In the early days much was said about the phenomena and how to prevent them, especially in steel castings, however, little was known of their formation mechanisms. It can be considered that the real study of hot tearing formation mechanisms was started in 1928, when Körber and Schitzkowski conducted systematic study of hot tears in carbon steels<sup>7</sup>. In their study, hot tears were intentionally produced in flanged steel bars by hindered contraction and it was found that hot tears most likely occurred in a temperature range from 1250 to 1300C (2282 to 2372F). Thereafter, it was believed for years that hot tears were formed at temperatures below solidus based on their experiments<sup>8,9</sup>.

In early 1930s, to “continue” Körber and Schitzkowski’s work, Briggs and Gezelius<sup>10, 11</sup> studied the stress evolution during solidification in a steel bar. The bar was designed in a way that there is no sharp thermal gradient in the casting therefore they did not break under contraction. Their work didn’t show the actual amount of stress necessary to cause hot tears, but intentionally showed the load-carrying ability of steel under hindered contraction<sup>8</sup>.

In 1936, Verö<sup>12</sup> proposed in his study of the hot-shortness of aluminum alloys that hot tearing was caused by the stress developed from the contraction of the primary crystals during solidification of the alloy. In the first stage of solidification, coherent network does not form and hot tears would not occur. As the dendrites grow and come into contact, a coherent network forms. Further solidification would produce stress when the alloy contraction is restrained by the mold. He also first clarified the importance of the influence of eutectic constituents. If the remaining eutectic liquid is sufficient, it would feed and ‘heal’ the incipient tears.

Pumphrey et al.<sup>13</sup> proposed that even though the strength of the metal increases with decreasing solidification temperatures, hot tears still could develop as long as a small amount of residual liquid remained. They thought that the alloy had a “brittle temperature range” between the temperature at which a coherent dendrite structure was first developed and the solidus temperature. In this temperature range, the metal possessed little ductility and was prone to hot tear.

These early studies all considered that hot tearing was induced by the stress buildup in the metal during solidification and cooling due to the hindered contraction. The importance of the “healing effects” of the remaining liquid was also addressed.

In 1952, Pellini et al. studied the initiation of hot tear by means of radiography and thermal analysis of solidifying castings and introduced the concept of liquid film in their study<sup>14</sup>. It was found that the tear started at the time when the metal temperature was above the solidus. At this time there was a thin continuous liquid film remaining between the solidified dendrites. It was suggested that the mechanism of hot tearing was the separation of the film at the solidification stage when the solidus was being approached and a minute amount of liquid remained. At the same time Pellini<sup>15</sup> published his strain theory of hot tearing based on strain accumulation and the concept of liquid films. It was said that hot tearing was a strain-controlled phenomenon. It would occur when the strain accumulated in a hot spot reached a critical value. As the

temperature just entered the film stage, the film was relatively thick and completely continuous. At this point, the load required to deform (to develop extension of) the hot spot (the liquid film) should be near zero; but the deformation (extension) needed to open the liquid film for initiating the hot tear should be relatively high. As the metal approached to the end of the solidification, the film became thinner and thinner and the deformation (extension) tended to concentrate on the few remained hot zones, which would produce a high unit strain. Total strain developed during film life depended on two factors: (1) strain rate; (2) time of film life. According to this theory the liquid film provided the condition that permitted hot tearing, and the actual occurrence of hot tearing was determined by mechanical factors inherent to the rate of deformation. The hot tearing of semisolid metal was not possible unless the strain rate was high enough. Pellini and his coworkers' further work<sup>14-16</sup> conducted at the Naval Research Laboratory in the 1950s, confirmed that the hot tearing temperature was above the solidus of a metal. Since Pellini et al.'s work it was recognized that the temperature interval was critical for hot tearing.

Campbell<sup>2</sup> postulated that a hot tear was a uniaxial tensile failure in weak portion of material and suggested that the theories based on feeding difficulties should be dismissed, since the hydrostatic (i.e. a triaxial) stress resulted from feeding problems would be associated with pores or layer porosity formation among dendrites, but dendrites themselves are not affected. He quantified Pellini's theory and expressed the strain ( $\epsilon$ ) in the hot spot as:

$$\epsilon = \alpha \Delta T L / l \quad (1)$$

- L: the length of the casting;
- $\alpha$ : coefficient of thermal expansion;
- $\Delta T$ : length of mushy zone;
- l: length of a hot spot.

From this equation it is clear that strain can be reduced by refining the grains, reducing lengths between hot spots, and minimizing the temperature difference.

Recently, Davidson and coworkers conducted experiments to confirm the hot tearing temperature<sup>17</sup>. They used a hot tear test rig, which was equipped with a window over the hot spot region, to measure the load imposed on the mushy zone and simultaneously observe the hot tear formation and growth. It was found that in Al-Cu alloys the hot tear started at a very low load and at a temperature between 93% and 96% solid.

Metz and Flemings<sup>6</sup> conducted a fundamental study of hot tearing using a shear test. They suggested that the strain rate was critical to hot tearing formation. Hot tearing formation was considered to be the result of progressive separation of dendrites to accommodate strain.

### 2.1 Theories based on other principles

In 1961, Saveiko developed a theory based on interdendritic liquid film<sup>18</sup>. The surface tension of the liquid film was considered of very importance in his theory. The model demonstrating the hot tearing formation on a microscopic scale in this theory is shown in Figure 1. In the model the grains were simplified and assumed to be cubical in shape. As shrinkage progresses, the grains at A and B move in their arrow directions respectively and the extension between them increases. If the movement reaches a certain value, a tear may form along one of the liquid films. To separate the liquid film to form two new surfaces, work must be done to overcome the molecular adhesion force. The force required to tear apart the liquid film is:

$$P = 2\alpha F / 1000gb \quad (2)$$

Where  $\alpha$  is surface tension of the liquid, erg/cm<sup>2</sup>; F is the area of contact between the plates and liquid, cm<sup>2</sup>;  $b$  is the thickness of the liquid layer between the plates, cm; and  $g$  is gravitational acceleration constant, cm/s<sup>2</sup>.

The film thickness is considered to be much more important than surface tension since film thickness varies to a greater extent than surface tension with the change of grain size. This explains why alloys with fine grains are more resistant to hot tearing.



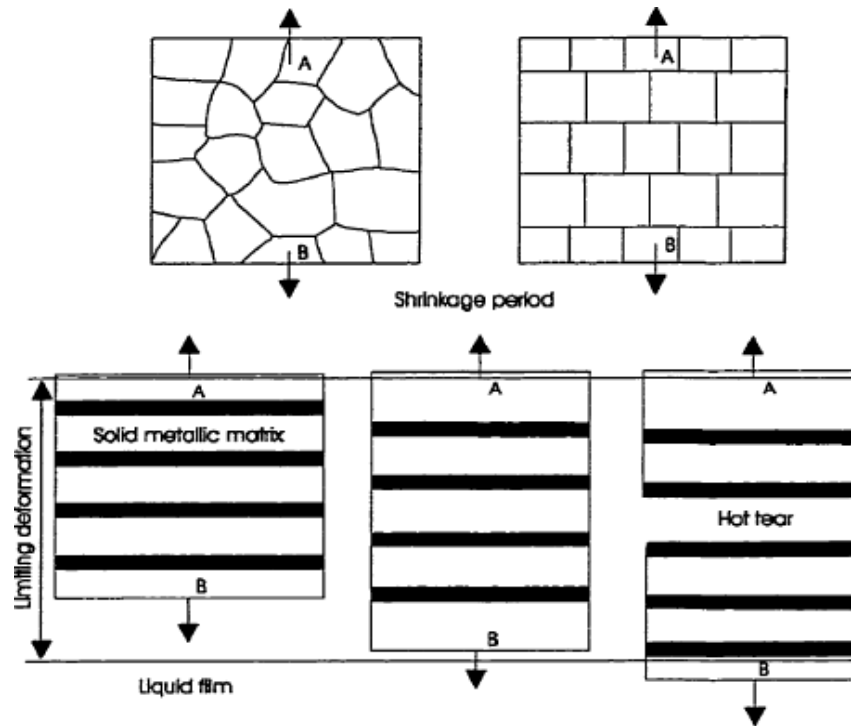


Figure 1: Hot tearing formation based on an interdendritic liquid film concept<sup>18</sup>.

Sigworth suggested considering liquid metal embrittlement to investigate hot tearing<sup>4</sup>. Griffith's crack theory was used to approach liquid metal embrittlement. In the model, the strain energy stored in the deformed material contributes to create a new surface when cracks grow. In ductile materials most of the fracture energy is consumed at the root of the growing crack tip in plastic deformation. However, when certain liquid metals are present, the ductility nearly vanishes, the fracture stress decreases remarkably, and the cleavage energies calculated are very close to the measured surface free energy. It is concluded that liquid metal embrittlement (and also hot tearing) is caused by small surface-free energy between liquid and solid, which create liquid cracks.

In 1961, Rosenberg R.A., Flemings M.C. and Taylor H.F. published their study on hot tearing of nonferrous binary alloys and pointed that the hindered feeding of the solid phase by the liquid was the main cause of hot tearing<sup>19</sup>. Hot tear would not occur as long as there was sufficient feeding during solidification. In a quantitative study of the solidification and an evaluation of cracking in aluminum-magnesium alloys, Clyne and Davies<sup>20</sup> focused on the solidification time in the mushy state; and thought that hot tear was the result of uniaxial tension. The last stage of freezing was critical to hot tearing. At this stage the grains were no longer able to move freely

and the strain applied would cause hot tearing. Based on this theory a CSC (crack susceptibility criterion) hot tearing criterion was established<sup>2</sup>.

Though the subject of hot tearing is not a simple one, we can generally summarize the theories into two groups:

- One group of theories is based on stress, strain and strain rate, and these are related to thermo-mechanical properties of the alloy.
- The other group of theories is based on liquid film and lack of feeding which is related to metallurgical factors.

From the study, it can be concluded that hot tearing is a complex phenomenon which combines the metallurgical and thermo-mechanical interactions. Though the basic phenomena involved in hot tearing formation are understood, there is still no agreement on what (controlling factor) causes its formation.

### **3. Hot Tearing Variables**

#### **3.1 Alloy factors**

##### **3.1.1 Effects of Alloy Chemistry**

Systematic investigation of the effects of alloy composition on hot tearing started from Ver ö's work<sup>12</sup>. He studied the Al-Si alloys by measuring the average length of hot tearing of a "U" shape permanent mold casting. The work showed that the severity of hot tearing increased with the increase of Si content up to 1.9%, then tearing rapidly decreased with the further increase of Si. Since then this field has been extensively explored and many other alloy systems were studied.

In early 1940's, Pumphrey et al. did a systematic study of six Al binary alloys, Al-Si, Al-Cu, Al-Mg, Al-Fe, Al-Mn, and Al-Zn, made from high purity Al and high purity master alloys or virgin metals<sup>21</sup>. Ring-casting test was used and the total length appearing on all ring surfaces were measured as the severity index of cracking. In the ring test each alloy was cast at three pouring temperatures with superheat of 20C (68F), 60C (140F), and 100C (212F), respectively. The addition of each element was in the range, in which pronounced cracking occurred in each system. In all systems an initial increase in cracking occurred from the initial addition of the

alloying element to super-purity Al, followed by a subsequent decrease to zero cracking at some higher element level. The alloy composition and superheat determined alloy grain structure and thus the hot tearing susceptibility. In Al-Si, Al-Cu, Al-Mg, and Al-Zn system the grain structure changed from columnar to transitional to equiaxed with increasing amount of alloy element at a given superheat, which corresponded to decreasing cracking length.

In a study of hot tearing of nonferrous binary alloys, Rosenberg and Flemings et al. developed a test and studied Al-Mg, Al-Sn, Al-Cu, Mg-Al and Mg-Zn alloy systems<sup>19</sup>. Hot tear resistance was rated as the maximum length of test casting which could be made free of tears. The greater the length, the greater the resistance to tearing. The lengths for pure Al and Mg were about 12” (30.48 cm). With a small amount of addition of the solute the hot tearing resistance decreased. Various alloying elements affected hot tearing in different ways, some more dramatically than others. For example, the resistance to hot tearing (the maximum length) reduced by a factor of 3 when 0.5% Ti was added in Al, while similar addition of Cu had relatively small effect. In all alloys studied, tear resistance was a minimum at one or more composition in the range of 0.25 to 10% alloy addition. After this point tear resistance starts to increase with further increase of alloy addition. For example, it was 0.15-5% Sn for Al-Sn alloy, 5% Cu for Al-Cu alloy, 4-6% Mg for Al-Mg alloy. Their experimental results of hot tearing susceptibility of Al-Sn and Al-Cu alloys are shown in Figure 2. In Al-Cu alloy the effect of Cu on tear resistance was coincident with its effect on alloy freezing range. When Cu addition increased the alloy freezing range it decreased tear resistance and vice versa. The minimum tear resistance corresponded to the Cu addition, which rendered the maximum freezing range to the alloy. However, this relation was not observed in other alloy system.

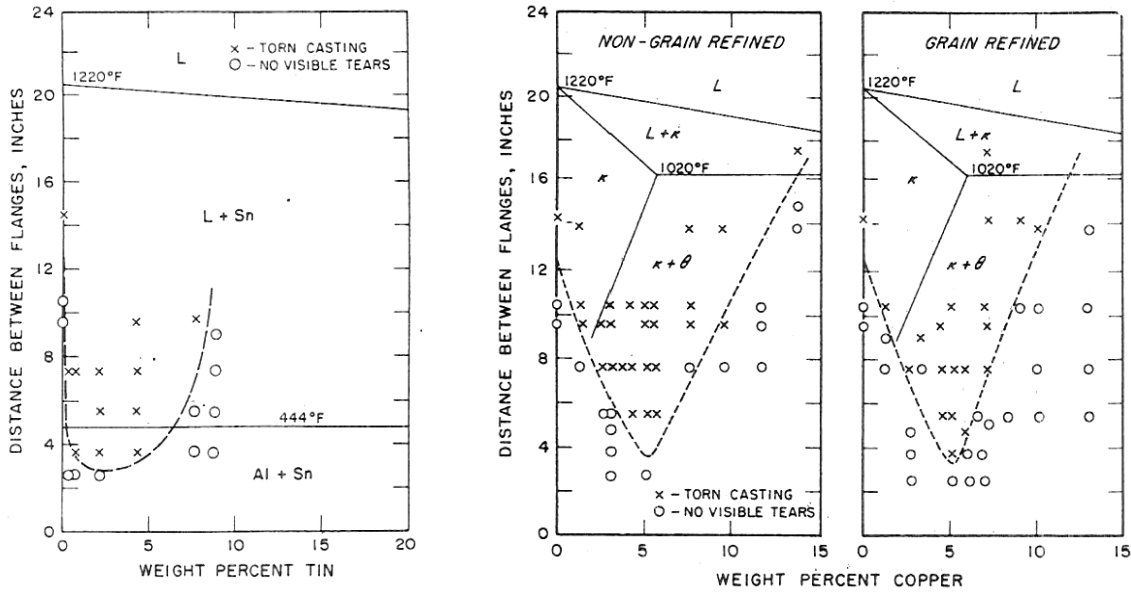


Figure 2: Hot tearing of restrained bar test in binary Al-Sn and Al-Cu systems<sup>19</sup>.

The effect of alloy composition on hot tearing has been established. For most binary alloys, the relationship between hot tearing tendency and alloy composition is considered as the so called lambda curve<sup>2, 22</sup>, as shown in Figure 3. Generally, the larger the freezing range, the more the alloy is prone to hot tearing since the alloy spends a longer time in the vulnerable stage.

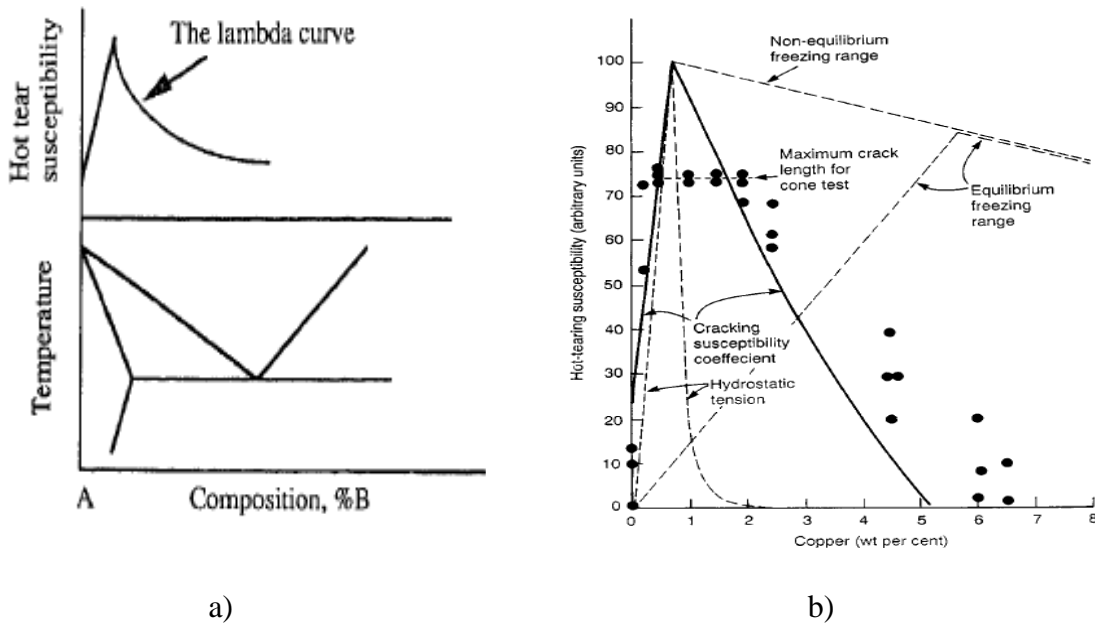


Figure 3: a) Schematic illustration of hot tearing susceptibility as a function of a binary alloy, shown as a lambda curve<sup>22</sup>; b) Hot tearing for Al-Cu alloys, showing a peak at approximately 0.7%Cu from the conical ring die test<sup>2</sup>.

Chamberlain et al. and Sigworth et al.'s work showed that not only the amount of the alloy additions but also their interactions had effects on the hot tearing<sup>23, 24</sup>. It was found that both Mg:Zn ratio and total Mg+Zn content in Al-Mg-Zn alloy system were critical to hot tearing. The propensity to hot tearing decreased with increasing Mg:Zn ratio. There was no hot tearing with Mg:Zn ratio greater than 1.4:1 and with the same Mg:Zn ratio the resistance to hot tearing increased with increasing magnesium content.

Many studies demonstrated the importance of the amount of eutectic to hot tearing in Al-Si and Al-Cu alloys<sup>12, 19, 25</sup>. All the work showed that hot tearing tendency was related to the amount of eutectic liquid present during the latter stages of solidification. The presence of a small amount of eutectic was observed to aggravate hot tearing tendency. However, when it was beyond a certain value, hot tearing decreased with increasing eutectic content. Rosenberg et al. thought that the different effects of different alloy additions were due in part to the shape or the resultant film or pockets<sup>19</sup>. When enough alloying elements were added to a pure metal so that eutectic was present in amounts greater than necessary to completely surround the primary grains with a thin film, resistance to hot tearing increased due to improved feeding. However, Pumphrey et al. indicated in their brittleness theory<sup>13</sup> that stress accommodation and healing were more significant with an increase in the amount of eutectic.

Eskin et al. presented a comprehensive review on hot tearing susceptibility of aluminum alloys<sup>5</sup>. The review covered many alloy systems, including Al-Cu, Al-Mg binary alloys, Al-Cu-Mg, Al-Cu-Si, Al-Mg-Si and Al-Cu-Li ternary alloys, and AA2XXX (Al-Cu-Mg), AA6XXX (Al-Mg-Si) and AA7XXX (Al-Zn-Mg) series commercial alloys, etc. To "continue" the work in Eskin's review, many other alloy systems were studied to relate their hot tearing susceptibility or other features to alloy compositions.

Clyne et al. studied Al-Mg system alloys using a "dog-bone" specimen<sup>20</sup>. High purity aluminum (total Fe+Si=0.03%) with a range of Mg was used in their first series of tests. Maximum susceptibility was observed at about 1%Mg. The test showed that even the high purity base alloy (without addition of Mg) had a significant degree of cracking. However, when super high purity aluminum was used the crack was eliminated. It was concluded that the onset of cracking was rapid at very low solute content. They further studied various level of Mg at different pouring temperatures using commercial purity aluminum (0.29%Fe, 0.44%Si). The results are shown in

Figure 4, which indicate that the maximum cracking susceptibility is dependent on both composition and pouring temperature. As pouring temperature increases the maximum in the cracking susceptibility curves is raised and moved to lower Mg content.

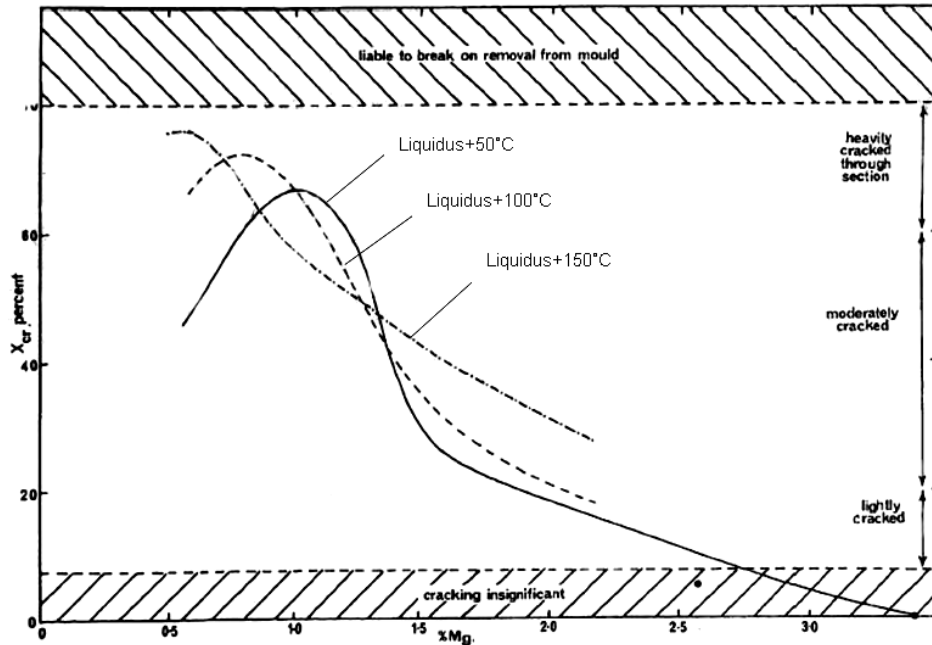


Figure 4: The variation of hot tearing susceptibility of Al-Mg alloys with different levels of superheat<sup>20</sup>.

Spittle and Cushway studied Al-Cu with Cu up to 15% using the dog-bone test casting<sup>26</sup>. The experiments showed that the alloy composition determined the crack formation mechanism. In their testing condition, the cracking was only detected in the alloys with Cu of less than 7%. The actual composition range, in which the cracking was observed, depended on alloy grain structure and pouring temperature (superheat).

### 3.1.2 Effects of Grain, its Grain Size and Morphology on Hot Tearing

The effects of grain refinement on hot tearing have been studied to a large degree<sup>6, 19, 27-30</sup>. Most of the results showed that grain refinement improved resistance to hot tearing by making it better able to accommodate local strains. A fine equiaxed grain structure was normally desired in aluminum castings. However, in Rosenberg and Flemings et al.'s work they "surprisingly" found that the grain refining did not have any effect on hot tearing in their experiments<sup>19</sup>.

Moreover, Warrington et al. found that the alloy could still have high hot tearing susceptibility when grain refiner was added depending on the amount of addition<sup>31</sup>. They studied alloys 7010 and 7050 using a test similar to the ingot shell zone of semi-continuous direct chill casting and found that the alloys had columnar structures and high cracking susceptibility without adding grain refiner. With moderate addition of grain refiner the alloys formed equiaxed-dendritic grains and gained resistance to cracking. However, with higher addition equiaxed-cellular grains formed and the cracking susceptibility turned to be high again.

Easton et al. studied how grain refinement affected hot tearing. The CAST hot tearing rig was used in their study and the load development with temperature of the test bar was measured<sup>29, 30</sup>. Alloy 6061 was studied with grain refiner additions of 0.001 (no addition), 0.005, 0.01, and 0.05% Ti. Figure 5 shows the measured load versus temperature curves and the cracks and microstructures of the castings are shown in Figure 6. It was found that the onset of load development was delayed and the load developed during cooling decreased with addition of grain refiner. They proposed three mechanisms, by which the grain refinement affected hot tearing.

- (1) Grain refinement changes grains from columnar to equiaxed morphology, and as a result the permeability length scale is changed from secondary dendrite arm spacing (for columnar grain) to grain size (for equiaxed grains),
- (2) Changing the region over which feeding occurs,
- (3) Changing the capillary pressure. The liquid films between grains become thinner at a given fraction solid due to smaller grain size, and therefore capillary pressures to be overcome before a crack propagate become greater.

These mechanisms were incorporated in the recent RDG hot tearing prediction model and were used in predicting hot tearing susceptibility of castings in their study. By comparing the predictions and the experimental results they concluded that grain refinement decreased the hot tearing susceptibility by causing a columnar to equiaxed transition and by reducing the equiaxed grain size. An important factor was that the point, at which the mush began to behave more like a solid than a liquid, was delayed. However, the prediction shows that if the grain size is reduced, the permeability of the mush would decrease causing the hot tearing susceptibility to increase. They thought that Warrington et al.'s work "with high addition the cracking susceptibility got

high”, mentioned earlier, supported that refinement of cellular equiaxed grains might increase the hot tearing susceptibility.

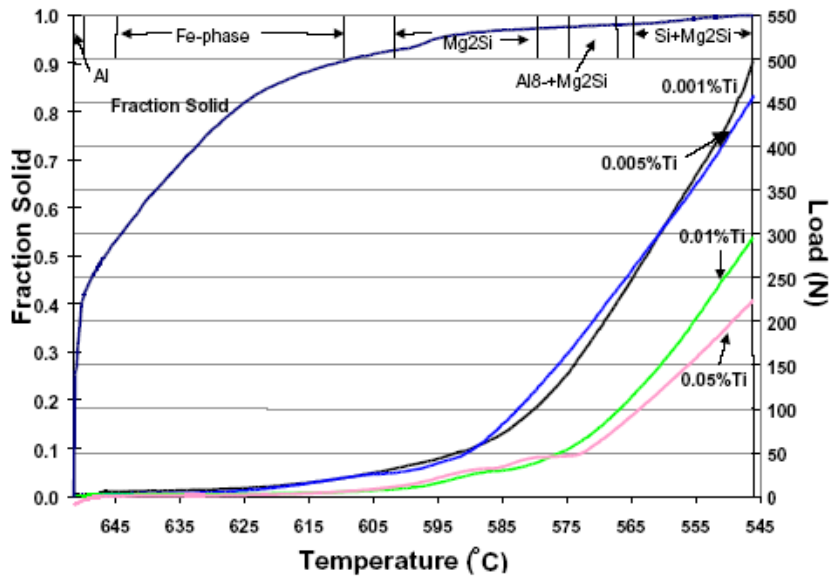


Figure 5: Load development of alloy 6061 during solidification with different grain refiner levels. Fraction solid value and phase formation as temperature decreases are also indicated<sup>29</sup>.

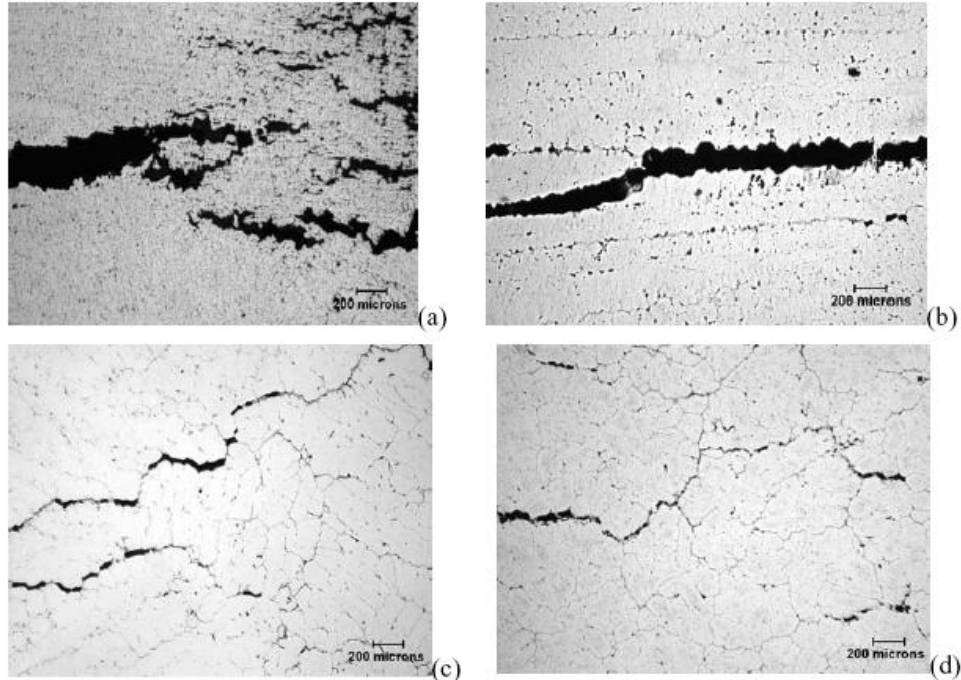


Figure 6: Optical micrographs showing microstructural features in hot spot area of cast bars for alloy 6061<sup>29</sup>; (a) 0.001% Ti, (b) 0.005% Ti, (c) 0.01% Ti and (d) 0.05% Ti.



Matsuda et al. studied the effect of adding elements on solidification crack susceptibility of Al-Zn-Mg welding alloys<sup>32</sup>. The alloy studied was synthesized weld alloy, Al-2%Zn-2-3%Mg. The elements added were Ti+B, Ti, Zr, Fe, Mn, B, Si, Be, Ni, Cr, V, Misch metal, and Cu, and added amount was up to 0.5% (up to 0.06% for Ti-B). The experiment was conducted using the ring casting crack test and crack length was used as susceptibility index. It was found that among the thirteen added elements the most favorable ones were Ti+B, Ti, and Zr, and the detrimental element was Cu. The effects of Ti+B, Ti, and Zr, are shown in Figure 7. The optimal amounts are greater than 0.05% for Ti-B, 0.14% for Ti, and 0.24% for Zr. They also found that when more than one element was added together they might react with each other. For example, small addition of Ti was favorable to the Ti-B addition, but small addition of Zr was likely to cancel the beneficial effect of Ti-B. The study showed that the effects of these elements were related to their grain refining effects and showed that when large columnar grains were dominant the crack length was likely to reach the saturated value, and with grain becoming equiaxed and smaller in size the crack length (hot tearing susceptibility) reduced, which was independent of the kind and amount of added elements. The relation between the measured crack length and mean grain size is shown in Figure 8.

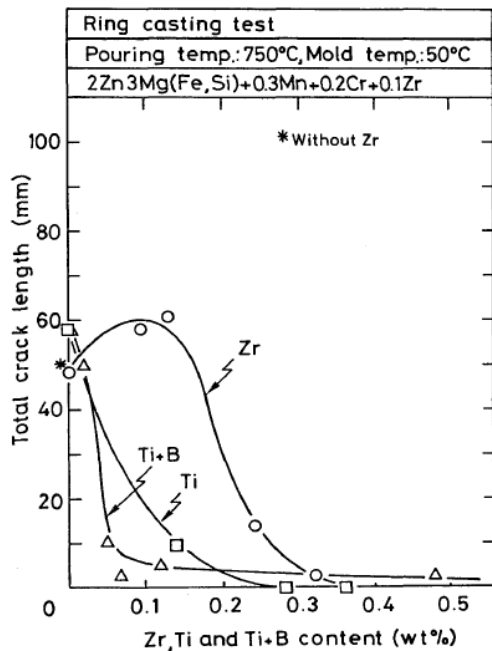


Figure 7: Effects of Ti+B, Ti and Zr additions on total crack length of Al-Zn-Mg system<sup>32</sup>.

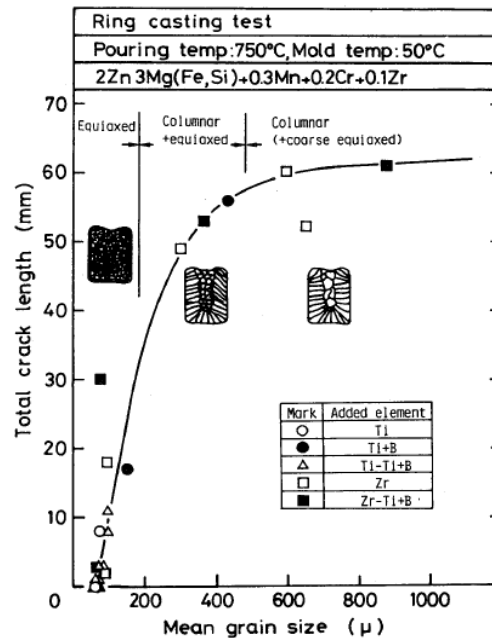


Figure 8: Relation between mean grain size and total crack length of Al-Zn-Mg alloy system with and without Ti+B, Ti and Zr<sup>32</sup>.

Clyne and Davies<sup>20</sup> studied the effect of grain refinement for two Al-Mg alloys, one was Al-2%Mg, which had low cracking susceptibility, and another was Al-1%Mg, which had high cracking susceptibility. Both alloys had columnar grain structure when no grain refiner (Ti) was added. It was found that the low susceptibility alloy showed an increased cracking tendency over a narrow range of Ti contents despite the grain structure was changed to finer and equiaxed. However, the high susceptibility alloy was unaffected by the Ti additions except at high level (>0.2%Ti) even though the grain was altered from columnar to equiaxed. So, they pointed out that there was a complex interaction between impurity content, grain structure, and cracking susceptibility.

Pumphrey et al.'s experiments demonstrated the effect of grain morphology<sup>21</sup>. In their study the grain structure changed from columnar to transitional to equiaxed in Al-Si, Al-Cu, Al-Mg, and Al-Zn binary systems with increasing alloy element content. This morphology change corresponded to the crack length decreases.

## **3.2 Processing Parameters**

### **3.2.1 Melt Superheat (Pouring Temperature)**

As pointed out by Pellini<sup>15</sup>, “at any meeting where the subject of hot tearing is discussed, the steel foundry community would divide into groups with distinctly opposite opinions regarding carbon and pouring temperature effects depending on the general types of casting produced and the foundry practices used by the individuals expressing the opinions”. For example, in earlier study of hot tearing of steel, Singer et al. believed that high pouring temperature would minimize hot tearing<sup>33</sup>. While, Middleton<sup>9</sup> et al. showed that hot tearing was likely to occur and was severer at high casting temperatures than at low temperatures. These conflicting experimental results and contradictory opinions were also seen in non-ferrous alloys. Pumphrey et al. studied six aluminum binary alloy systems and their experiments showed that at any given alloying element level the cracking susceptibility decreased with decreasing superheat<sup>21</sup>. However, in the study of a magnesium alloy, AZ91D, Bichler et al. found that the variation of pouring temperature did not have significant effects<sup>34</sup>.

Couture and Edwards<sup>35</sup> thought that two factors could be attributed to this controversy. A higher superheat might spread the hot spot, which was expected to reduce hot-tearing tendency and high superheat also might increase the liquid film life, which was expected to increase the tendency to

hot tearing. However, Briggs thought high superheat levels can increase the temperature gradients during solidification and result in the promotion of columnar dendritic growth<sup>8</sup>. Generally, the alloys with columnar structure have higher hot tearing tendency than the alloys with equiaxed structures in normal situations. Several studies also showed that the effects of superheat changed with different test methods and were dependent on some other factors such as cooling rate, presence of grain refiners, and healing phenomena, etc.

### 3.2.2 Mold temperature

Generally, it is considered that the effect of mold temperature on hot tearing is through its effect on cooling rate. Mold temperature directly affects the casting cooling rate and thus the casting microstructure and performance, including hot tearing. On the other hand, controlling cooling rate is generally through controlling mold temperature. In fact, most of studies on hot tearing, which involve mold temperature, were using it to control cooling rate or the solidification pattern, like in Clyne<sup>20</sup> et al. and Spittle<sup>26</sup> et al.'s tests. Very limited work on this topic was found in the published literatures.

Bichler<sup>34</sup> et al. studied the effects of mold temperature on Mg alloy, AZ91D. The tests were conducted at pouring temperature was 700°C (1292°F) and mold temperatures of 140, 180, 220, 260, 300, 340, and 380°C (284, 356, 428, 500, 572, 644, and 716°F). It was found that mold temperature had significant effect on hot tearing. The severity of hot tearing decreased progressively with increasing mold temperature. They thought that 220°C (392°F) was critical, which corresponded to cooling rate of 18-20°C/s. At mold temperatures below 220°C (392°F) cracks initiated from all surfaces, propagated toward center and were connected transiting the entire cross section. At higher than 220°C (392°F) cracks were hairline-like and were not connected. The mold temperatures above 340°C (644°F) were sufficient to significantly alleviate hot tears. They thought this was probably because that higher temperature improved feeding.

Zhen<sup>36</sup> et al. studied the effects of mold temperature in the range of 250 to 500°C (482 to 932°F) for binary Mg-Al alloys. They found that increasing the mold temperature decreased hot tearing susceptibility and the higher mold temperature led to higher crack onset temperature and longer propagation time. The mechanism they gave was that cracks were initiated at all the mold temperatures, but at higher mold temperature the cracks could be refilled by the remaining liquid and healed. This was because the higher mold temperature led to lower cooling rate, and thus a

coarser microstructure. The coarser structure led to thicker and more continuous remaining liquid. This coupled with higher onset temperature made the refilling easier. Limmaneevichitr et al. mentioned the effect of mold temperature when studying the role of grain refinement<sup>37</sup>. They were “quite surprised to find” that cracking were severer in lower mold temperature experiments, e.g. 220°C (392°F) (compared with 250°C (482°F)). However, looking at their entire data presented, only in two conditions the cracking was severer in lower mold temperature, but all seven other cases did not support their finding.

Few literatures were found so far in studying the effects of casting and mold temperatures on the hot tearing. Different studies showed controversies about casting temperature effect but all of the limit work about the effect of mold temperature showed that higher mold temperature reduces hot tearing susceptibility and gave the mechanism of better feeding and initial crack refilling.

#### **4. Hot Tearing Measurements**

Many techniques for studying hot tearing and assessing hot tearing susceptibility have been developed over the years. These apparatuses were designed to induce cracking during solidification by constraining the casting to resist solidification shrinkage and thermal contraction. Eskin<sup>5</sup> et al. summarized the various measurement techniques in their recent review, which include ring type testing, backbone mold testing, cold finger testing and tensile testing. In this paper only test methods those were not included in the 2004 review<sup>5</sup> are presented. Generally, the testing methods can be classified into the following categories<sup>38</sup>:

- 1) Tests by observation of hot tears;
- 2) Tests using mechanical techniques;
- 3) Other tests including physical property testing, etc.

The ring mold testing, backbone mold testing, cold finger testing and their relatively modified tests belong to the first category - tests by observation of hot tears. Other tests to this category include flanged bar test<sup>7, 39</sup>, cylindrical bar test<sup>19, 40</sup>, ball-bar casting test<sup>35</sup>, I-beam casting test<sup>41, 42</sup>, “U” shape casting test<sup>43</sup>, and N-Tec hot tearing mold test\*.

The N-Tec hot tearing mold testing is a variation of the backbone mold testing. The casting consists of five 'Dog Bone' sections of different lengths, constrained at each end, and with a hot

---

\*: N-Tec is a trademark of N-Tec Ltd.

spot along the gauge length. The hot tearing mold and the set up are shown in Figure 9. Metal is poured into the mold by means of a pouring sleeve that is located in the mold by a clamp ring. The top of the sleeve should be used as the pivot point for the ladle when pouring. Therefore, this sets the pouring height to a repeatable level so ensuring accurate and consistent test results. Moreover, a heater plate was placed under the mold, so the temperature can be precisely controlled.



Figure 9: N-Tec hot tearing mold (a) and setup (b)\*.

Hot tearing usually appears in the longer sections due to the increasing constrained shrinkage with the increasing lengths of the sections. This testing provides both qualitative and semi-quantitative measures of hot tearing susceptibility. Hot Cracking (Index) is obtained by recording the number of cracked ‘Dog Bones’. Hot Tearing (characteristic) can be obtained by plotting all visible cracks on a control sheet.

A common point in the many tests in this category is that each section has a heavier end to provide a restriction to its contraction. When the metal is solidified, the contraction of the section will take place, and hot tears will occur at the hot spot if the section is greater than a critical length. The severity of hot tearing in these tests is usually evaluated by its total crack length and/or the crack width, or critical length (diameter) that the casting is free of tear. Obviously, only a qualitative or semi-quantitative assessment data can be obtained. Moreover, internal cracks in the casting were difficult to be estimated and measured.

Another approach to investigate hot tearing is to simultaneously measure the strength development of alloys at high temperatures or to measure certain characteristics such as contraction force and/or linear displacement during solidification of casting. Eskin<sup>5</sup> et al.

reviewed numerous testing techniques for measuring the mechanical properties of semi-solid model and commercial aluminum alloys. The methods include tensile test at higher temperatures<sup>5, 44, 45</sup>, direct chill casting tensile test<sup>46</sup>, stress and strain measurement in half-ring mold testing<sup>5, 47</sup>, variable tensile strain test<sup>48</sup>, and hot tear test rig<sup>49, 50</sup>. More recently, several testing systems which measure contraction force and/or linear displacement have been developed and some typical ones are described below.

Instone et al. developed a constrained solidification test rig for characterizing tensile strength development and hot tearing behavior of solidifying material<sup>49, 50</sup>. The apparatus simulates the DC casting process where two solidification fronts met at the center of the test bars and measures the load imposed in the semi-solid region during solidification. A schematic view of the mold is shown in Figure 10. The mold has a pouring reservoir at the center, which ensures hot tears form at the central location of the bars. One test bar is used for temperature measurements and microstructural examination. The other test bar is connected to a displacement transducer and a load cell, to measure the load and displacement developed during solidification. The schematic diagram of the test rig is shown in Figure 11. A modified Instron tensile testing machine with a 5kN load cell is used as the basis of the test rig.

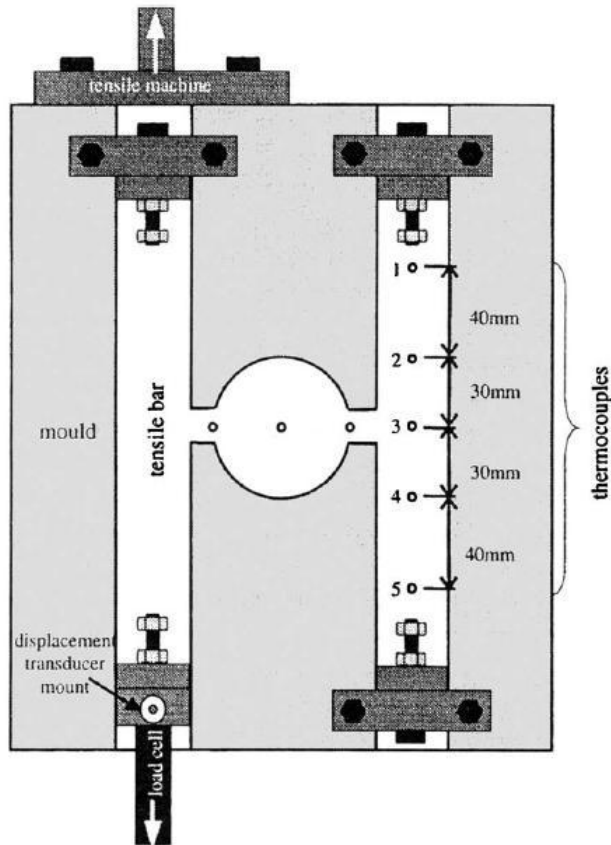


Figure 10: Plan view of the test mold developed by Instone et al.<sup>49</sup>

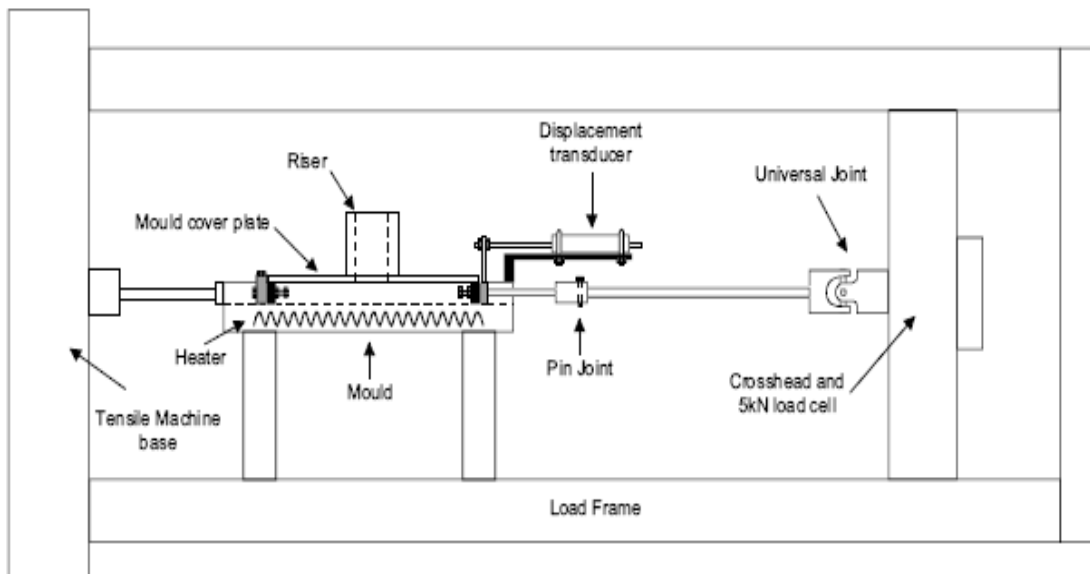
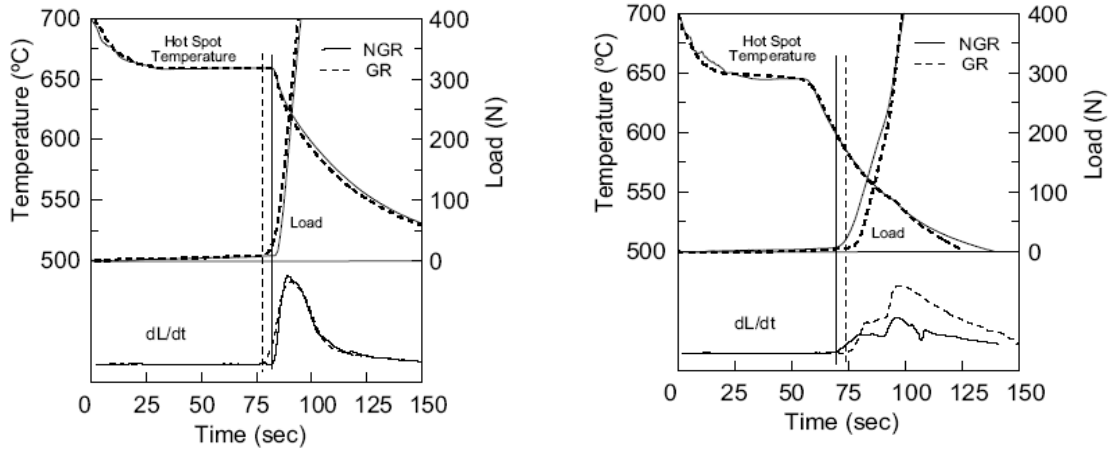


Figure 11: Schematic diagram of the hot tear rig<sup>50</sup>.

Viano et al. used this test rig to investigate hot tearing in Al-Cu alloys<sup>50</sup>. The temperature and load recorded as a function of time are shown in Figure 12. The first derivative of the load is also plotted to determine the point where load begins to develop. Figure 13 shows load recorded at solidus temperature as a function of solute content.



a) 0.25 wt% Cu

b) 4 wt% Cu

Figure 12: Temperature and load development as a function of time<sup>50</sup>.

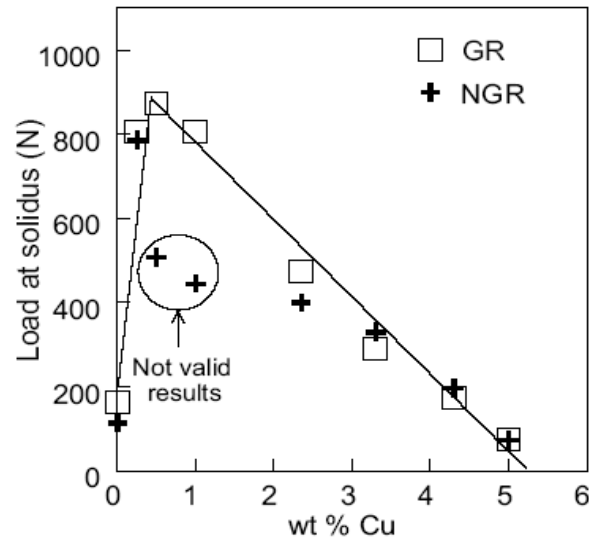


Figure 13: Load recorded at solidus T as a function of solute content<sup>50</sup>.

More recently, Davidson et al. modified the hot tear test rig developed by Instone to directly observe the hot spot region during solidification<sup>17</sup>. A mold lid with a glass window is located



directly above the hot spot region. A video camera was used to record the images of the hot spot region during solidification. By this technique, it is possible to observe the initiation and propagation of the tear.

Based on the idea suggested by Novikov<sup>3</sup>, Eskine et al. developed an apparatus to measure the linear contraction of alloys upon solidification<sup>51,52</sup>. The diagram of the setup is shown in Figure 14. It consists of a T-shaped mold which is made of graphite and a moving block which can slide in horizontal directions along the mold cavity. A connection screw is embedded into the moving block and is used to attach the solidifying metal. A linear displacement sensor (linear variable differential transformer (LVDT)) was attached to the moving wall from the outside to measure the linear displacement of the solidified shell of the casting. Stangeland et al. measured the linear solidification contraction using this set up and related the experimental results to thermal strain, which causes hot tearing<sup>53</sup>.

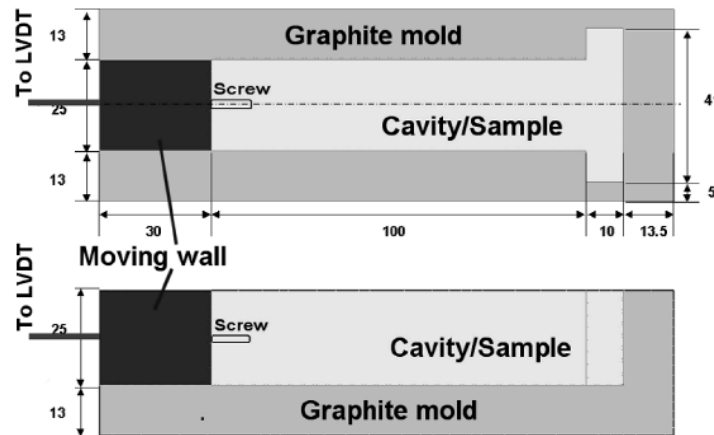


Figure 14: Diagram of the casting mold with a moving wall<sup>52</sup>.

Cao et al. developed an instrumented constrained rod casting method for quantitatively analyzing hot tearing and used it in studying the Mg-Al and Mg-Al-Ca alloys<sup>54</sup>. The experimental set-up is shown in Figure 15. It consisted mainly of a steel mold, a load cell, and a thermocouple. The bottom rod was connected to the load cell at one end and a thermocouple was buried at the junction area between the rod and the sprue, near the potential place of the crack. The mold was equipped with a graphite pouring cup with a graphite sleeve to maximize test reproducibility and a graphite felt to minimize the interference of the rising tension near the sprue end of the rods. Bottom pouring crucible and gas protection were used to ensure a consistent pouring head each

time and no contamination.

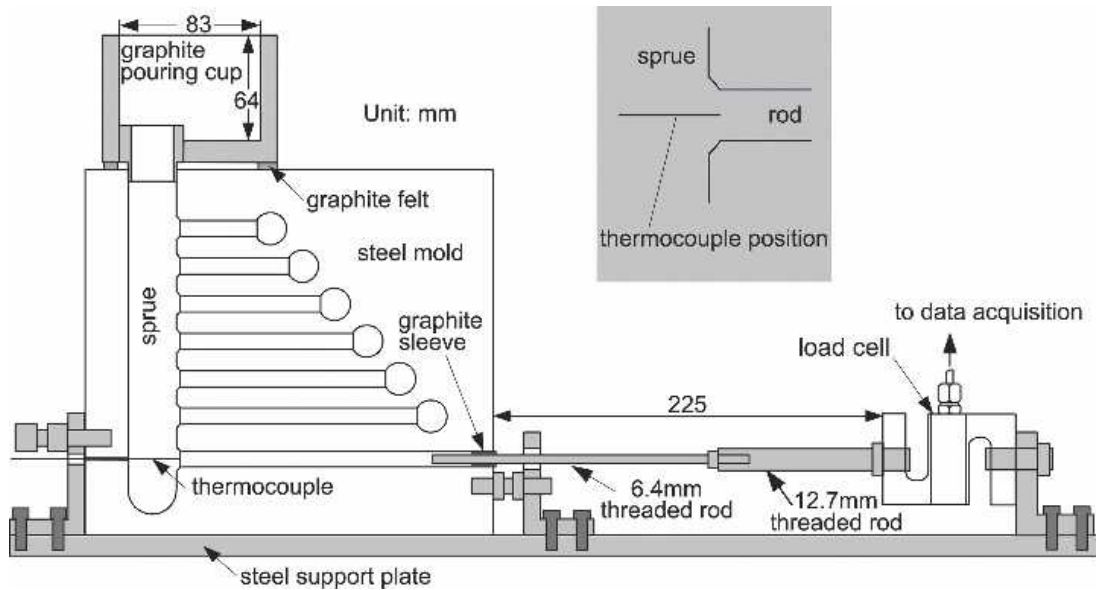


Figure 15: Schematic of the instrumented constrained rod testing apparatus<sup>54</sup>.

The hot tearing susceptibility was evaluated based on the crack width, rod length and crack location. They correlated the load and cooling vs. time curve to hot tearing and said the load and cooling curves reflected the phase formation and crack onset, healing, propagation and the final crack width. The crack onset time and temperature can be determined from the load curve and its first derivative.

Their study found that the higher (larger) the freezing temperature range, the higher the hot tearing susceptibility. The element Ca had a significant effect on the susceptibility of ternary Mg-Al-Ca alloys to hot tearing. In Mg-4Al-yCa alloys, the crack susceptibility decreases sharply as the Ca content (y) increases from 0 to 2.5 %. The susceptibility of Mg-xAl-2.5Ca to hot tearing did not change significantly as the Al content (x) increased from 4 to 6%.

Zhen et al. developed a system and used it in studying Mg-Al alloys<sup>55</sup>. Figure 16 shows a schematic of the experimental setup. It consists of a constrained rod steel mold, a contraction force measurement system with a load cell, and a data acquisition system. The principle of the test is to measure the contraction force induced by solidification and thermal shrinkages to monitor the evolution of hot tearing. When a hot tear occurs during solidification, the induced contraction force is accordingly released. A drop can be observed on the force curve. The

behavior of hot tearing can then be investigated by analyzing force development. This includes the initiation of hot tearing, the evolution and the final size of the hot crack and so on. Their mold design minimized the friction between the solidifying casting and the inner wall of the mold and thus eliminated the error in measuring contraction force. The operation procedure was that once the casting started the force measurement system was activated. The force, temperatures of the mold at different positions including at the hot spot area were recorded. They used total volume value as the measure of hot tearing severity. With this method they studied the influence of mold temperature and found that increasing mold temperature decreased hot tearing susceptibility. The contraction force curves also indicated that the liquid refilling played an important role in partially or completely healing the cracks.

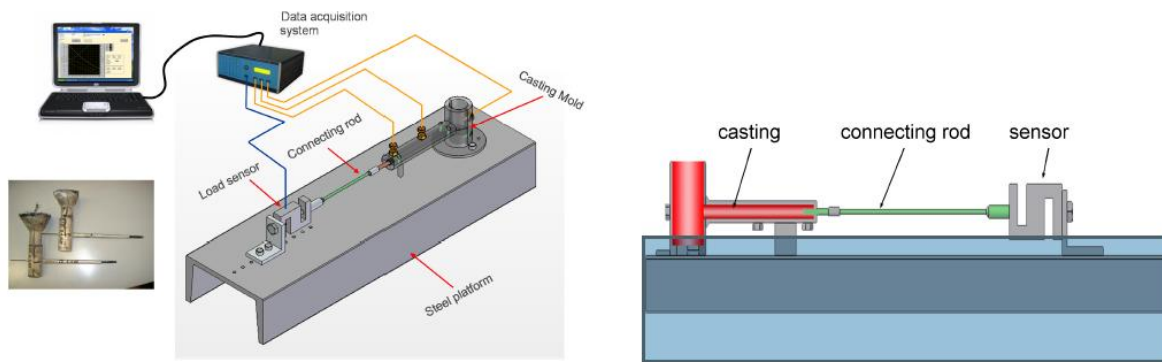


Figure 16: Schematic of the experimental setup by Zhen<sup>55</sup> et al.

## 5. Hot Tearing Criteria and Models

It is of practical importance to be able to predict hot tearing in casting. Efforts have been made for decades to develop hot tearing criteria and models and implement them into casting simulation. Based on the theories of hot tearing formation mechanism, the hot tearing criteria can be classified into following groups<sup>5</sup>: 1) strain-based criteria, 2) stress-based criteria, 3) strain rate-based criteria, and 4) criteria based on nonmechanical principles.

An extensive review of hot tearing criteria<sup>5</sup> was done by Eskin et al. in 2004 and “a quest for a new hot tearing criterion<sup>56</sup>” was recently presented. It was pointed out most of the criteria can successfully predict the hot tearing susceptibility of some binary alloys for their composition sensitivity, i.e. the so called lambda curve showing the maximum susceptibility for a certain composition range. However, the results are not satisfying when consideration is given to other

process parameters. Moreover, none of the existing model can predict whether hot tearing will occur or not. A generic reliable hot tearing prediction model is still not available. It is suggested that the mechanisms of nucleation and propagation of a crack should be considered when developing new hot tearing model and criterion<sup>56</sup>. On the other hand, the limitation of the existing models suggests the need for reliable quantitative input data, which are not easily available and need to be measured experimentally.

A summary of the hot tearing criteria are given at the end of the paper as Appendix. The reader is referred to the excellent reviews<sup>5, 56</sup> and the references listed in the table for more detailed information.

## **6. Concluding Comments**

Much work on hot tearing has been done over the years and resulted in copious information and the establishment of mechanisms, which revealed the nature of hot tearing. It is a complex phenomenon that involves heat flow, melt flow and mass flow, and stress/strain development in the coherent network. Its occurrence is well recognized to be a result of combined thermo-mechanical and metallurgical interactions. In this work, a chronological review of hot tearing theories, the affecting variables and recently developed hot tearing test methods have been presented. The important area of hot tearing model and simulation was not covered in this paper. Only a summary of hot tearing criteria (equations) is provided at the end of the paper.

Though the basic knowledge associated with hot tearing are established and understood, a globally reliable standard hot tearing test method is still not available. Moreover, none of the existing model can predict whether hot tearing will occur or not. A generic reliable hot tearing prediction model is still not available. Reliable quantitative measurement of hot tearing as well as reliable modeling and prediction of the problem will be of great value to the casting industry.

## **7. Acknowledgements**

The authors gratefully acknowledge the member companies of the Advanced Casting Research Center (ACRC) for their support of this work, and for their continued support of research focused on the science and technology of metal casting at Worcester Polytechnic Institute.

## 8. References

1. Monroe, C., and Beckermann, C., "Development of a Hot Tear Indicator for Steel Castings," *Materials Science and Engineering A*, vol. 413-414, pp. 30-36. (2005)
2. Campbell, J., 1991, "Castings," Oxford: Butterworth-Heinemann.
3. Novikov, I. I., "Goryachelomkost Tsvetnykh Metallov i Splavov (Hot Shortness of Non-Ferrous Metals and Alloys)," pp. 299. (1966)
4. Sigworth, G. K., "Hot Tearing of Metals," *AFS Trans*, vol. 104, pp. 1053-1062. (1996)
5. Eskin, D. G., Suyitno, and Katgerman, L., "Mechanical Properties in the Semi-Solid State and Hot Tearing of Aluminum Alloys," *Progress in Materials Science*, vol. 49, pp. 629-711. (2004)
6. Metz, S. A., and Flemings, M. C., "A Fundamental Study of Hot Tearing," *AFS Trans*, 78, pp. vol. 453-460. (1970)
7. Körber, F., and Schitzkowski, G., "Determination of the Contraction of Cast Steel," *Stahl Und Eisen*, vol. 15, pp. 128-135. (1928)
8. Briggs, C.W., 1946, McGraw-Hill, (London), pp. 317-338.
9. Middleton, J. M., and Protheroe, H. T., "The Hot-Tearing of Steel," *Journal of the Iron and Steel Institute*, vol. 168, pp. 384-397. (1951)
10. Briggs, C. W., and Gezelius, R. A., "Studies on Solidification and Contraction in Steel Castings II-Free and Hindered Contraction of Cast Carbon Steel," *AFA Trans*, vol. 42, pp. 449-476. (1934)
11. Briggs, C. W., and Gezelius, R. A., "Studies on Solidification and Contraction in Steel Castings IV-the Free and Hindered Contraction of Alloy Cast Steels," *AFA Trans*, vol. 44, pp. 1-32. (1936)
12. Ver ö J., "The Hot-Shortness of Aluminum Alloys," *The Metals Industry*, 48, pp. 431-434, 442. (1936)
13. Pumphrey, W. I., and Jennings, P. H., "A Consideration of the Nature of Brittleness at Temperature above the Solidus in Castings and Welds in Aluminum Alloys," *J. Inst. Metals*, vol. 75, pp. 235. (1948)
14. Bishop, H. F., Ackerlind, C. G., and Pellini, W. S., "Metallurgy and Mechanics of Hot Tearing," *AFS Trans*, vol. 60, pp. 818-833. (1952)
15. Pellini, W. S., "Strain Theory of Hot Tearing," *Foundry*, vol. 80, pp. 125-199. (1952)

16. Bishop, H. F., Ackerlind, C. G., and Pellini, W. S., "Investigation of Metallurgical and Mechanical Effects in the Development of Hot Tearing," AFS Trans, vol. 65, pp. 247-258. (1957)
17. Davidson, C., Viano, D., Lu, L., StJohn, D., "Observation of Crack Initiation during Hot Tearing," International Journal of Cast Metals Research, vol. 19, pp. 59-65. (2006)
18. Saveiko, V. N., "Theory of Hot Tearing," Russian Castings Production, vol. 11, pp. 453-456. (1961)
19. Rosenberg, R. A., Flemings, M. C., and Taylor, H. F., "Nonferrous Binary Alloys Hot Tearing," AFS Trans, vol. 69, pp. 518-528. (1960)
20. Clyne, T. W., and Davies, G. J., "A Quantitative Solidification Test for Casting and an Evaluation of Cracking in Aluminium-Magnesium Alloys," The British Foundrymen, vol. 68, pp. 238-244. (1975)
21. Pumphrey, W. I., and Lyons, J. V., "Cracking during the Casting and Welding of the More Common Binary Aluminum Alloys," J. Inst. Met., vol. 118, pp. 439-455. (1948)
22. Upadhyaya, G., Cheng, S., and Chandra, U., "A Mathematical Model for Prediction of Hot Tears in Castings," Light Metals, pp. 1101-1106. (1995)
23. Chamberlain, B., and Watanabe, S., "A Natural Aging Aluminum Alloy, Designed for Permanent Mold use," AFS Trans, vol. 85, pp. 133-142. (1977)
24. Sigworth, G. K., Rios, O., Howell, J., Kaufman, M., "Development Program on Natural Aging Alloys," AFS Trans, vol. 112, pp. 387-408. (2004)
25. Dodd, R. A., Pollard, W. A., and Meier, J. W., "Hot Tearing of Magnesium Casting Alloys," AFS Trans, vol. 65, pp. 100-118. (1957)
26. Spittle, J. A., and Cushway, A. A., "Influence of Superheat and Grain Structure on Hot-Tearing Susceptibilities of Al-Cu Alloy Castings," Metals Technology, vol. 10(1), pp. 6-13. (1983)
27. Fortier, M., Lahaine, D. J., Bouchard, M., Langlais, J., "Mold Surface Roughness Effects on the Microstructure and the Hot Tearing Strength for an Al-4.5% Wt Cu Alloy," Light Metals. (2001)
28. Sadayappan, M., Sahoo, M., Shkuka, M., Yang, B.J. and Smith, R.W., "Effect of Melt Processing and Magnetic Field on the Hot Tearing of Al-Cu Alloy A201," AFS Trans, vol. 110, pp. 407-415. (2002)

29. Easton, M., Wang, H., Grandfield, J. StJohn, D. and Sweet, E., "An Analysis of the Effect of Grain Refinement on the Hot Tearing of Aluminum Alloys," *Materials Science Forum*, vol. 28, pp. 224-229. (2004)
30. Easton, M., Grandfield, J., StJohn, D., Rinderer, B., "The Effect of Grain Refinement and Cooling Rate on the Hot Tearing of Wrought Aluminum Alloys," *Materials Science Forum*, vol. 30, pp. 1675-1680. (2006)
31. Warrington, D., and McCartney, D. G., "Hot-Cracking in Aluminum Alloys 7050 and 7010 – a Comparative Study," *Cast Metals*, vol. 3(4), pp. 202-208. (1991)
32. Matsuda, F., Nakata, K., and Shimokusu, Y., "Effect of Additional Element on Weld Solidification Crack Susceptibility of Al-Zn-mg (Report I)," *Transactions of JWRI*, vol. 12(1), pp. 81-87. (1983)
33. Singer, K., and Benek, H., "Contribution to Hot Tears in Steel Castings," *Stahl and Sisen*, vol. 51, pp. 61-65. (1931)
34. Bichler, L., Elsayed, A., Lee, K., "Influence of Mold and Pouring Temperatures on Hot Tearing Susceptibility of AZ91D Magnesium Alloy," *International Journal of Metalcasting*, vol. 2(1), pp. 43-54. (2008)
35. Couture, A., and Edwards, J. O., "The Hot-Tearing of Copper-Base Casting Alloys," *AFS Trans*, vol. 74, pp. 709-721. (1966)
36. Zhen, Z., Hort, N., Utke, O., "Investigations on Hot Tearing of mg-Al Binary Alloys by using a New Quantitative Method," *Magnesium Technology*. (2009)
37. Limmaneevichitr, C., Saisiang, A., and Chanpum, S., "The Role of Grain Refinement on Hot Crack Susceptibility of Aluminum Alloy Permanent Mold Castings," *Proceedings of the 65th World Foundry Congress*. (2002)
38. Lin, S., "A Study of Hot Tearing in Wrought Aluminum Alloys" PhD thesis, University of university of Quebec at Chicoutimi, Chicoutimi (1999)
39. Hall, H. F., "The Strength and Ductility of Cast Steel during Cooling from the Liquid State in Sand Mold," *Journal of the Iron and Steel Institute*, vol. 15, pp. 65-93. (1936)
40. Singer, A. R. E., and Jennings, P. H., "Hot-Shortness of the Aluminium-1043 Silicon Alloys of Commercial Purity," *J. Inst. Metals*, vol. 72, pp. 197-211. (1946)
41. Oya, S., Hanma, U., Fujii, J., "Evaluation of Hot Tearing in Binary Al-Si Alloy Castings," *Aluminium*, vol. 60(20), pp. 777. (1984)

42. Paray, F., Kulunk, B., and Gruzleski, J. E., "Hot Tearing in 319 Alloy," *Int. J. Cast Metals Res.*, vol. 13, pp. 147-159. (2000)
43. Gamber, E. J., "Hot Cracking Test for Light Metal Casting Alloys," *AFS Trans*, vol. 67, pp. 237-241. (1959)
44. Singer, A. R. E., and Jennings, P. H., "Properties of the Al-Si Alloys at Temperatures in the Region of the Solidus," *J. Inst. Metals*, vol. 73, pp. 33. (1947)
45. Langlais, J., and Gruzleski, J. E., "A Novel Approach to Assessing the Hot Tearing Susceptibility of Aluminum Alloy," *Materials Science Forum*, vol. 331-337, pp. 167-172. (2000)
46. Hamaker, J. C., and Wood, W. P., "Influence of Phosphorus on Hot Tear Resistance of Plain and Alloy Gray Iron," *AFS Trans*, vol. 60, pp. 501-510. (1952)
47. Guven, Y. F., and Hunt, J. D., "Hot-Tearing in Aluminum Copper Alloys," *Cast Metals*, vol. 1(2), pp. 104-111. (1988)
48. Taumura, H., Kato, N., Ochiai, S., Katagiri, Y., "Cracking Study of Aluminum Alloys by the Variable Tensile Strain Hot Cracking Test," *Trans. Jpn. Welding Soc.*, vol. 8(2), pp. 63-69. (1977)
49. Instone, S., StJohn, D., and Grandfield, J., "New Apparatus for Characterizing Tensile Strength Development and Hot Cracking in the Mushy Zone," *International Journal of Cast Metals Research*, vol. 12(6), pp. 441-456. (2000)
50. Viano, D., StJohn, D., Grandfield, J., C áceres, C., "Hot Tearing in Aluminium-Copper Alloys," *Light Metals*. (2005)
51. Eskine, D., Zuidema, J. J., and Katgerman, L., "Linear Solidification Contraction of Binary and Commercial Aluminium Alloys," *Int. J. Cast Metals Res.*, vol. 14, pp. 217-224. (2002)
52. Eskin, D. G., Suyitno, Mooney J.F., Katgerman, L., "Contraction of Aluminum Alloys during and After Solidification," *Metallurgical and Materials Transactions A*, vol. 35A, pp. 1325-1335. (2004)
53. Stangeland, A., Mo, A., Dielsen, Ø., Eskin, D., M'Hamdi, M., "Development of Thermal Strain in the Coherent Mushy Zone during Solidification of Aluminum Alloys," *Metallurgical and Materials Transactions A*, vol. 35A, pp. 2903-2915. (2004)
54. Cao, G., and Kou, S., "Hot Tearing of Ternary mg-Al-Ca Alloy Castings," *Metallurgical and Materials Transactions A*, vol. 37A, pp. 3647-3663. (2006)



55. Zhen, Z., Hort, N., Huang, Y., "Quantitative Determination on Hot Tearing in mg-Al Binary Alloys," *Materials Science Forum*, vol. 618-619, pp. 533-540. (2009)
56. Eskin, D. G., and Katgerman, L., "A Quest for a New Hot Tearing Criterion," *Metallurgical and Materials Transactions A*, vol. 38A, pp. 1511-1519. (2007)
57. Suyitno, Kool, W. H., and Katgerman, L., "Evaluation of Mechanical and Non-Mechanical Hot Tearing Criteria for DC Casting of an Aluminum Alloy," *Light Metals*, pp. 753-758. (2003)
58. Dickhaus, C. H., Ohm, L., and Engler, S., "Mechanical Properties of Solidifying Shell of Aluminum. Alloys," *AFS Trans*, vol. 101, pp. 677. (1994)
59. Lahaie, D. J., and Bouchard, M., "Physical Modeling of the Deformation Mechanisms of Semisolid Bodies and a Mechanical Criterion for Hot Tearing," *Metallurgical and Materials Transactions B*, vol. 32B, pp. 697. (2001)
60. Williams, J. A., and Singer, A. R. E., "Deformation, Strength, and Fracture above the Solidus Temperature," *J. Inst. Met.*, vol. 96, pp. 5-12. (1968)
61. Zhao, L. Y., Baoyin, Wang, N., Sahajwalla, V. and Pehlke, R.D., "The Rheological Properties and Hot Tearing Behavior of an Al-Cu Alloy," *Int. J. Cast Metals Res.*, vol. 13(3), pp. 167-174. (2000)
62. Suyitno, Kool, W. H., and Katgerman, L., "Hot Tearing Criteria Evaluation for Direct-Chill Casting of an Al-4.5 Pct Cu Alloy," *Metallurgical and Materials Transactions A*, vol. 36A, pp. 1537-1546. (2005)
63. Magnin, B., Maenner, L., Katgerman, L., "Ductility and Theology of an Al-4.5%Cu Alloy from Room Temperature to Coherency Temperature," *Mater Science Forum*, vol. 1209, pp. 217-222. (1996)
64. Prokhorov, N. N., "Resistance to Hot Tearing of Cast Metals during Solidification," *Russian Castings Production*, vol. 2, pp. 172-175. (1962)
65. Rappaz, M., Drezet, J.-M., and Gremaud, M., "A New Hot Tearing Criterion," *Metallurgical and Materials Transactions A*, vol. 30A, pp. 449-455. (1999)
66. Braccini, M., Martin, C. L., Su éry, M., Br échet, Y., "Modeling of Casting," *Welding and Advanced Solidification Processes IX*, Aachen, pp. 18-24. (2000)
67. Clyne, T. W., and Davies, G. J., "*Solidification and Casting of Metals*," *Proc. Conf. on Solidification and Castings of Metals*, Anonymous Metals Society, pp. 275-278. (1979)

68. Katgerman, L., "A Mathematical Model for Hot Cracking of Aluminum Alloys during DC Casting," J. of Metals, vol. 34, pp. 46-49. (1982)
69. M'Hamdi, M., Mo, A, Fjær, H.G., "TearSim: A Two-phase Model Addressing Hot Tearing Formation during Aluminum Direct Chill Casting," Metallurgical and Materials Transactions A, vol. 37A, pp. 3069-3083. (2006)

**Appendix: Summary of Hot Tearing Criteria and Models [5, 57]**

Classification	Author(s)	Mathematical Expression	Comments	References
<b>Stress-based Criteria</b>	Novikov	$\sigma_{fr} = 2\gamma / b$	$\sigma_{fr}$ : the fracture stress $\gamma$ : the surface tension $b$ : the film thickness	[3]
	Dickhaus et al.	$F_z = \frac{3\pi\eta R^4}{8t} \left( \frac{1}{b_1^2} - \frac{1}{b_2^2} \right)$ $b = \frac{(1-f_s)d}{2}$	$F_z$ : the force required to increase the film thickness from $b_1$ to $b_2$ $\eta$ : the dynamic viscosity $R$ : the radius of a plate $t$ : the time required to increase the film thickness from $b_1$ to $b_2$ $f_s$ : the fraction of solid $d$ : the average thickness of a solidifying grain	[58]
	Lahaie & Bouchard	$\sigma_{fr} = \frac{4\eta}{3b} \left( 1 + \left( \frac{f_s^m}{1-f_s^m} \right) \varepsilon \right)^{-1}$	$m=1/3$ : equiaxed structure $m=1/2$ : columnar structure	[59]
	Langlais & Gruzleski	$HTS=1 / \text{the maximum tensile strength}$	$HTS$ : hot tearing susceptibility	[45]
	Williams & Singer	$\sigma_{fr} = \sqrt{\frac{8G\gamma}{\pi(1-\nu)A V_L^{1/2}}}$ Modified equation: $\sigma_{fr} = \sqrt{\frac{16G\gamma}{\pi(1-\nu)} \left[ \frac{1}{0.07D + 0.47AV_L^{1/2} + 0.37D^{1/2}V_L^{1/4}} \right]}$	$\sigma_{fr}$ : the fracture stress $A$ : a constant dependent on grain size and the dihedral angle $G$ : the shear modulus $\gamma$ : the effective fracture surface energy $V_L$ : the volume of liquid $\nu$ : Poisson's ratio	[60]

Strain-based Criteria	Novikov	$P_r = \frac{S}{\Delta T_{br}}$ <p>If <math>\varepsilon_p</math> and <math>\varepsilon_{sh}</math> curves cross in the brittle temperature range,</p> $P_r = \frac{S_1 - S_2}{\Delta T_{br}}$	<p><math>P_r</math>: reserve of plasticity in the solidification range  <math>\Delta T_{br}</math>: the brittle temperature range  S: the difference between the average integrated value of the elongation to failure (<math>\varepsilon_p</math>) and the linear shrinkage/contraction (<math>\varepsilon_{sh}</math>)  <math>S_1</math>: the area between the (<math>\varepsilon_p</math>) and (<math>\varepsilon_{sh}</math>) curves.  <math>S_2</math>: is the area in which in the (<math>\varepsilon_p</math>) and (<math>\varepsilon_{sh}</math>) curves cross in the brittle temperature range.</p>	[3, 57, 61, 62]
	Magnin et al.	$HCS = \frac{\varepsilon_{\theta\theta}}{\varepsilon_{fr}}$ <p>If <math>HCS &gt; 1</math>, a hot tear will develop.</p>	<p><math>\varepsilon_{\theta\theta}</math>: the circumferential plastic strain at solidus temperature  <math>\varepsilon_{fr}</math>: the experimentally determined fracture strain, close to solidus temperature</p>	[63]
	Prokhorov	$\frac{\Delta \varepsilon_{res}}{BTR} = \frac{D_{min} - (\Delta \varepsilon_{free} + \Delta \varepsilon_{app})}{BTR}$ $\varepsilon_{res} = \varepsilon_{min} - \varepsilon_{free} - \varepsilon_{app}$ <p>If <math>\varepsilon_{res} \leq 0</math>, a hot tear will form.</p>	<p><math>BTR</math>: the brittle temperature range  <math>D_{min}</math>: the minimum fracture strain in <math>BTR</math>  <math>\Delta \varepsilon_{res}</math>: the reserve of hot tearing strain  <math>\Delta \varepsilon_{free}</math>: the free thermal contraction strain  <math>\Delta \varepsilon_{app}</math>: the actual strain in the solidifying body</p>	[5, 64]

<b>Strain rate-based criteria</b>	Rappaz, Drezet, and Gremaud  (RDG Criterion)	$\Delta p = \Delta p_{sh} + \Delta p_{mec} + \rho gh = \frac{180\mu\Delta T}{G\lambda_2^2} \left[ v_T \beta A + \frac{(1+\beta)B\varepsilon\Delta T}{G} \right] + \rho gh$ $A = \frac{1}{\Delta T} \int_{T_{end}}^{T_{mf}} \frac{f_s^2 dT}{(1-f_s)^2}$ $B = \frac{1}{\Delta T} \int_{T_{end}}^{T_{mf}} \frac{f_s^2 \cdot F_s(T)}{(1-f_s)^3} dT$ $F_s(T) = \frac{1}{\Delta T} \int_{T_{end}}^T f_s dT$ <p>If <math>\Delta p &gt; \Delta P_c</math>, a hot tear will occur.  <math>\Delta p_c = 2 KPa</math></p>	<p><math>\Delta p</math>: the depression pressure over mush  <math>\Delta p_{sh}</math> &amp; <math>\Delta p_{mec}</math>: the pressure drop contributions in the mush associated with the solidification shrinkage and the deformation induced fluid flow  <math>\mu</math>: dynamic viscosity of the liquid phase  <math>G</math>: thermal gradient  <math>\lambda_2</math>: dendrite arm spacing  <math>v_T</math>: casting velocity  <math>\beta</math>: solidification shrinkage factor  <math>\varepsilon</math>: viscoplastic strain rate  <math>F_s</math>: volume fraction of solid  <math>T_{end}</math>: temperature at which bridging of the dendrite arms between grains occurs  <math>T_{mf}</math>: mass feeding temperature</p>	[62, 65]
	Braccini et al.	$\dot{\varepsilon}^c = \left( 1 - \frac{e}{l} \right) \left[ \frac{\lambda - a}{\lambda} \left( \frac{\frac{2}{3} P_C - P_M}{K(T, f_s)} \right) \right]^{1/m} + \frac{e}{l} \frac{2\kappa}{(\lambda - a)^2} \frac{P_C}{\eta_L}$ $P_C = \frac{4 \cos \theta \sigma_{lv}}{e}$ $P_M = \bar{\rho} gh$ $\bar{\rho} = \rho_l f_l + \rho_s f_s$ $\kappa = \frac{e^2}{32} (1 - f_s) (f_s^c - f_c)^{1.3}$	<p><math>\dot{\varepsilon}^c</math>: critical strain rate for hot tearing  <math>e</math>: liquid film thickness  <math>l</math>: gage length  <math>a</math>: length of the tear  <math>P_C</math>: cavitation pressure  <math>P_M</math>: metallostatic pressure  <math>K</math>: a constitutive parameter that is a function of T and <math>f_s</math>  <math>m</math>: strain-rate sensitivity  <math>k</math>: permeability of the mushy zone  <math>\eta_L</math>: viscosity of the liquid  <math>h</math>: distance below the melt level  <math>f_s^c</math>: solid fraction at which the liquid network becomes disconnected</p>	[66]

	Stangeland, Mo, and Eskin	$\dot{\varepsilon}_s^{th} = \frac{1}{3} \Psi(g_s) \beta_T \dot{T} I \quad \text{with} \quad \text{for } g_s \leq g_s^{th}$ $\Psi(g_s) = \begin{cases} 0 & \text{for } g_s > g_s^{th} \\ \left( \frac{g_s - g_s^{th}}{1 - g_s^{th}} \right)^n & \end{cases}$	$\dot{\varepsilon}_s^{th}$ : thermal strain rate in the mushy zone that may cause hot tearing $\beta_T$ : volumetric thermal expansion coefficient $\dot{T}$ : cooling rate, $I$ : the identity tensor $g_s$ : solidification fraction, $g_s^{th}$ : solid fraction at onset of contraction, $n$ : a material parameter.	[53]
	M'Hamdi, Mo, Fjaer	$\Delta\varepsilon(w_v, w_d) = \begin{cases} 0 & \\ \int_{t(p_l=p_c)}^{(g_s=g_s^{nof})} \left( w_v \cdot \text{tr}(\dot{\varepsilon}_s^p) + w_d \cdot \dot{\varepsilon}_s^p \right) dt & \end{cases} \quad (1) \quad (2)$ <p>(1) for <math>p_l(g_s = g_s^{nof}) \geq p_c</math>  (2) for <math>p_l(g_s = g_s^{nof}) &lt; p_c</math>  if <math>\Delta\varepsilon &gt; \Delta\varepsilon_c</math>, hot tearing occurs</p>	$\Delta\varepsilon$ : the effective tearing strain, which is a measure of the hot tearing susceptibility $p_l$ : are liquid pressure, $p_c$ : critical pressure, $g_s$ : volume fraction of solid in the mushy zone, $g_s^{nof}$ : solid fraction when no continuous film exist, $\Delta\varepsilon_c$ : critical value	[69]
	Feurer	$SPV = \frac{f_l^2 d^2 P_s}{24\pi c^3 \eta L^2}$ $P_s = P_o + P_M - P_C$ $P_M = \bar{\rho} gh$ $\bar{\rho} = \rho_l f_l + \rho_s f_s$ $P_C = \frac{4\gamma_{SL}}{\lambda_2}$	$SPV$ : maximum volumetric flow rate(feeding term) through a dendritic network $SRG$ : volumetric solidification shrinkage $d$ : the secondary dendrite arm spacing $P_s$ : the effective feeding pressure $P_o, P_M, \text{ and } P_C$ : atmospheric, metallostatic, and capillary pressure, respectively.	[62]

<b>Criteria based on other principles</b>		$SRG = \left( \frac{\partial \ln V}{\partial t} \right) = - \frac{1}{\rho} \frac{\partial \bar{\rho}}{\partial t}$ <p>If <math>SPV &lt; SRG</math>, hot tearing is possible.</p>	<p><math>L</math>: the length of porous network  <math>c</math>: the tortuosity constant of dendrite network  <math>\eta</math>: the viscosity of the liquid phase</p>	
	Clyne & Davies	$HCS = \frac{t_v}{t_R} = \frac{t_{99} - t_{90}}{t_{90} - t_{40}}$	<p><math>t_v</math>: vulnerable time period (hot tearing susceptibility)  <math>t_R</math>: time available for stress relief process (mass feeding and liquid feeding)  <math>t_{99}</math>: the time at the solid fraction <math>f_s=0.99</math></p>	[67]
	(Modified) Clyne & Davies	$CSC^* = \frac{t_v}{t_r} (\Delta T) g_s$	<p><math>g_s</math>: grain size  <math>\Delta T</math>: solidification range</p>	
	Katgerman	$HCS = \frac{t_{99} - t_{cr}}{t_{cr} - t_{40}}$	<p><math>t_{cr}</math>: determined using Feurer's criterion when <math>SPV=SRG</math></p>	[68]

# Characterization of Hot Tearing in Al Cast Alloys:

## *methodology and procedures*

### **Abstract**

Hot tearing is perhaps the pivotal issue defining castability. It is affected by alloy composition as well as processing conditions and variables. Hot tearing is a complex phenomenon in that it lies at the intersection of heat flow, fluid flow and mass flow. Over the years many theories and models have been proposed and accordingly many tests have been developed. Unfortunately many of the tests that have been proposed are qualitative in nature. The need exists for a simple, reliable and repeatable quantitative test to evaluate hot tearing. MPI and CANMET MTL- both members of the Light Metal Alliance joined forces to address this need. A quantitative hot tearing test was developed and the methodology is presented and discussed. Application results utilizing the apparatus for alloy A356 and M206 are presented and discussed. A protocol and standardized procedures that can be adapted by the metal casting industry is presented.

**Keywords:** Hot tearing, Aluminum cast alloys, Test apparatus, Quantitative measurement, Contraction

### **1. Introduction**

Hot tearing, also referred to as hot cracking and solidification cracking, is a common and severe defect that occurs during solidification in aluminum alloy castings.<sup>1</sup> It is generally believed that hot tearing is a complex phenomenon linked to the inadequate liquid feeding to compensate solidification shrinkage and the accumulation of thermally induced stresses/strain during solidification contraction. When the stress exceeds the strength of the mush<sup>2</sup> and not enough liquid metal is available to fill the incipient cracks hot tearing is observed. Once it occurs, the casting has to be repaired or to be scraped, which result in significant productivity loss. It is desirable in industry to have a reliable test, which can be used to predict the susceptibility of various alloys and evaluate the effects of process parameters and casting geometries on hot tearing.<sup>3</sup>



Over the years, much effort has been devoted to understanding the fundamentals of hot tearing. Many theories have been proposed and can be mainly summarized into two categories. One group of theories considers the metallurgical factors related to the role of liquid feeding or interdendritic liquid film in the mush during solidification.<sup>4-6</sup> The other group of theories is based on stress and strain. It is thought hot tearing is associated with thermally induced stress/strain caused by non-uniform cooling.<sup>7-10</sup> In fact, hot tearing is a complex phenomenon that involves both of the metallurgical and mechanical factors.

In addition to the theoretical investigations, researchers have developed various tests to evaluate hot tearing tendency. Among these tests, the I-beam or dog bone type tests and ring mold tests are the classical tests<sup>11</sup>, which do have certain limitations. The severity of hot tearing is usually measured by either the length or width of the crack; nevertheless, only a qualitative index can be obtained from such tests for assessing hot tearing tendency. Eskin et al. published an excellent review that covers various methods of evaluating hot tearing tendency.<sup>11</sup> Many other researchers have carried out extensive work in this area on a variety of systems and also in an attempt to quantitatively evaluate and investigate hot tearing behavior.<sup>12-18</sup>

In parallel, mathematical models have been pursued for hot tearing,<sup>19-24</sup> and these have been useful in our understanding of the nature of the problem. Most of the criteria can successfully predict the hot tearing susceptibility of some binary alloys for their composition sensitivity, i.e. the so called lambda ( $\lambda$ ) curve showing the maximum susceptibility for a certain composition range. However, the results are not satisfying when consideration is given to other process parameters. Moreover, none of the existing model can predict whether hot tearing will occur or not. A generic reliable hot tearing prediction model is still not available.<sup>11,15</sup> The limitation of the existing models suggests the need for reliable quantitative input data, which are not easily available and need to be measured experimentally.

The objectives of this project are to develop a simple quantitative test that can be used by both industry and the research laboratory and use the test to evaluate alloy and processing variables affecting hot tearing of Al based casting alloys. This paper will focus on the test development. The team at MPI in USA and CANMET in Canada has collaborated on the development of such a foundry test that is easy to use and yield quantitative data. Compared with the test apparatus

developed earlier by Instone et al. which was designed to simulate the DC casting process where two solidification fronts met at the center of the casting and the load was generated in the semi-solid region at the center,<sup>15</sup> the test method presented in this study is to reproduce shape casting processes. Both tests were designed to measure the contraction force and temperature during the casting solidification and relate them to the formation of hot tearing. The differences were in the mold and apparatus designs, thus the solidification patterns, the parameter controlled, and the consideration of affecting factors etc. The apparatus developed in this project has been successfully used in quantitatively determining the effects of various parameters (mold temperature, pouring temperature and grain refinement) on hot tearing of different alloys. The main purpose of this paper is to give a detailed description of the design and working principles of the apparatus and present the methodology of result analysis. Its applications on studying the effects of processing variables will be presented in other papers.

## **2. Universal Hot Tearing Apparatus**

### Instrumented Constrained Rod Mold:

The strains and stresses imposed on the solid network in the mush are induced by solidification and thermal contraction. The deformation behavior is very critical for the development of hot tearing. In order to study the solidification and deformation behavior of cast aluminum alloys, an instrumented constrained rod mold was developed. The mold was designed to simultaneously measure the load/time/temperature developed during solidification for a restrained casting or shrinkage (contraction)/time/temperature for a relaxed casting. The details and development considerations on the setup is given below.

Fig. 1 is a schematic diagram showing the components of the apparatus. An exploded view of the mold plate assembly is shown in Fig. 2. Two different molds are available, one made of copper and the other made of H13 steel. The results presented in this paper were carried out using H13 mold. The mold temperature is controlled precisely with heat plates. Different casting configurations and dimensions can be obtained by using different inserts (shown in Fig. 2). The casting used in this study is shown in Fig. 3. The test piece has two arms. The arms were designed with a slight taper to reduce friction between the mold and casting. One arm is constrained at one end with a steel bolt, which is embedded in the end of the casting. This end

section will solidify first and fast because of the embedded lower temperature bolt. A graphite stopper anchors the bolt. Because the bolt cannot move, this structure keeps the arm from contraction; this causes tension development and hence cracking may be induced during solidification. The other arm is used for temperature and load/displacement measurements. This end is connected to a rod, which has one end embedded in the arm and the other end connected to a load cell (Loadstar iLoad Pro Analog 500lb.) or linear variable differential transformer (LVDT, Macro Sensors HSTA 750-1000). The accuracy of both load cell and LVDT is 0.25% of full-scale output. The LVDT is unrestrained and can move horizontally and freely (Fig. 4) while the load cell will offer a resistance (Fig. 5) to the contraction and may cause cracking in the casting. Two K-type thermocouples are used for the temperature measurement of the casting. One is positioned at the riser end ( $T_1$ ) where hot tears were expected to occur and the other at the end of the rod ( $T_2$ ) as shown in Fig. 4 and 5. The mold was closed by a hydraulic system under consistent pressure for each test.

After pouring the melt into the mold, temperatures and load/displacement were recorded by a PC-based NI (National Instrument) data acquisition system. The system consists of SCXI-1303 terminal block, PCI-6043E interface card and LabVIEW software (DASYLab). The data was acquired at a rate of 200HZ. The whole experimental setup was shown in Fig. 6.

The parameters affecting hot tearing that can be controlled in the test are casting size, alloy composition, casting temperature, mold temperature and grain refiner addition.

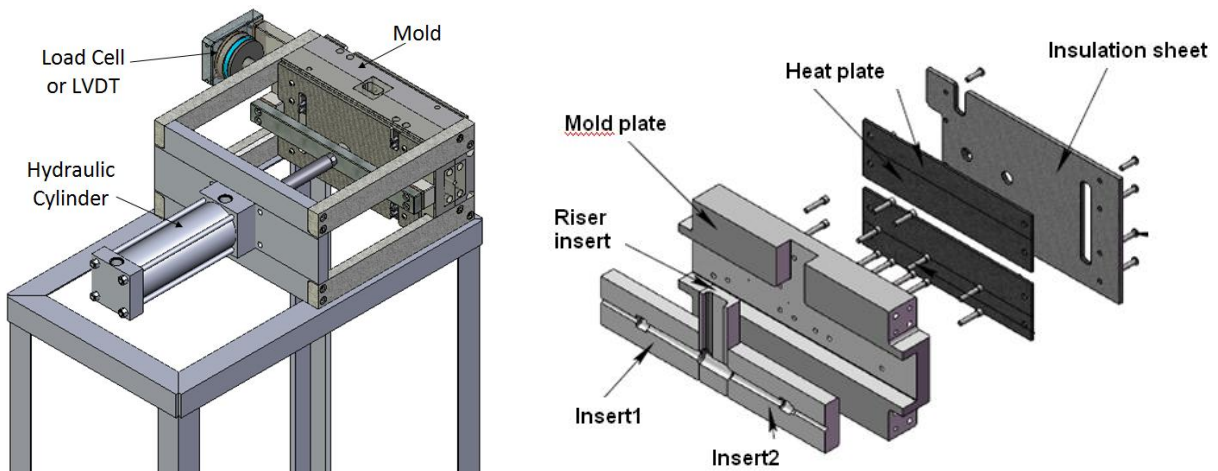


Fig. 1: Mold assembly

Fig. 2: Exploded view of mold plate assembly

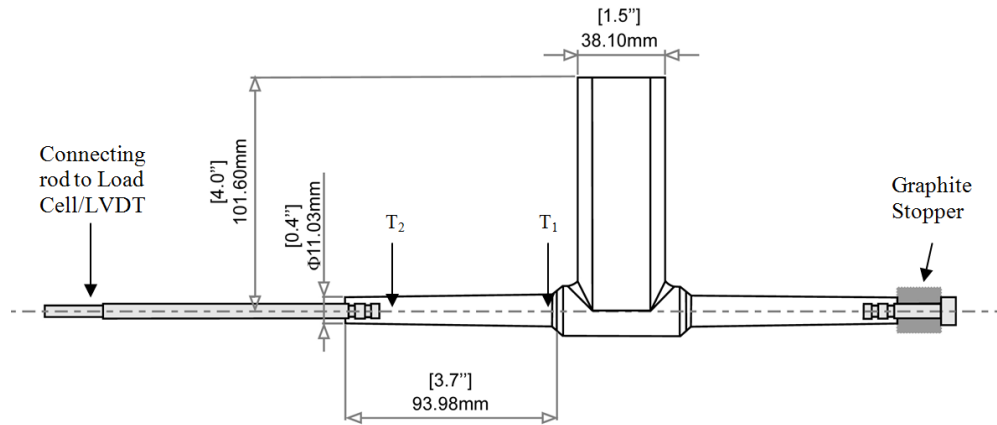


Fig. 3: The dimensions of the casting

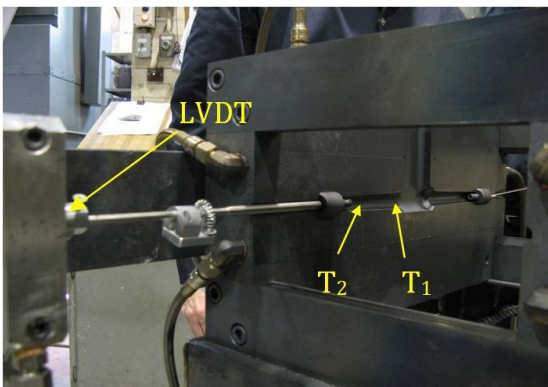


Fig. 4: LVDT set-up

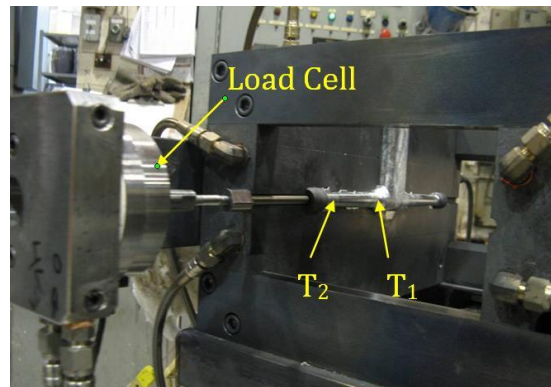


Fig. 5: Load cell set-up



Fig. 6: Experimental set-up

### 3. Experimentation

The experiment presented in this paper is the one for calibrating, evaluating, and fine-tuning the apparatus, and setting up the procedures for operation and the methodology for interpreting the data. The results presented in this paper are also set as the reference for further study of other affecting factors for comparison.

#### A. Tested alloys

Aluminum casting alloys A356 and 206 were selected as model alloys. As is well known, alloy A356 is widely used in industry for many applications due to its high mechanical strength, ductility and fatigue resistance. It has excellent fluidity making it easy to cast and resists hot tearing. It is selected as the reference alloy for comparison, since it is considered the ideal case. Alloy 206 has excellent mechanical properties and high temperature strength and is used today for automotive and aerospace industries. However, it is widely recognized as being difficult to cast, mainly because of its susceptibility to hot tearing. For the experiments, commercial Al-Si alloy A356.2 ingots was used, but Al-Cu alloy 206 used in this study was purposely modified slightly that it did not contain Ti; grain refiner was added later to study the effects of grain refinement. The base 206 alloy was made using commercial pure Al, Al-50%Cu, Al-25%Mg and

Al-50%Mn master alloys and was tagged as M206. The chemical compositions of A356 and M206 were measured using a spark emission spectrometer and are given in Table 1. It can be observed that a very low level of Ti (0.006%) was detected in M206.

Table 1: Chemical composition of alloy M206 and A356 (wt %)

Alloy	Si	Fe	Cu	Mn	Mg	Ti	Al
M206	0.05	0.05	4.55	0.36	0.25	0.006	Bal.
A356.2	6.70	0.06	<0.01	<0.001	0.38	0.14	Bal.

### B. Melting and process parameters

Melting was conducted in an induction furnace and the melt was well degassed with argon using a rotating impeller degasser for 30 minutes before pouring. Graphite lubricant spray was applied to the mold to reduce the friction between the mold wall and the casting and facilitate the removal of casting from the mold. The mold was preheated to  $300 \pm 2$  °C before pouring. The pouring temperatures for both alloys are at 100 °C above their liquidus, respectively. The castings were extracted from the mold after full solidification and then examined for cracks. No grain refinement was applied during these tests. Each test was repeated for 5-7 times. It was found that when the temperatures/load or temperatures/displacement were measured at the same time the temperature measurement would interfere the others, since the thermocouples placed inside the casting would add resistance to the casting contraction. So temperature data was then measured separately in parallel tests. After acquiring the data, the cooling curve, load vs. time curve and displacement vs. time were processed to obtain critical information about solidification process and hot tearing formation.

### C. Microstructure

Four samples were sectioned from the specimen for each set of tests for microstructure examination (Fig. 7). One sample was cut at the riser end of the constrained test arm (left in the figure) and its transverse cross section was examined for microstructure including the DAS and/or grain size. The entire arm, which is connected to load cell or LVDT, and the conjunction region were precisely sectioned into three pieces (for easy sample preparation) in the axial direction. These samples were used for characterizing hot tears (their morphology, width, length

and locations) and microstructures. All the samples are cold mounted in epoxy, ground and polished following standard procedures. The dendrite arm spacing and/or grain size were measured using standard linear intercept method.

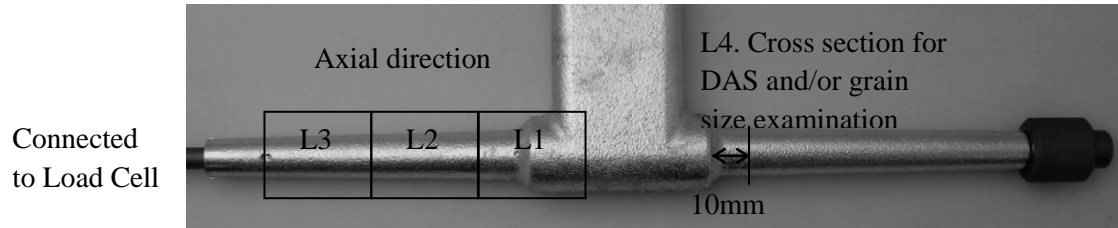


Fig. 7: Sample locations for microstructure examination

#### 4. Results and Discussion

##### A. Load (contraction force), displacement and temperature measurements

The temperature, load and displacement recorded during casting of A356.2 and M206 are shown in Fig. 8 and 9, respectively. The load represents the tensile force developed in the rod during cooling due to solidification shrinkage and thermal contraction, and the displacement represents the linear contraction when the rod was relaxed. Two temperatures were measured at locations  $T_1$  (riser side) and  $T_2$  (edge) as shown in Fig. 3, 4 and 5, at the centerline of the constrained rod. The temperatures at the surface of the rod were also recorded in parallel test. In the data and curves the time zero was normalized to correspond to the moment when thermocouple 1 starts to react the increase of the temperature upon pouring. The first derivatives of load/displacement with respect to time were calculated and presented, which is the rate of load/displacement increase and pictorially demonstrates the change in the curve. In both of load and displacement measurements, slight decrease in the reading were observed shortly after pouring, possibly due to the melt pressure head.

The solidification related data derived from the cooling curves are presented in Table 2. Cooling rate is determined using the total solidification range divided by the corresponding solidification time. Dendrite coherency points listed in the table were adopted from reference 25 for comparison purpose. It refers to the temperature or fraction solid when the individual dendrites first impinge upon their neighbors.

The important load and linear displacement data of A356 of M206 are summarized in Table 3 and 4. Fig. 8(a) shows the measured temperatures and load recorded in casting as a function of time for alloy A356 at mold temperature of 300°C. From Fig. 8(b), it is observed that the contraction load started to develop noticeably at 8.6 seconds (contraction onset point) and increased with time during entire cooling process, the solidification period and beyond. The load curve is perfectly smooth and no noticeable changes (except the inflection point) are reflected in the first derivative curve, which suggests no hot tears occurred during solidification. At this load onset point, the temperature at the centerline of the rod ( $T_{C1}$  at riser side) was around 561°C, in which the solid fraction was around 0.89 according to the calculations using Pandat Scheil simulation. The temperature near the end of the casting ( $T_{C2}$ ) was around 449°C; at which the casting end was firmly solidified. According to Backerud et al.,<sup>25</sup> when alloy A356.2 is solidified at a cooling rate of 0.6°C, coherency is achieved around 610°C and the fraction solid is 0.21. There is a considerable difference between the coherency point measured by Backerud et al.<sup>25</sup> and the load onset point measured by this experiment. This suggests the solid network started transferring tensile forces at a very late stage of solidification, though a continuous dendritic network formed at a relatively early stage. However, it should be noticed the alloy compositions were very close but cooling rate was higher in this test. After the rod was completely solid (472°C), the rod contracted approximately linearly upon cooling.

Fig. 8(d) shows the measured displacement and its first derivative with respect to time for alloy A356. It is observed that shrinkage/contraction started at around 6.5 seconds and increased rapidly during solidification and cooling. At 6.5 seconds, the temperature of  $T_{C1}$  was 575°C, in which the solid fraction was around 0.47. From the cooling data, solidification was complete at around 39.8 seconds. The total linear shrinkage/contraction (displacement) of the solidification range was around 0.44mm compared to the effective length of the rod of 75mm. The maximum displacement rate was 0.033 mm s<sup>-1</sup>. It is noticed the displacement developed before the non-equilibrium eutectic temperature was so small (Table 4), which suggests that there is almost no strain developed before this point.

Fig. 10(a) is a mosaic optical micrograph showing the longitudinal cross section of the neck region (hot spot) for A356 load measurement specimen. No hot tears were seen in the critical region. Fig. 10(b) shows the dendritic structure of A356 and the measured dendrite arm space is 18.7 μm.



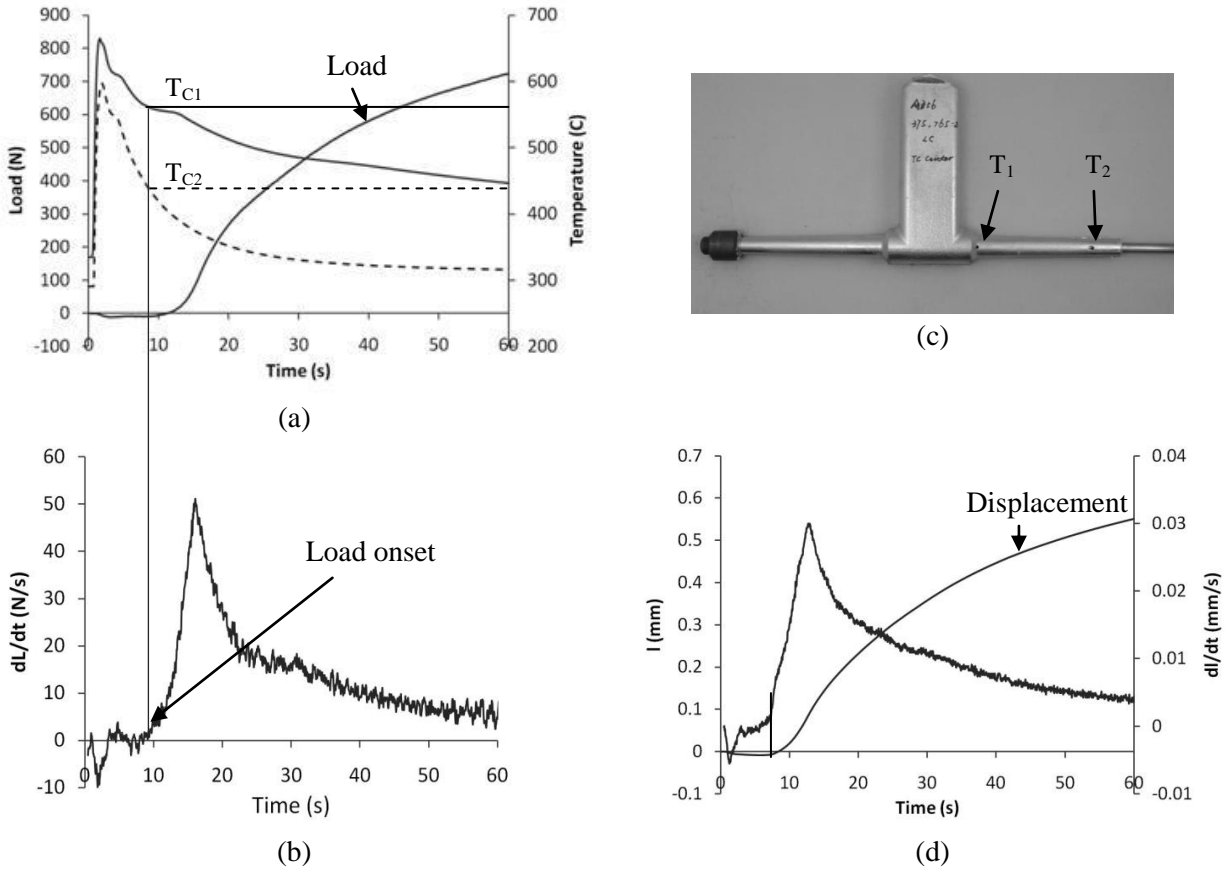


Fig. 8: (a) Temperatures and load development as a function of time of A356,  $T_{C1}$  and  $T_{C2}$  are thermocouples located at centerline of the rod defined in Fig. 3; (b) Derivative of load vs. time curves; (c) Photograph of the constrained casting showing thermocouple locations; (d) Measured displacement and its derivative as a function of time.

Table 2: Solidification characteristics data

Alloy	$T_1$ (°C)	$T_{nes}$ (°C)	$\Delta T$ (°C)	Cooling rate (°C s <sup>-1</sup> )	SDAS ( $\mu\text{m}$ )	Dendrite coherency point <sup>25</sup> (°C)/ $f_s$
A356	615	472	143	3.85	18.7	610/ 0.21
M206	647	485	164	5.13	22.4	641/ 0.30

$T_l$ : liquidus,  $T_{nes}$ : non-equilibrium solidus,  $\Delta T$ : solidification range,  $f_s$ : fraction of solid

Table 3: Contraction force (load) measurement data

Alloy	Load onset temp./ $f_s$ (°C)/ $f_s$		Maximum loading rate (N s <sup>-1</sup> )	Cracking initiation temp. (°C) / $f_s$		Major crack temp. (°C) / $f_s$		Load at $T_{nes}$ (N)
	$T_{CI}/f_s$	$T_{SFI}/f_s$		$T_{CI}$	$T_{SFI}$	$T_{CI}$	$T_{SFI}$	
A356	561/0.89	487/-	51	No crack	No crack	No crack	No crack	578
M206	601/0.80	530/0.976	36	562/0.885	518/0.98	544/0.90	508/0.99	360

$T_{CI}$ : temperature at the center of the rod,  $T_{SFI}$ : temperature at the surface of the rod.

Table 4: Linear displacement measurement data

Alloy	Onset temp. ( $T_{CI}$ )/ $f_s$ (°C)/ $f_s$	Displacement at $T_{eu}$ (mm)	Displacement at $T_{nes}$ (mm)	Displacement at cracking initiation (mm)	Displacement at major cracking (mm)	Maximum displacement rate (mm s <sup>-1</sup> )
A356	575/0.47	-0.0079	0.44	No Crack	No Crack	0.033
M206	636/0.42	0.31	0.67	0.21	0.27	0.048

$T_{eu}$ : eutectic temperature

The load and displacement measurement results of M206 are shown in Fig. 9. The load started to develop rapidly at 6.8 seconds and increased with time. When the load started the temperature at the centerline of the rod ( $T_{CI}$ ) is 601°C and the solid fraction is about 0.80. In the first derivative curve of the load shown in Fig. 9(b), a slight decrease was first observed at 10.1 seconds. This indicated that hot tearing initiated. At this point the corresponding loading rate reached 36N s<sup>-1</sup>. The temperature at the centerline of the rod ( $T_{CI}$ ) was 562°C and at the surface of the casting ( $T_{SFI}$ ) was 518°C. The corresponding fraction solids at those temperatures were 0.885 and 0.98 respectively (Pandat Scheil calculation). It suggests that hot tearing formed in the eutectic temperature range. In the micrograph showing cracks in the hot spot region (Fig. 10b), it appears that hot tear initiated at the surface of the casting and propagated towards the center. The nucleation of hot tear may be caused by surface curvature against a non-wetted mold.<sup>10</sup> The curve and data show that shortly after the tear initiation, a slight increase in the rate was seen at about 11.1 seconds, which suggests cracking might stop or partially filled by remaining liquid. On the other hand, the connected solidified part was gaining strength during cooling. Right after the slight increase, the load rate dropped abruptly from 33N s<sup>-1</sup> at about 12.5 seconds to 10N s<sup>-1</sup>

at 16.6 seconds. The temperatures of  $T_{C1}$  and  $T_{SF1}$  at 12.5 seconds are  $544^{\circ}\text{C}$  and  $508^{\circ}\text{C}$ , respectively, at which the corresponding fraction solids are 0.9 and 0.99 (Pandat Scheil calculation). This abrupt rate decrease suggests that the load increase was stopped and significant cracking (the first major crack) occurred/propagated suddenly. In Fig. 10(b), we can see two major cracks (one at the top and one at bottom) initiated from the surface and propagated towards the center and stopped at some lengths. The two cracks might start at the same or nearly the same time. The width of bottom crack was slightly smaller than that of the top crack, possibly due to the gravity effect. A small internal crack can be seen at the left. Such internal cracks can be caused by internal folded-oxides.<sup>10</sup> It can also be observed that there are many minor “filled” cracks around the two major cracks and all the cracks seem to follow the intergranular paths. These tears might be the incipient cracks but filled by remaining liquid considering there was still a large amount of liquid around in the early stage. From the first derivative curves, a short unstable (variation) stage before load onset point was observed. This would represent the process of “tearing” and “filling” at the early stage. Photographs of the constrained casting showing hot tearing locations are shown in Fig. 9(c). All cracks formed in the hot spot in the neck region, the general stress concentration area.

Fig. 9(d) shows the measured displacement and its first derivative as a function of time for alloy M206. It is observed that shrinkage/contraction started at around 4.9 seconds and increased rapidly during and after solidification. At 4.9 seconds, the temperature of  $T_{C1}$  is  $636^{\circ}\text{C}$  and the solid fraction is around 0.42. The data and the curves show that the solidification was complete at around 37 seconds. The total linear shrinkage/contraction (displacement) in the solidification range is around 0.67mm out of the effective rod length of 75mm and the maximum displacement rate is  $0.048\text{ mm s}^{-1}$ , which are greater than those of A356. This displacement is expected to correlate to hot tearing susceptibility of the alloy.

For displacement measurement, there should be no obvious change in the first derivative curve, since the casting rod was relaxed. However, it was observed that the curve was not perfectly smooth around 10 to 15 seconds (Fig. 9d). This is probably due to the fact that the casting was being separated from the mold surface during this time range of solidification and that the process was not smooth. On the other hand, in the unrestrained displacement measurement samples, some minor “filled” cracks were also observed in the neck region (Fig. 11), which could cause the “un-smoothness”. However, such small “filled” cracks were not found in A356

samples. This indicates that 206 has much higher hot tearing tendency than A356. The venerable mushy zone of M206 may initiate cracks in the stress concentration area.

From the measured data, it seems that the load onset point does not necessarily correspond to the onset of LVDT movement for both A356 and M206. It appears that the load starts recording only when “tensile coherency” is achieved in the hot spot, but shrinkage/contraction can begin in the unrestrained rod and “tensile coherency” is not required.

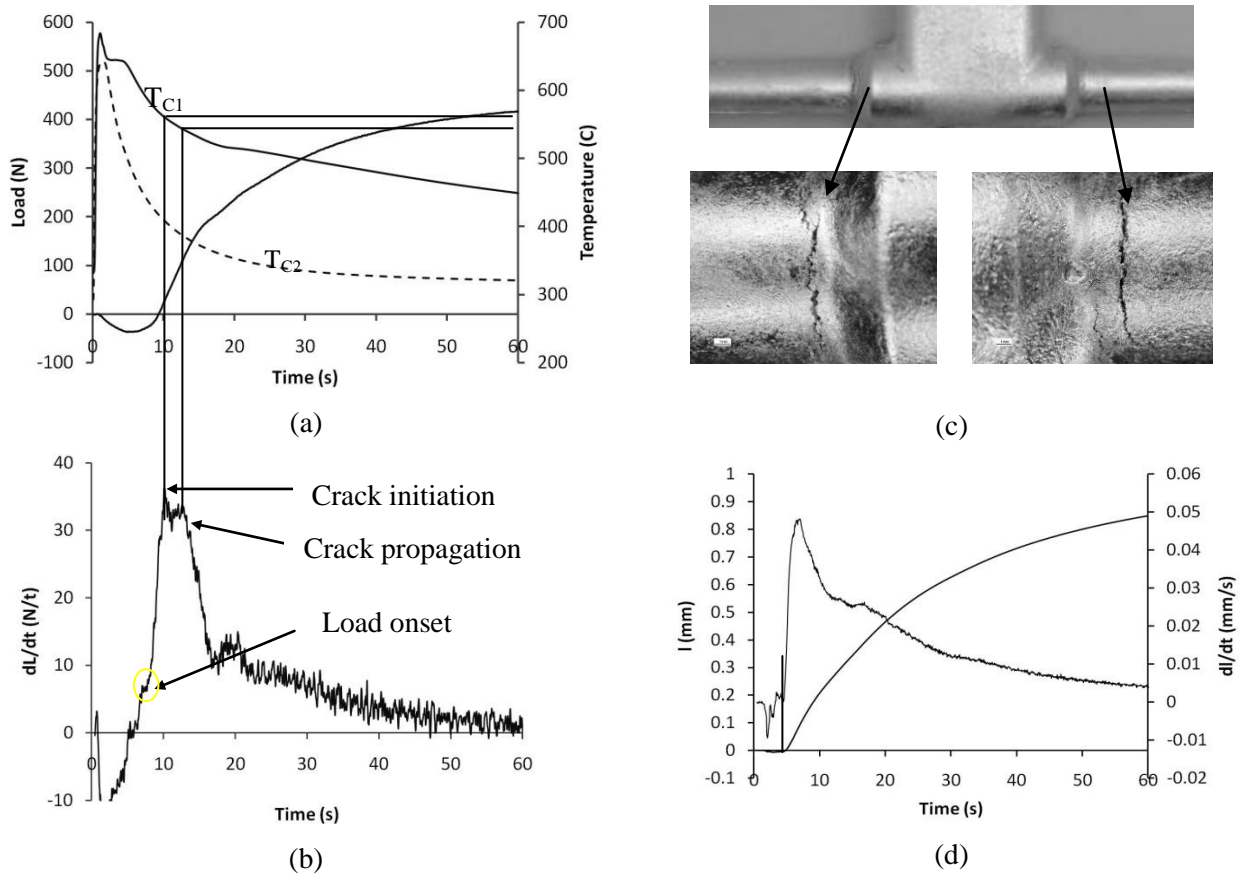


Fig. 9: (a) Temperatures and load development as a function of time for M206,  $T_{C1}$  and  $T_{C2}$  are thermocouples shown in Fig. 3 and 4; (b) Derivative of load vs. time curves; (c) Photographs of the constrained casting showing cracking locations; (d) Measured displacement and derivative of displacement as a function of time.

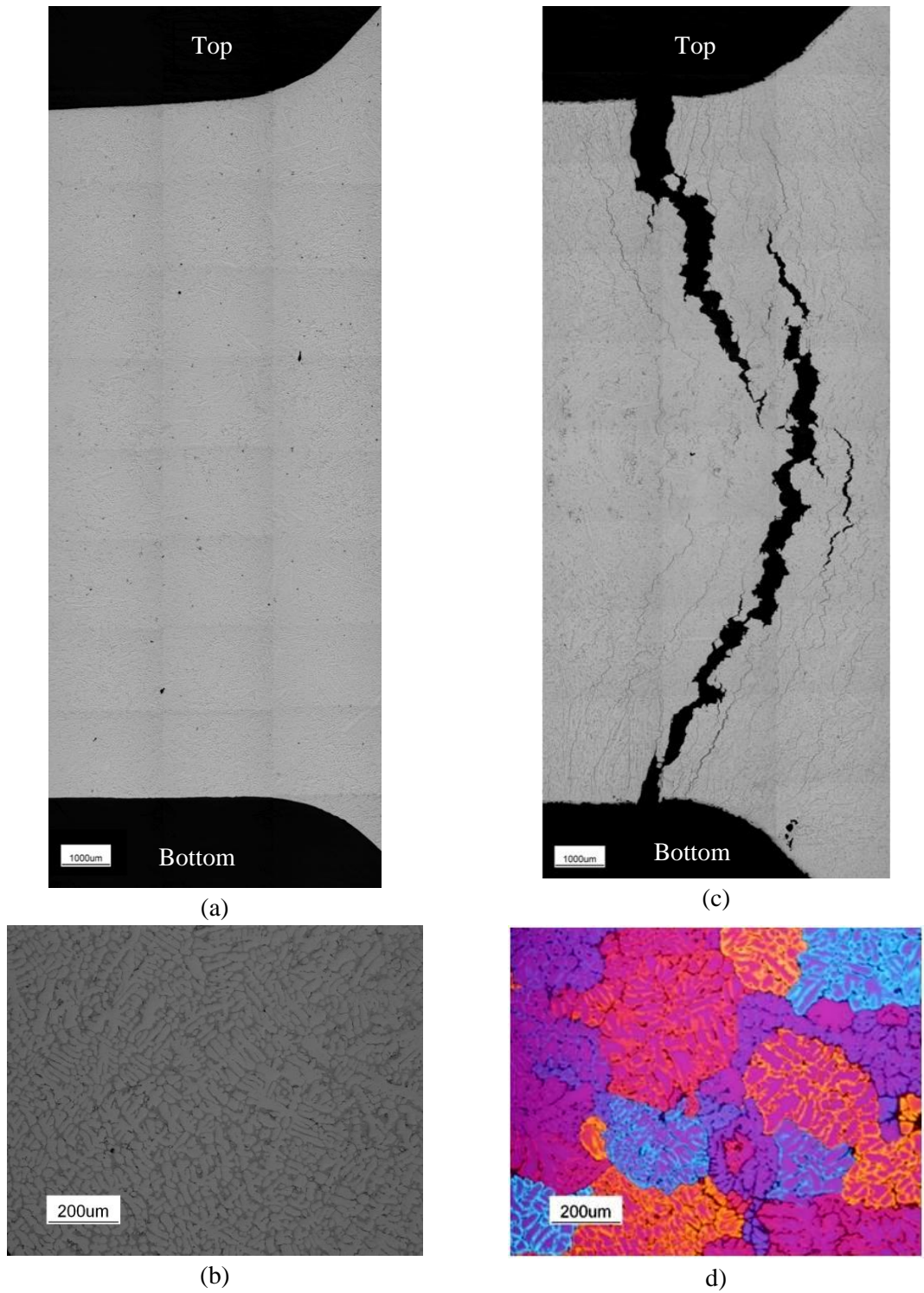


Fig. 10: (a) Mosaic optical micrograph showing the longitudinal cross section of the neck region of A356; (b) Dendritic microstructure of A356; (c) Mosaic micrograph showing hot tears in the neck region of M206; (d) Microstructure of M206 showing grain and dendritic morphology.

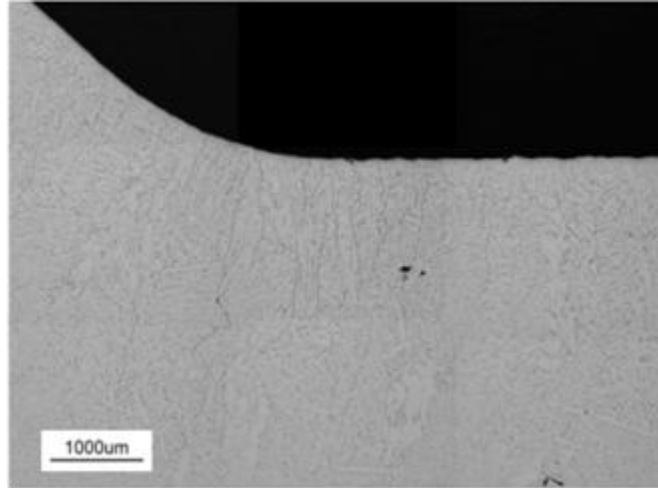


Fig. 11: Micrographs of neck region of M206 displacement measurement sample

### B. Reproducibility of the Experimental Setup

One of the objectives of this project is to develop a robust and repeatable quantitative test to evaluate hot tearing in Al cast alloys. In order to examine the reproducibility, tests were conducted under same casting conditions for A356 and M206 alloys. Fig. 12 (a) shows two load measurement results for alloy A356. Both the load curves and derivative curves coincide well with each other. The loading starting point and the maximum loading rates are close to each other. Good repeatability for displacement measurement is also shown in Fig. 12 (b).

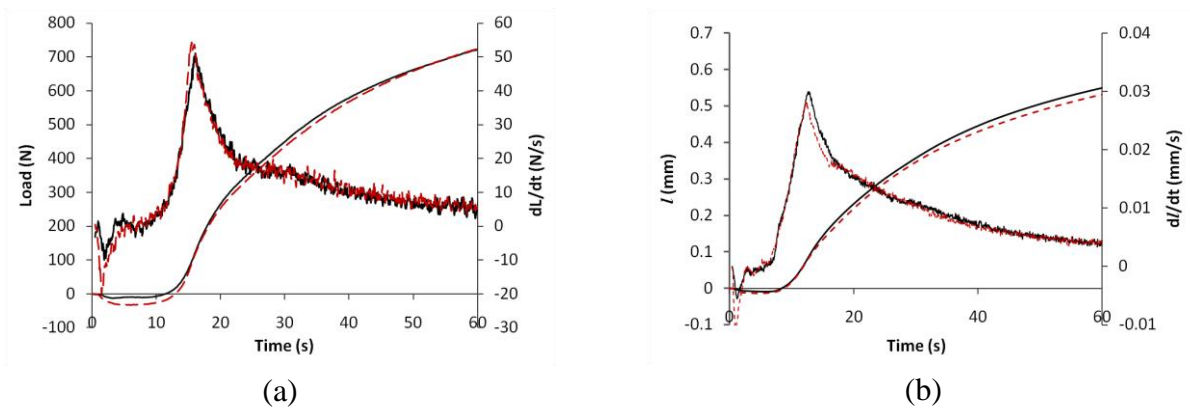


Fig. 12: Test reproducibility for hot tearing assessment of A356 (Melt temperature: 710°C, Mold temperature: 300°C). (a) Load measurement; (b) Displacement measurement.

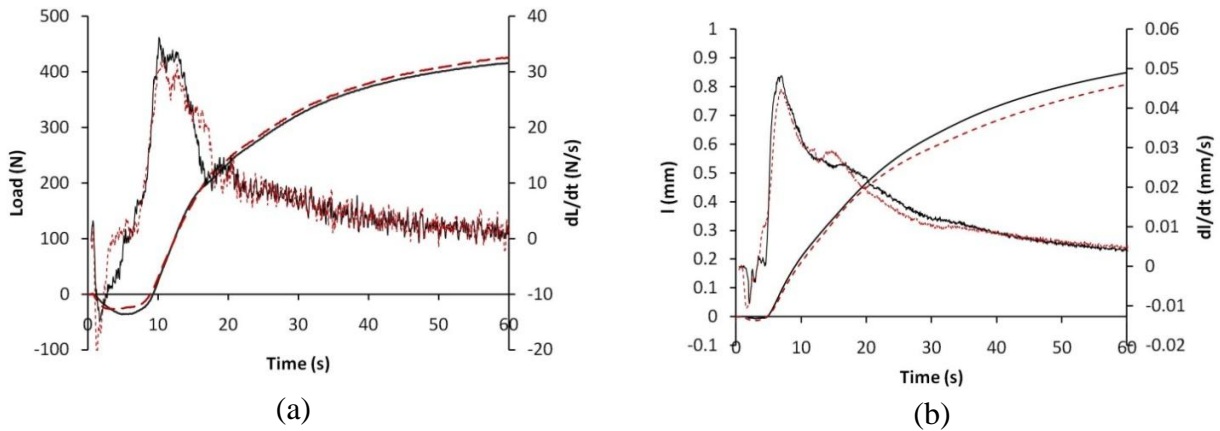


Fig. 13: Test reproducibility for hot tearing assessment of M206 (Melt temperature: 750°C, Mold temperature: 300°C). (a) Load measurement; (b) Displacement measurement.

The results for alloy M206 are shown in Fig. 13. The time and temperature of hot tearing onset and major cracks are very close. For example, the hot tearing onset temperature for test 1 (black line/curve) and test 2 (dashed red) are 562°C and 558°C, respectively. The major crack in test 1 occurred at 544°C, and it occurred at 543°C in test 2. The two temperatures are very close. Good repeatability for displacement measurement is shown in Fig. 13 (b).

## 5. Conclusions

- A quantitative method to characterize hot tearing behavior of Al alloys has been developed. The apparatus is designed to measure the contraction force/displacement and temperature developed during casting. The casting rod was designed with a slight taper to reduce friction between the mold and casting. The testing results are repeatable and reliable.
- Hot tearing is alloy dependent. Alloy A356 has high resistance to hot tearing, while M206 shows significant hot tearing tendency under the same conditions.
- The “tensile coherency” can be determined from load curve and its first derivative curve. In A356, the development of the tensile load-bearing solid network starts at about 561°C and fraction solid of 0.89. In M206, the solid network, which can transfer forces, forms at about 601°C at fraction solid of 0.80.

- The onset of hot tearing can be determined from load curve, its first derivative and temperature curve for M206. The initiation temperature at the centerline of the rod ( $T_{Cl}$ ) was 562°C and at the surface of the casting ( $T_{SF1}$ ) was 518°C, which is around the eutectic temperature range. The corresponding fraction solids at those temperatures were 0.885 and 0.98 respectively (Pandat-Scheil calculation). The propagation of hot tearing was detected from the derivative of the load curve.
- Linear shrinkage/contraction of A356 and M206 was quantitatively measured and the measured displacements are 0.44 mm and 0.67 mm out of their effective rod length of 75 mm, respectively.
- Interdendritic cracking is evident in M206. “Filled” cracks were seen around the transition area. Liquid refilling plays an important role in filling the incipient cracks.

### Acknowledgements

The authors gratefully acknowledge the member companies of the Advanced Casting Research Center (ACRC) for their support of this work, and for their continued support of research focused on the science and technology of metal casting at Worcester Polytechnic Institute. The authors also thank Jim Thomson, Geethe Nadugala and Stuart Amey of CANMET Material Technology Laboratory for their support during this work.

### References

1. D. Warrington and D.G. McCartney: *Cast Metals*, 1996, 3, 134-143.
2. C. Davidson, D. Viano, L. Lu and D. StJohn: *Int. J. Cast. Met. Res.*, 2005, 19, 59-65.
3. J. B. Mitchell, S. L. Cockcroft, D. Viano, C. Davidson, and D. StJohn: *Metall. Mater. Trans. A*, 2007, 38A, 2503-2512.
4. R. A. Rosenberg, M. C. Flemings, and H. F. Taylor: *AFS Trans*, 1960, 69, 518-528.
5. V. N. Saveiko: *Russian castings production*, 1961, 11, 453-456.
6. U. Feurer: *Giesserei-Forschung*, 1976, 28, 75-80.



7. J. Verö *The Metals Industry*, 1936, 48, 431-434.
8. W. I. Pumphrey and P. H. Jennings: *J. Inst. Metals*, 1948, 75, 235.
9. W. S. Pellini: *Foundry*, 1952, 80, 125-199.
10. J. Campbell: 'Castings'. 2nd edn, 2003, Oxford: Butterworth-Heinemann.
11. D. G. Eskin, Suyitno and L. Katgerman: *Progress in Materials Science*, 2004, 49, 629-711.
12. J. V. Eeghem and A. D. Sy: *AFS Trans*, 1965, 73, 282-291.
13. S. A. Metz and M. C. Flemings: *AFS Trans*, 1970, 78, 453-460.
14. Y. F. Guven and J.D. Hunt: *Cast Metals*, 1988, 1(2), 104-111.
15. S. Instone, D. StJohn and J. Grandfield: *Int. J. Cast. Met. Res.*, 2000, 12(6), 441-456.
16. D. Viano, D. StJohn, J. Grandfield and C. C áceres: *Light Metals*, 2005, 1069.
17. G. Cao and S. Kou: *Metall. Mater. Trans. A*, 2006, 37A, 3647-3663.
18. Z. Zhen, N. Hort, Y. Huang, N. Petri, O. Utke and K. U. Kainer: *Materials Science Forum*, 2009, 618-619, 533-540.
19. N. N. Prokhorov: *Russian Castings Production*, 1962, 2, 172-175.
20. T. W. Clyne and G. J. Davies: Proc. Conf. on 'Solidification and Castings of Metals', London, UK, 1979, 275-278.
21. I. I. Novikov, 'Goryachelomkost tsvetnykh metallov i splavov (Hot Shortness of Nonferrous Metals and Alloys)', 1966, Nauka, Moscow.
22. L. Katgerman: *J. of Metals*. 1982, 34, 46-49.
23. M. Rappaz, J.-M. Drezet, and M. Gremaud: *Metall. Mater. Trans. A*, 1999, 30A, 449-455.
24. A. Stangeland, A. Mo, M. M'Hamdi, D. Viano, and C. Davidson: *Metall. Mater. Trans. A*, 2006, 37A, 705-714.
25. L. Backerud, G. Chai and J. Tamminen: 'Solidification characteristics of aluminum alloys, Foundry alloys,' vol. 2, 1990, AFS/Skanaluminium, Sweden.

# **Why Some Aluminum Alloys Hot Tear and others do not?**

## *– Effects of mold temperature and pouring temperature*

The effects of mold temperature and pouring temperature on hot tearing formation and contraction behavior of Al-Cu alloy 206 have been studied. The experiments were conducted using a newly developed Constrained Rod Mold, which simultaneously measures the contraction force/time/temperature during solidification for the restrained casting or linear contraction/time/temperature for a relaxed casting, and hence investigate hot tearing formation in alloys. Three mold temperatures (200 to 370°C) and three pouring temperatures (superheat from 50 to 150°C) were studied and alloy A356 was used as reference for comparison. The results showed alloy A356 has high resistance to hot tearing. No hot tearing forms under three different mold temperatures, while M206 shows significant hot tearing tendency under the same casting conditions. The severity of hot tearing and linear contraction in alloy 206 decreased significantly with increasing the mold temperature. Increasing pouring temperature resulted in severer hot tearing in alloy M206, but the effect is not as significant as that of mold temperature within the stated range. The results and underlying mechanism of these effects are discussed in correlation with alloy's thermo-mechanical properties and microstructures.

### **1. INTRODUCTION**

Hot tearing is a common and severe defect that encountered during solidification of castings. It is identified as cracks, either on the surface or inside the casting. Hot tears are usually large and visible to the naked eye. Sometimes, they can be also very small and only visible under magnetic particle or penetrant inspection.<sup>[1]</sup> The main tear and its numerous minor offshoots generally follow intergranular paths and the failure surface usually reveals a dendritic morphology.<sup>[2]</sup> The subject of hot tearing has been extensively studied and many tests and techniques were developed. The studies show that hot tearing is a complex phenomenon, it lies at

the intersection of heat flow, fluid flow and mass flow, and various factors have influences on its formation. These factors include alloy composition, its solidification and thermo-mechanical characteristics, alloy treatment, casting and mold design, mold material, and process parameters etc. Over the years many theories and models have been proposed. Now it is generally accepted that hot tears would form when thermally induced stresses (strains) accumulated during solidification contraction exceed the strength of the mush <sup>[3]</sup> and liquid feeding is insufficient to fill the incipient cracks. However, the experimental results were conflicting and the opinions were contradictory on many important aspects. Moreover, the increasing demands for high performance alloys now shed more light on the importance of hot tearing study as new alloys encounter this problem and the knowledge and database are needed in the alloy developments. So, hot tearing study remains as the hot research area in the casting sector. To push this study to an advanced level, MPI teamed up with CANMET MTL developed a simple and reliable quantitative test and used it to evaluate hot tearing in Al cast alloys. The test has been used in characterizing hot tearing behavior and in studying the effects of various variables for alloys 206 and A356. The work will be presented in a series of papers. This paper will focus on studying the effect of process parameters: the melt superheat and mold temperature.

#### **A. Melt Superheat (Pouring Temperature)**

Previous experimental studies relating to the effects of superheat on hot tearing are limit and conflicting. As pointed out by Pellini, opposite opinions regarding pouring temperature were always raised at any meeting where the subject of hot tearing is discussed. <sup>[4]</sup> For example, in earlier study of hot tearing of steel, Singer et al. believed that high pouring temperature would minimize hot tearing. <sup>[5]</sup> While, Middleton et al. showed that hot tearing was likely to occur and was severer at high casting temperatures than at low temperatures. <sup>[6]</sup> These conflicting experimental results and contradictory opinions were also seen in study of non-ferrous alloys. Pumphrey et al. studied six aluminum binary alloy systems <sup>[7]</sup> and their experiments showed that at any given alloying element level the cracking susceptibility decreased with decreasing superheat. However, in the study of a magnesium alloy, AZ91D, Bichler et al. found that the variation of pouring temperature did not show significant effect. <sup>[8]</sup>

Couture et al. thought that two factors could be attributed to this controversy. <sup>[9]</sup> A higher superheat might spread the hot spot, which was expected to reduce hot-tearing tendency and high

superheat also might increase the liquid film life, which was expected to increase the tendency to hot tearing. However, Briggs thought high superheat levels can increase temperature gradients during solidification and result in the promotion of columnar dendritic growth.<sup>[10]</sup> Generally, the alloys with columnar structure have higher hot tearing tendency than the alloys with equiaxed structures in normal situations. Several studies also showed that the effects of superheat changed with different test methods and were dependent on factors such as cooling rate, presence of grain refiners, and healing phenomena, etc.<sup>[9-11]</sup>

## **B. Mold Temperature**

Mold temperature directly affects the casting cooling rate and thus the casting microstructure and performance, including hot tearing. In fact, most of studies on hot tearing, which involve mold temperature, were using it to control cooling rate or the solidification pattern, like in Clyne<sup>[12]</sup> et al. and Spittle<sup>[13]</sup> et al.'s tests. Limited work on this topic was found in the published literatures.

Bichler et al.<sup>[8]</sup> studied the effects of mold temperature on Mg alloy, AZ91D. The tests were conducted at pouring temperature of 700°C and mold temperatures from 140 to 380°C. It was found that mold temperature had significant effect on hot tearing. The severity of hot tearing decreased progressively with increasing mold temperature. The mold temperatures above 340°C were sufficient to significantly alleviate hot tears. Hot tears were eliminated for mold temperature above 380°C. They thought this was probably because that higher temperature improved feeding. Zhen et al. studied the effects of mold temperature in the range of 250 to 500°C for binary Mg-Al alloys.<sup>[14]</sup> They found that increasing the mold temperature decreased hot tearing susceptibility and the higher mold temperature led to higher crack onset temperature and longer propagation time. The mechanism they gave was that cracks were initiated under all the mold temperatures, but at higher mold temperature the cracks could be refilled by the remaining liquid and healed. This was because that higher mold temperature led to lower cooling rate, and thus a coarser microstructure. The coarser structure led to thicker and more continuous remaining liquid. This coupled with higher onset temperature made the refilling easier.

Limmaneevichitr et al. mentioned the effect of mold temperature when studying the role of grain refinement.<sup>[15]</sup> They were “quite surprising to find” that cracking were severer in lower mold temperature experiments, e.g. 220°C (compared with 250°C). However, looking at their entire

data presented, the cracking was severer only in two conditions in lower mold temperature but all seven other cases did not support their finding.

Few literatures were found in studying the effects of casting and mold temperatures on hot tearing. Different studies showed controversies about casting temperature effect but all the limit work about the effect of mold temperature showed that higher mold temperature reduces hot tearing susceptibility and gave the mechanism of better feeding and crack refilling. This study further studied these two aspects. On one hand, it aimed to clarify the controversies about pouring temperature effect and provide more and solid quantitative data for the effect of mold temperature. On the other hand, this study will look at these issues from a different angle. It will use the method developed in this project and relate the variations of casting and mold temperatures to the alloy's thermo-mechanical properties, e.g. the stress and strain development in the region prone to hot tearing to reveal their effects and underlying mechanisms.

## **2. EXPERIMENTATION**

### **A. Experimental Set-up**

The quantitative hot tearing test developed collaboratively by WPI and CANMET-MTL is used in this study. The apparatus used for the test is an Instrumented Constrained Rod Mold. It was designed and constructed to simultaneously measure the load/time/temperature during solidification for a restrained casting or shrinkage (contraction)/time/temperature for a relaxed casting. The whole set-up is shown schematically in Figure 1.

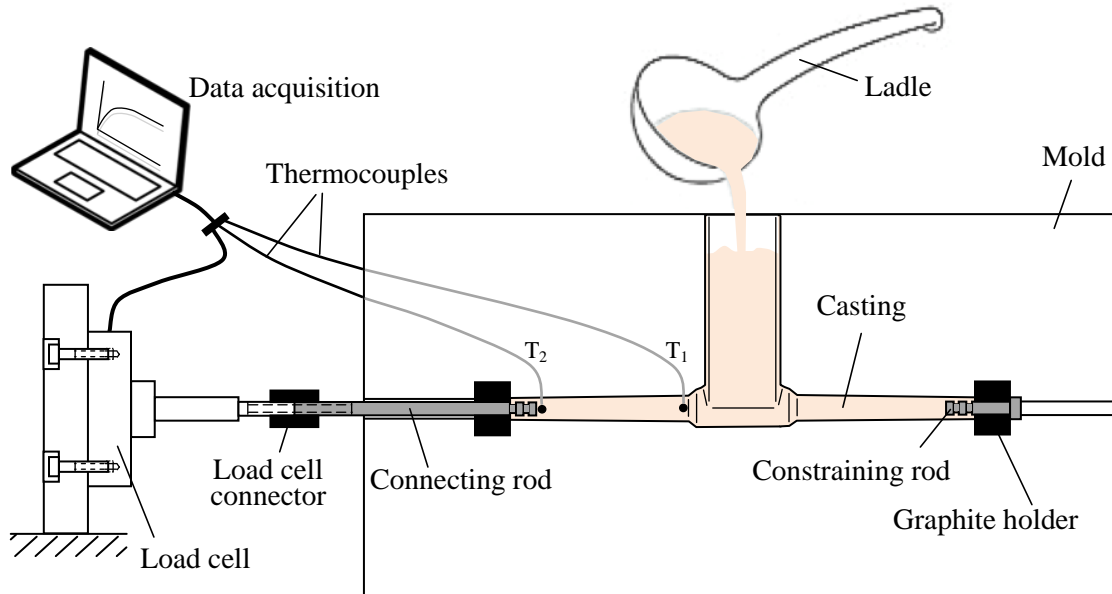


Fig. 1- Diagram of experimental set-up

The mold is made of H13 steel and consists of vertically partitioned two halves. A hydraulic device is used to open and close the mold. The test casting has two arms with a riser at the center. The arms were designed with a slight taper to reduce friction between the mold and casting during solidification. One arm (right arm in Figure 1) is constrained at the end with a steel bolt embedded in the casting. The bolt is anchored snugly by a graphite stopper. This end of casting will solidify first and fast because of the embedded bolt. Since the bolt cannot move, it will force the arm end in place without any movement and thus constrain the arm's contraction during solidification. This will cause tension development and hence may induce cracking at the latest solidified area of the arm. The other arm (left arm in Figure 1) is used for temperature and load/displacement measurements. Its end is connected to a rod, which has one end embedded in the arm and the other end connected to a load cell (Loadstar iLoad Pro Analog 500lb.) or linear variable differential transformer (LVDT, Macro Sensors HSTA 750-1000). The test casting with the embedded steel bolt and the connecting rod is shown in Figure 2. The load cell is bolted tightly on the apparatus frame to ensure no movement during casting solidification, which offers resistance to the contraction and may cause cracking in the arm while LVDT is unrestrained and can move horizontally and freely. Two K-type thermocouples are used for the temperature measurements of the casting. One is inserted to the centerline of the rod at the riser end ( $T_{C1}$ ), where hot tears were expected to occur and the other at the end of the rod ( $T_{C2}$ ) as shown in

Figures 1 and 2. The temperatures at the surfaces ( $T_{SF1}$  and  $T_{SF2}$ ) of the rods were also recorded in parallel tests.

After pouring the melt into the mold, temperatures and load/displacement are recorded by a PC-based NI (National Instrument) data acquisition system. The data was acquired at a rate of 200HZ.

The parameters affecting hot tearing that can be controlled in the test are alloy composition, casting temperature, mold temperature and grain refiner addition. A detailed description of the experimental setup for quantitatively measuring hot tearing onset and contraction during solidification of aluminum alloys can be found elsewhere.<sup>[16]</sup>

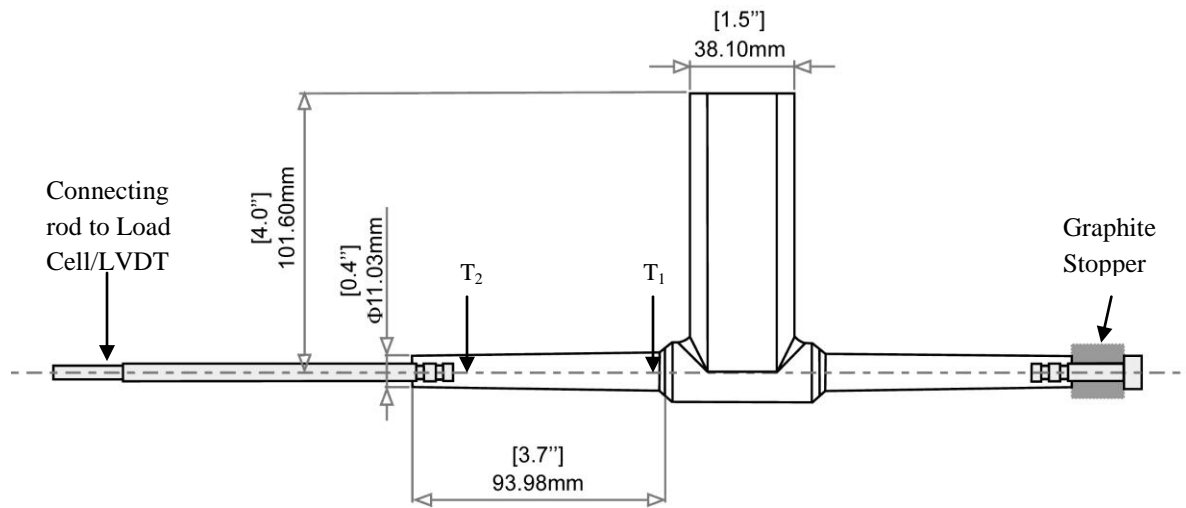


Fig. 2 – Dimensions of test casting

## B. Experimental matrix and procedures

Aluminum casting alloys A356 and 206 were selected as model alloys. As is well known, alloy A356 is widely used in industry for many applications due to its high mechanical strength, ductility and fatigue resistance. It has excellent fluidity making it easy to cast and resists hot tearing. It is selected as the reference alloy for comparison, since it was considered the ideal case. Alloy 206 has excellent mechanical properties and high temperature strength and is used today for automotive and aerospace industries. However, it is widely recognized as being difficult to cast, mainly because of its susceptibility to hot tearing. In the experiments commercial alloy A356.2 ingots was used, but the base 206 alloy used was not standard alloy. In

the specifications standard 206 and A206 alloys contain 0.15-0.3% Ti. Ti is added as grain refiner to improve alloy properties. However, one of the objectives of this project is to study the effect of grain refinement, so we needed to start from a base alloy without Ti addition, and so, we used a purposely modified 206 alloy, which has minimum Ti but has all other element within the specification. The base 206 alloy was made using commercial pure Al ingots, Al-50%Cu, Al-25%Mg and Al-50%Mn master alloys and was tagged as M206. The composition of A356 and M206 used was measured using a spark emission spectrometer and are given in Table 1. It can be observed that M206 contains a very low level of Ti (0.006%).

Table 1: Chemical Composition of Alloy M206 and A356 (wt%)

Alloy	Si	Fe	Cu	Mn	Mg	Ti	Al
M206	0.05	0.05	4.55	0.36	0.25	0.006	Bal.
A356.2	6.7	0.06	<0.01	<0.001	0.38	0.14	Bal.

Melt was prepared in a silicon carbide crucible coated with boron nitride in induction furnace and well degassed with argon using a rotating impeller degasser for 30 minutes before pouring. Graphite lubricant spray of controlled thickness was applied to the mold to reduce the friction between the mold wall and the casting and facilitate the removal of casting from the mold. The mold was preheated to desired temperature and held at this temperature at least 10 minutes. No grain refinement was applied in these tests. The independent variables of the experiments are shown in Table 2. The temperatures/load or temperatures/displacement were measured simultaneously for each set of conditions. Castings were extracted from the mold after full solidification and then examined for cracks. Each test was repeated for 5-7 times.

Table 2: Experimental Design for Alloy M206 and A356.

Alloy	Pouring Temp. ( °C)	Mold Temp. ( °C)	Grain Refinement
M206	~700 (50 superheat)	300	No
	~750 (100 superheat)		
	~800 (150 superheat)		
	~750 (100 superheat)	200	No
		300	
		370	
A356	~715 (100 superheat)	200	No
		300	
		370	



From each set of the tests samples were sectioned from one representative bar as shown in Figure 3 for microstructure examination. One sample was cut from the constrained arm near the riser and its transverse cross section was examined for microstructure including the DAS and/or grain size. The entire arm, which is connected to load cell or LVDT, including part of the arm-riser conjunction region was sectioned precisely along axial direction. Half of the sectioned arm was then cut into 3 pieces for easy sample preparation and analysis. These samples were used for characterizing hot tears (their morphology, width, length and locations) and microstructures in the longitudinal cross section using optical microscope and SEM. All the samples are cold mounted in epoxy, ground and polished following standard procedures. The dendrite arm spacing and/or grain size were calculated using standard linear intercept method.

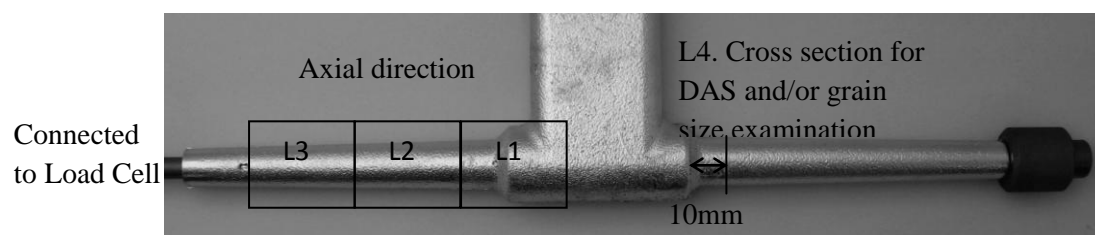


Fig. 3 - Sample locations for microstructure examination

### 3. RESULTS AND DISCUSSION

The setup developed in this project is to investigate the shrinkage/contraction behavior and hot tearing formation of aluminum alloys by measuring the strains and stresses induced by solidification and thermal contraction. A detailed description of the design, the working principles of the apparatus and analysis method of the results is given in reference.<sup>[16]</sup> The reproducibility of the test was also validated.<sup>[16]</sup>

#### A. Effect of Mold Temperature on Hot Tearing

Figure 4 shows typical micrographs of neck region (hot spot) of the restrained rods for M206 alloy cast at different mold temperatures. The crack area was calculated using image processing software (ImageJ) and results are given in Figure 5. The results clearly suggest that the mold temperature has a significant effect on hot tearing susceptibility of 206 alloys. The hot tearing

susceptibility decreases with increasing mold temperature. No hot tears were observed in the critical region of the restrained rods for all A356 castings at three mold temperatures.

Table 3, 4 and 5 summarize the important data from thermal analysis and the load/displacement measurement. The liquidus ( $T_l$ ) and non-equilibrium solidus ( $T_{nes}$ ) were determined from cooling curve. Cooling rate is calculated using the total solidification range divided by the corresponding solidification time. The solidification range ( $\Delta T$ ) reduced with increasing mold temperature, as well as the cooling rate. As a result, the dendrite arm spacing (SDAS) of both alloy A356 and M206 increased.

Table 3: Solidification characteristics data

Alloy	Mold temp. (°C)	$T_l$ (°C)	$T_{nes}$ (°C)	$\Delta T$ (°C)	Cooling rate (°C /s)	SDAS ( $\mu\text{m}$ )
A356	200	615	443	172	6.33	16.31
	300	615	472	143	3.85	18.70
	370	615	501	114	1.99	20.18
M206	200	647	463	186	8.38	16.75
	300	647	485	164	5.13	22.40
	370	647	497	152	2.78	24.70

$T_l$ : liquidus,  $T_{nes}$ : non-equilibrium solidus,  $\Delta T$ : solidification range

Table 4: Contraction force (load) measurement data

Alloy	Mold temp. (°C)	Load onset: temp./ fraction solid (°C)/ fs		Maximum loading rate (N/s)	Cracking initiation temp./ fraction solid (°C) / fs		Major crack temp. (°C) / fs	Load @ $T_{nes}$ (N)
		$T_{C1}/f_s$	$T_{SF1}/f_s$		$T_{C1}/f_s$	$T_{SF1}$		
A356	200	553/0.94	440/-	67	No crack		No crack	702
	300	561/0.89	487/-	51	No crack		No crack	578
	370	585/0.40	507/-	31	No crack		No crack	425
M206	200	624/0.66	478/-	62	593/0.831	471	593/0.831	160
	300	601/0.80	530/0.98	36	562/0.885	518	544/0.903	360
	370	592/0.83	577/0.87	18	~554/0.896	537	-/-	280

$f_s$ : fraction of solid,  $T_{nes}$ : non-equilibrium solidus,

$T_{C1}$ : temperature at the center of the rod,  $T_{SF1}$ : temperatures at the surface of the rod

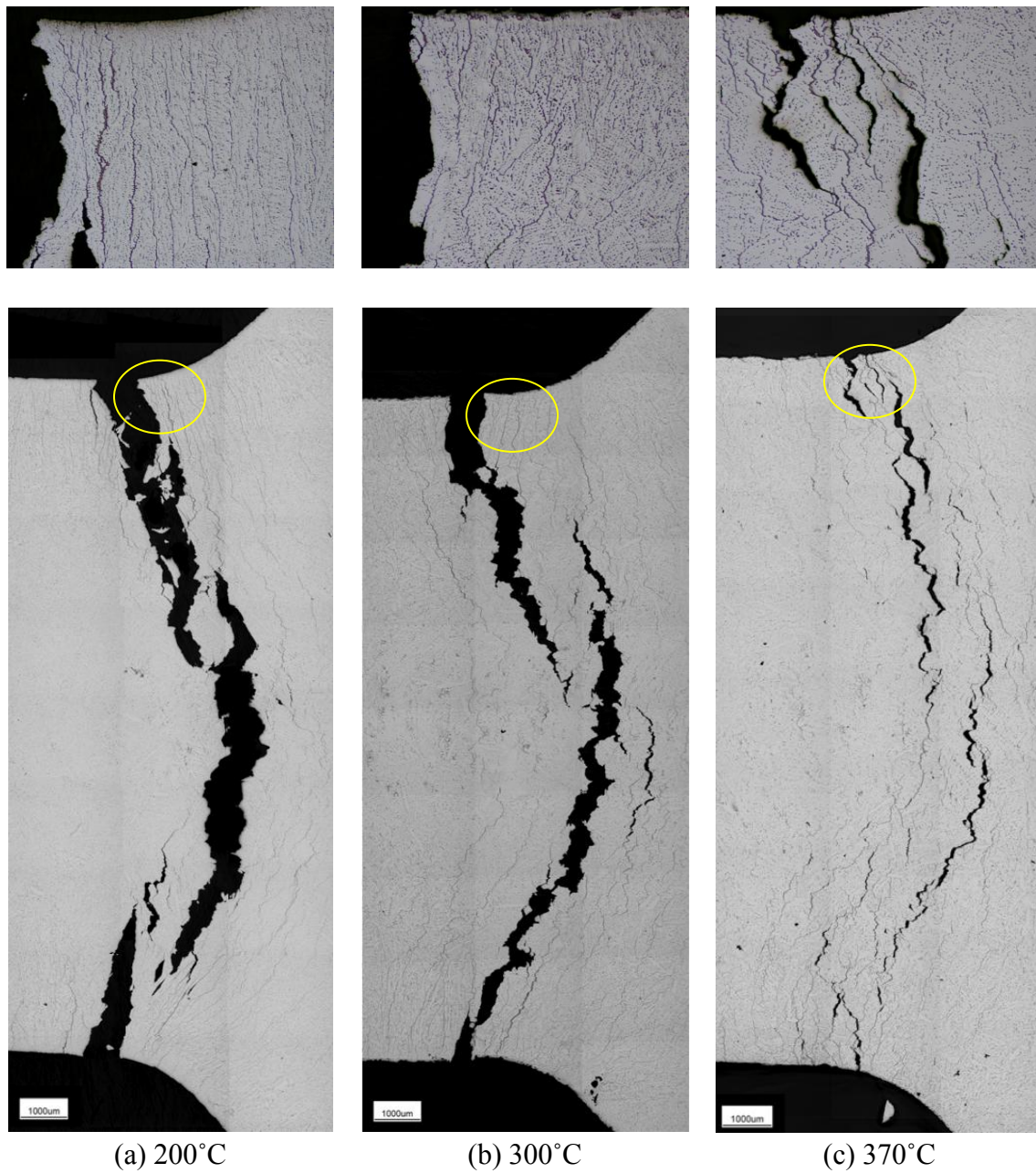


Fig.4 - Mosaic optical micrographs showing hot tears in neck region of M206 (sample sectioned from location 1 shown in Figure 3).

Mold temperature: (a) 200°C, (b) 300°C, (c) 370°C; Pouring temperature: 750°C.

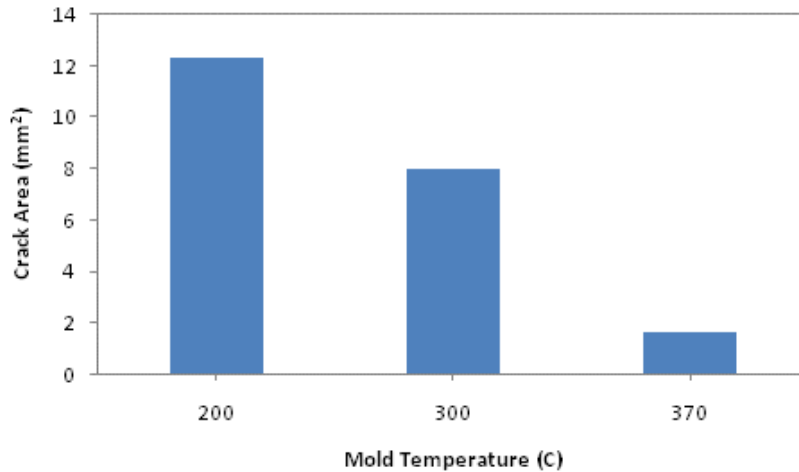


Fig 5 - Crack area under different mold temperatures for alloy M206.

Table 5: Linear displacement ( $l$ ) measurement data

Alloy	Mold temp. (°C)	Onset temp. (°C)/ fs	$l$ @ $T_{eu}$ (mm)	$l$ @ $T_{nes}$ (mm)	$l$ @ cracking initiation (mm)	$l$ @ major cracking (mm)	Maximum displacement rate (mm/s)
A356	200	559/0.69	-0.0010	0.47	No crack	No crack	0.037
	300	575/0.47	-0.0079	0.44	No crack	No crack	0.033
	370	591/0.34	-0.0022	0.31	No crack	No crack	0.017
M206	200	643/0.21	0.40	0.93	0.26	0.29	0.099
	300	636/0.42	0.31	0.67	0.21	0.27	0.048
	370	600/0.80	0.14	0.37	0.07	--	0.014

$l$ : displacement

The temperature, load and linear displacement recorded during casting of A356 and M206 at three mold temperatures are shown in Figure 6 and 7, respectively. The load represents the contraction force developed in the constrained rod during cooling due to solidification and thermal contraction. The measured displacement represents the linear contraction when the rod end was relaxed. The temperatures measured at location  $T_{C1}$  at the centerline of the constrained rod for three mold temperatures were shown in Figure 6 (a) and 7 (a). The time zero in the curves was normalized to correspond to the moment when thermocouple 1 starts to react the increase of the temperature. The first derivatives of load/displacement with respect to time were used to pictorially demonstrate the rate change of load/displacement and thus determine the time and

temperature of hot tearing. In both of load and displacement measurements, slight decrease in the reading (compressive force) were observed shortly after pouring, possible due to the melt pressure head and evolving of gas at the beginning. In the early stage, the liquid and solid are free to move, so the contraction can be accommodated by liquid flow and hot tearing should not occur. However, this mass feeding stage should be relatively short considering a solid shell would form rapidly after pouring due to the high cooling rate in this test. After the solid shell forms (dendrite coherency reaches), the strains and stresses due to thermal contraction will build up and impose on the shell and concentrated in the weak area of the casting. If it is larger than a value, it may tear apart the dendrites and cause hot tearing. But these tears can be filled by liquid refilling considering there is still a large amount of liquid around. From the first derivative curves, a short unstable (variation) stage after the mass feeding stage was observed. This would represent the process of tearing and filling described. The filled minor cracks are evident in the micrographs of the hot spot area of M206 castings (Figure 4.) After this unstable stage, the load starts increasing very fast when a coalesced solid networking forms and can transfer tensile force.<sup>[16]</sup> This can be identified from both the load curve and its first derivative curve. It is defined as the load onset point, which corresponds to the temperature/fraction solid where the solid network starts transferring tensile forces. It should be noted this load onset point is different from the dendrite coherency point, which refers to the moment when the dendrites begin to contact each other and a solid network forms. It is also considered as the moment when the mass feeding transits to interdendritic feeding to compensate shrinkage.<sup>[17,18]</sup> After the load onset point, the dendritic feeding becomes difficult or even impossible. If a hot tear forms, it is hardly to be filled by the remaining liquid and usually will propagate with further contraction.

It is observed from Figure 6, the load kept increasing with time after the load onset point for all three mold temperatures and there were no noticeable changes in the first derivative curves, which suggest no hot tears occurred during casting of A356. Similar conditions were also observed for displacement measurements as shown in Figure 6 (c). Load and displacement developed faster for low mold temperature than higher mold temperature. From Table 4, the load onset temperature decreased with decreasing mold temperature (increasing cooling rate), and correspondingly the fraction solid increased. This is probably due to dendrite refinement caused by the increased cooling rate. It is believed grain refinement resulted from grain refiner addition and dendrite refinement resulted from increased cooling rate delay contraction onset.<sup>[19]</sup> The

maximum loading rate decreased significantly with increasing mold temperature due to lower thermal gradient. Therefore, the load developed before non-equilibrium temperature ( $T_{nes}$ ) was lower for higher mold temperature.

Figure 6(c) shows the measured displacement and its first derivative with time for alloy A356. Similarly, the linear displacement onset temperature decreased with decreasing mold temperature (increasing cooling rate). Compared to the load onset temperatures (starting transferring tensile force) in Table 4, the linear displacement onset temperatures are slightly higher, which suggests the sense of shrinkage by LVDT starts slightly earlier. This is possible because the LVDT can move freely in the horizontal direction and detect the start of movement due to shrinkage, and the solid coalesced network which can transfer tensile force is not necessary. The time range for this early unstable load development should be less or even doesn't exist for LVDT measurement.

The cracks in the hot spot region of alloy M206 for three mold temperatures are shown in Figure 4. They were also detected from the load measurements as shown in Figure 7, which are different from those of A356. The differences for the load development at three mold temperatures also can be clearly observed. For a lower mold temperature (200°C), the load started developing (load onset) very early at around three seconds and increased very fast with time. The crack initiated at 5.3 seconds, at which the temperature at the center of the rod ( $T_{C1}$ ) was 593°C, correspondingly the fraction solid was 0.83 (Pandat Scheil calculation). The tear propagated very rapidly right after the initiation from the surface into the interior of the casting till the load suddenly stopped increasing. This suggests a severe crack (cracks) occurred and the bar was almost broken. For the case of mold temperature of 300°C, the load started developing at 6.8 seconds and increased very fast. From the first derivative curve shown in Figure 7(b), a slight decrease was observed at 10.1 seconds, which suggests hot tearing initiated at this point. The temperature at the center of the rod ( $T_{C1}$ ) was 561°C and at the surface was 518°C. Correspondingly the fraction solid was 0.88 and 0.98 respectively. Shortly after the initiation, a slight increase in the rate was observed, which suggests cracking might stop or partially filled by the remaining liquid. On the other hand, the connected solidified part was gaining strength during cooling. Followed after the slight increase, the rate decreased abruptly from 33N/s at about 12.5 seconds to 10N/s at 16.6 seconds, which suggests the load increase was interrupted and significant cracking (the first major crack) occurred/propagated. The reason why the load was still increasing after the initiation and

propagation is that the solidified part of casting was continuously grain strength during cooling. For a higher mold temperature (370C), the load started developing at 12 seconds and the crack initiated around 554C, at which corresponding fraction solid is 0.83. No sharp drop but a visible variation was still observed at around 24 seconds in the load curve and its first derivative curve, which suggests medium to mild cracks formed. It can be clearly seen from the first derivative curves hot tears propagated slower for higher mold temperature.

The important load measurement data for M206 were summarized in Table 4. The results show that the mold temperature (cooling rate) influences the load onset temperature, the maximum loading rate and hot tearing initiation temperature. The load onset temperature decreased with increasing mold temperature. This trend is opposite with that of A356. The reason for this difference is still unclear. It is possible due to the difference in the grain morphology between A356 and M206. There is no columnar structure in all A356 castings which cast at three mold temperatures due to grain refinement effect of quite amount of titanium in the composition. As pointed out, the dendrite refinement resulted from increased cooling rate was believed to delay contraction onset. However, for M206, columnar structures were seen in all three conditions and more obvious for lower mold temperatures, due to no grain refiner addition in the melt and high thermal gradient in the casting (Figure 8). It is possible that M206 cast at mold temperature of 200C developed a coherent solid network shell which could stand force very fast at an early stage but with lower fraction solid at the center. The crack initiation temperature decreases with increased mold temperature, which suggests the crack initiation is delayed (higher fraction solid) due to increased mold temperature. It should be pointed out the fraction solid at specific temperature was calculated based on the Scheil model. The fraction solid at the surface of the casting is not available, since the experimentally determined non-equilibrium solidus temperature is lower than the calculated value. However, it is believed that there were still some liquid in the surface area at the time when the cracks initiated by comparing the temperatures at the surfaces ( $T_{SF1}$ ) of the castings with the experimentally determined solidus (Table 3). The maximum loading (contraction) rate decreased with increased mold temperature.

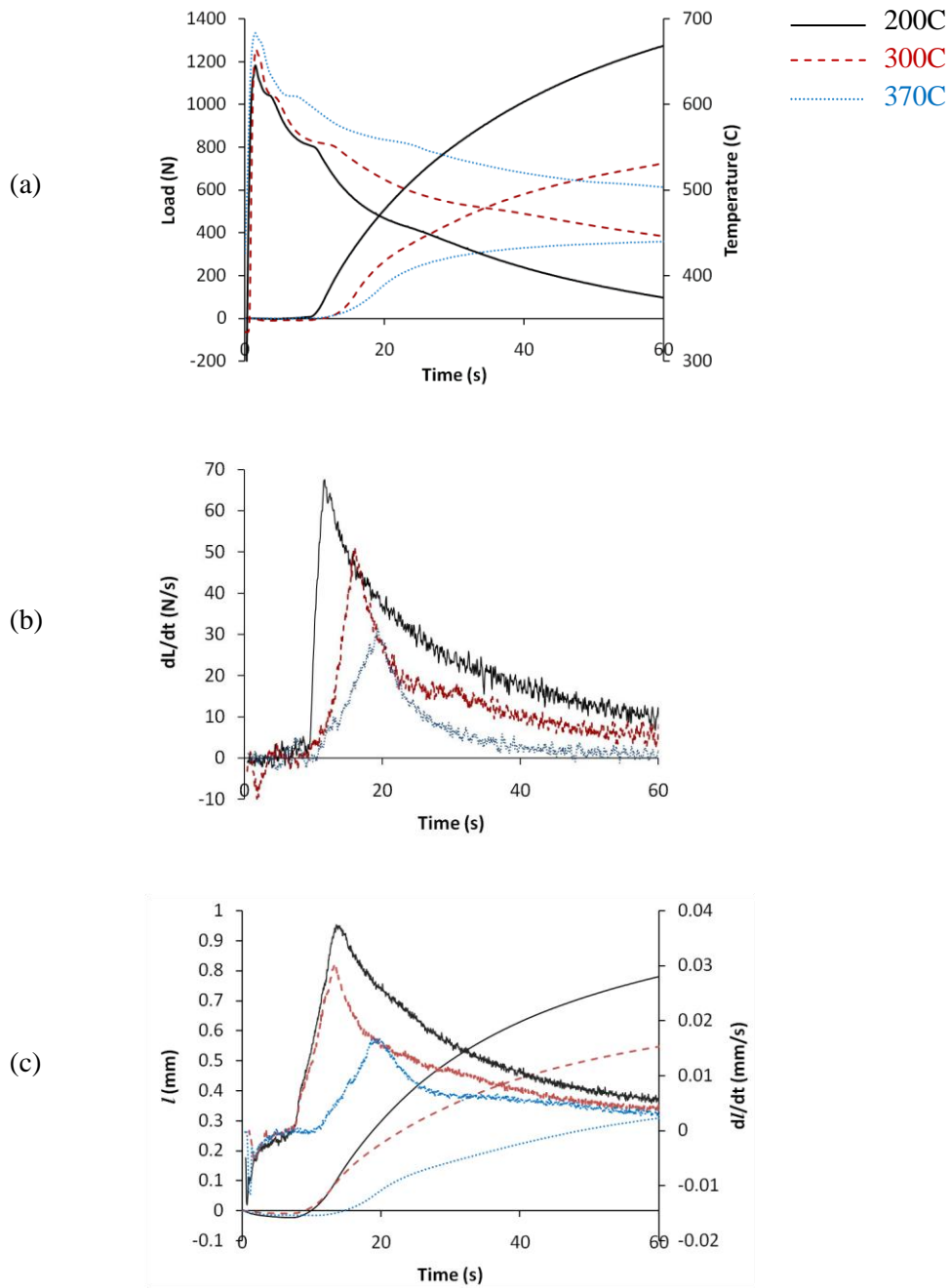


Fig. 6 - (a) Temperature and load development as a function of time for A356 at different mold temperatures, temperature measured at centerline of the rod at the riser end ( $T_{c1}$ ); (b) Derivative of load vs. time curves; (c) Measured displacement and its derivative as a function of time.



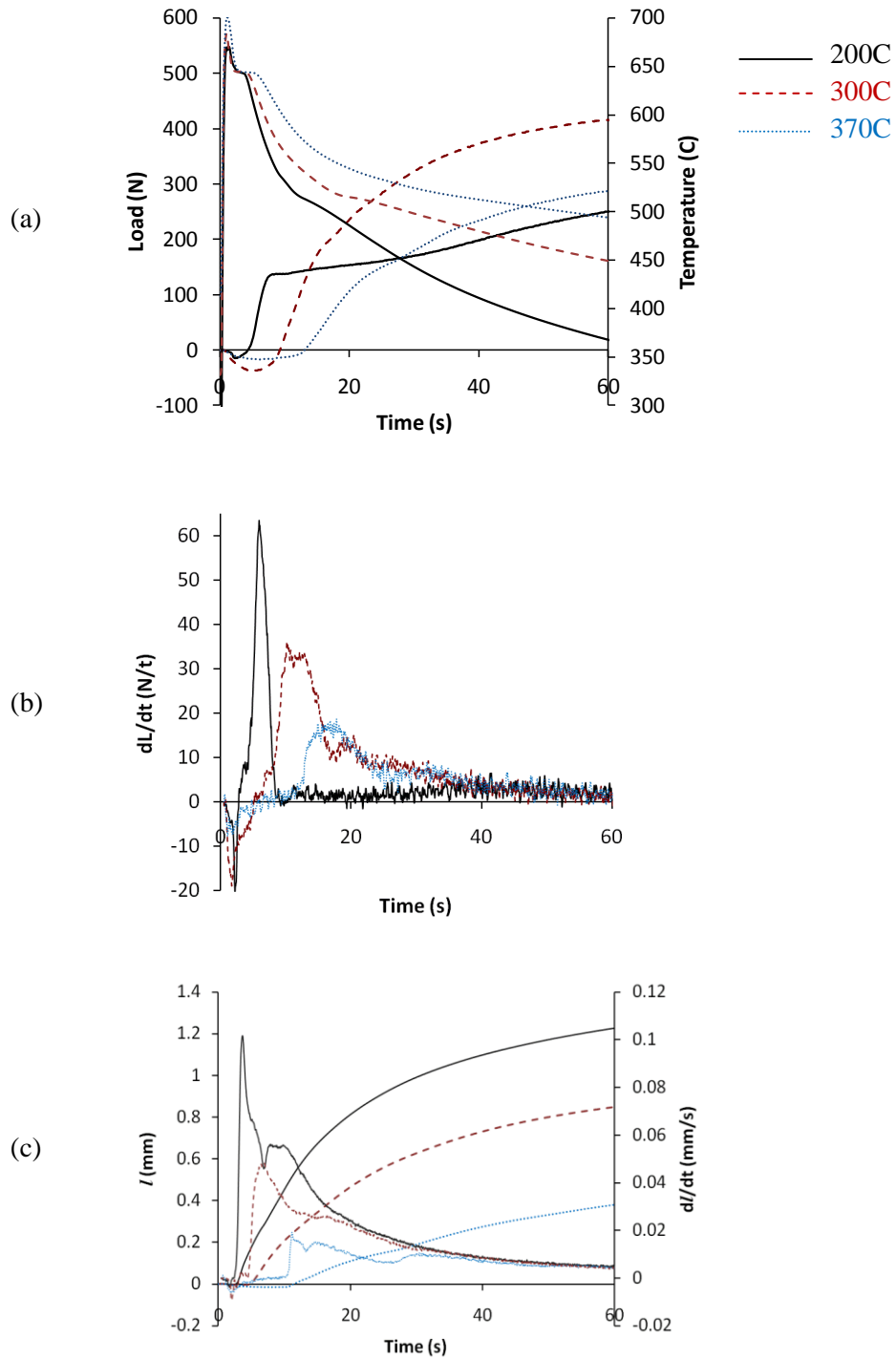


Fig. 7 - (a) Temperature and load development as a function of time for M206 at different mold temperatures, temperature measured at centerline of the rod at the riser end ( $T_{c1}$ ); (b) Derivative of load vs. time curves; (c) Measured displacement and its derivative as a function of time.

This is because higher mold temperature results in lower cooling rate, which slows down the load development, thus lower the loading rate. In addition, the thermal stresses on the solidifying metal (concentrated in the hot spot area) decreased with increased mold temperature. All the information is useful to help understand why increasing mold temperature decreased hot tearing susceptibility. On the other hand the thermal gradient influences the grain morphology during solidification.<sup>[14]</sup> For lower mold temperature, the columnar grains are growing very fast against the wall as shown in Figure 4 and Figure 8. The columnar structure is detrimental when it stands tensile force vertical to the growth direction, which favors the hot tearing formation. Moreover, the liquid flow between these columnar grains is limited. For a higher mold temperature (370°C), there are less columnar grains and more equiaxed grains in the microstructure. However, all the grains are equiaxed dendritic at the center of the casting rod (Figure 8). The average grain size and dendrite arm spacing increased with increasing mold temperature.

The microstructure (grain morphology) of the casting determined by thermal gradient and the contraction rate by cooling rate are the most important factors for hot tearing formation in this study.

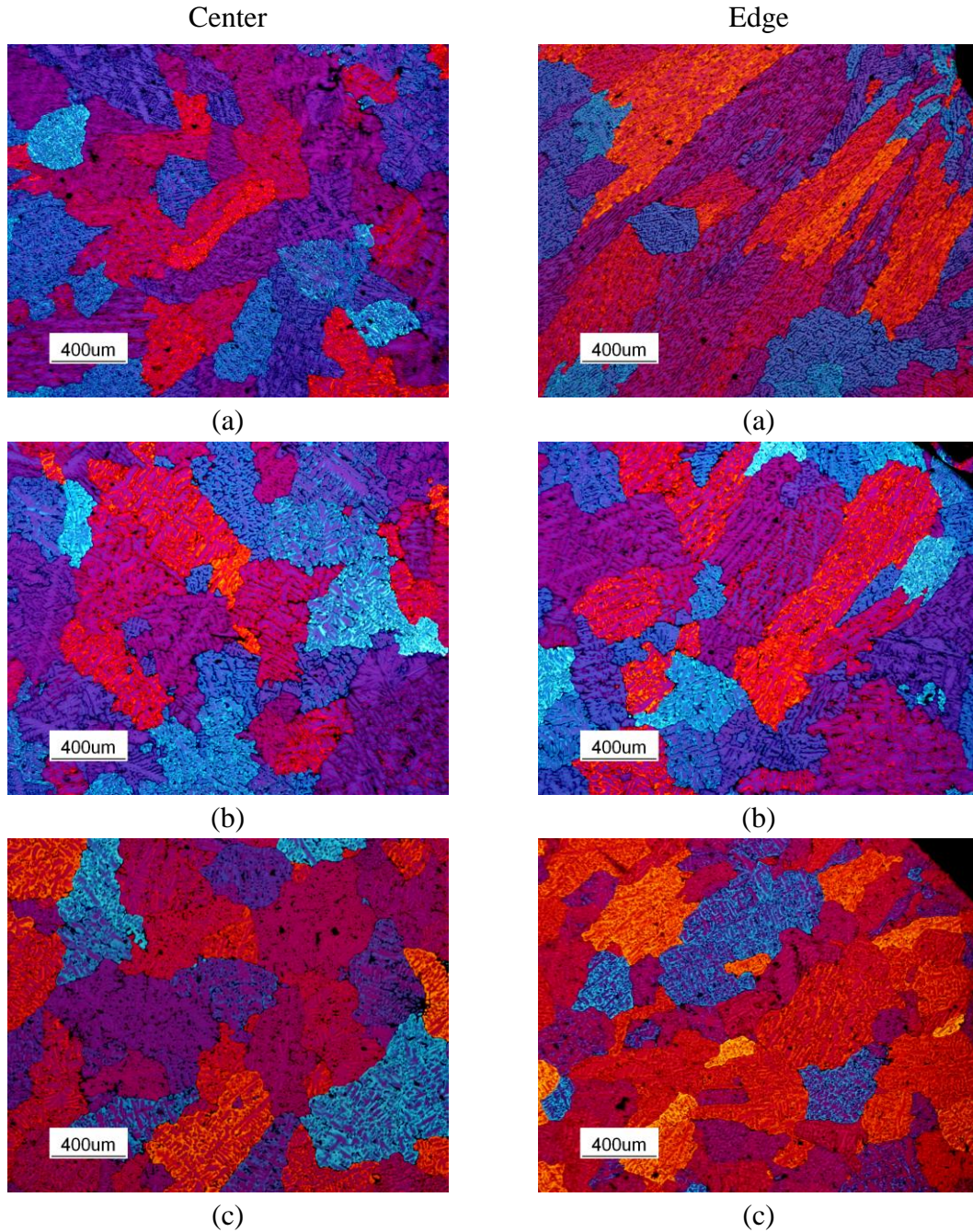


Fig. 8 - Microstructure of M206 showing grain and dendritic morphology of center and edge of the rod (sample sectioned from location 4 shown in Figure 3);

Pouring Temperature: 750°C, Mold Temperature: (a) 200°C, (b) 300°C, (c) 370°C

The linear displacements below the eutectic temperature were measured for both A356 and M206. Negligible displacement was developed for A356, but considerable displacement for M206. This is due to the difference of solidification process for these two alloys.

Let's use the binary Al-Si and Al-Cu systems to estimate the A356 and 206 alloys solidification process. The eutectic temperature for A356 is 577°C, at which 1.65% of Si is dissolved in Al and 12.5% is in liquid. For 206 the eutectic temperature is ~540C, at which 5.65% of Cu is dissolved in Al and 33.2% is in liquid. Si content in A356 is ~7% and Cu content in 206 is ~5%. This means 356 has about 50% liquid but 206 almost solidifies completely or only very small amount liquid left when reaching at eutectic temperature. So, comparing with 206, 356 will solidify at a higher eutectic temperature for a longer time, which provides larger amounts of liquid and allows for a longer time for interdendritic and mass feeding to compensate the contraction, resulting in reducing the contraction amount.

As a whole, the test bar solidifies from its end to the riser, where are the hot spot and the possible hot tearing sites. When solidification progresses the solidified part in 356 contains 1.65% Si in solid solution and 5.35% as Si particle in eutectic, but in 206 almost all Cu in solid solution. There is an expansion when Si particles form. This process releases a large amount of heat because of high heat of fusion of the Si. The Si expansion reduces the solidification contraction and thus the stress in the bar. Moreover, large amount of released heat slows the solidification and reduce the stress increase rate and the strain rate in the mushy zone in front of solidification front. For A356 all these factors are favorable to prevent the hot tearing formation.

### **B. Effect of Pouring Temperature on Hot Tearing**

Figure 9 shows typical micrographs of neck region (hot spot) of the restrained rods for M206 alloy cast at different mold temperatures. All the castings showed severe tears. The crack area was calculated and results are shown in Figure 10. The results suggest that hot tearing susceptibility slightly increased with increasing pouring temperature. Grain morphology are columnar at the surface layer and equiaxed dendritic at the center for all three castings cast under different pouring temperatures (Figure 11).

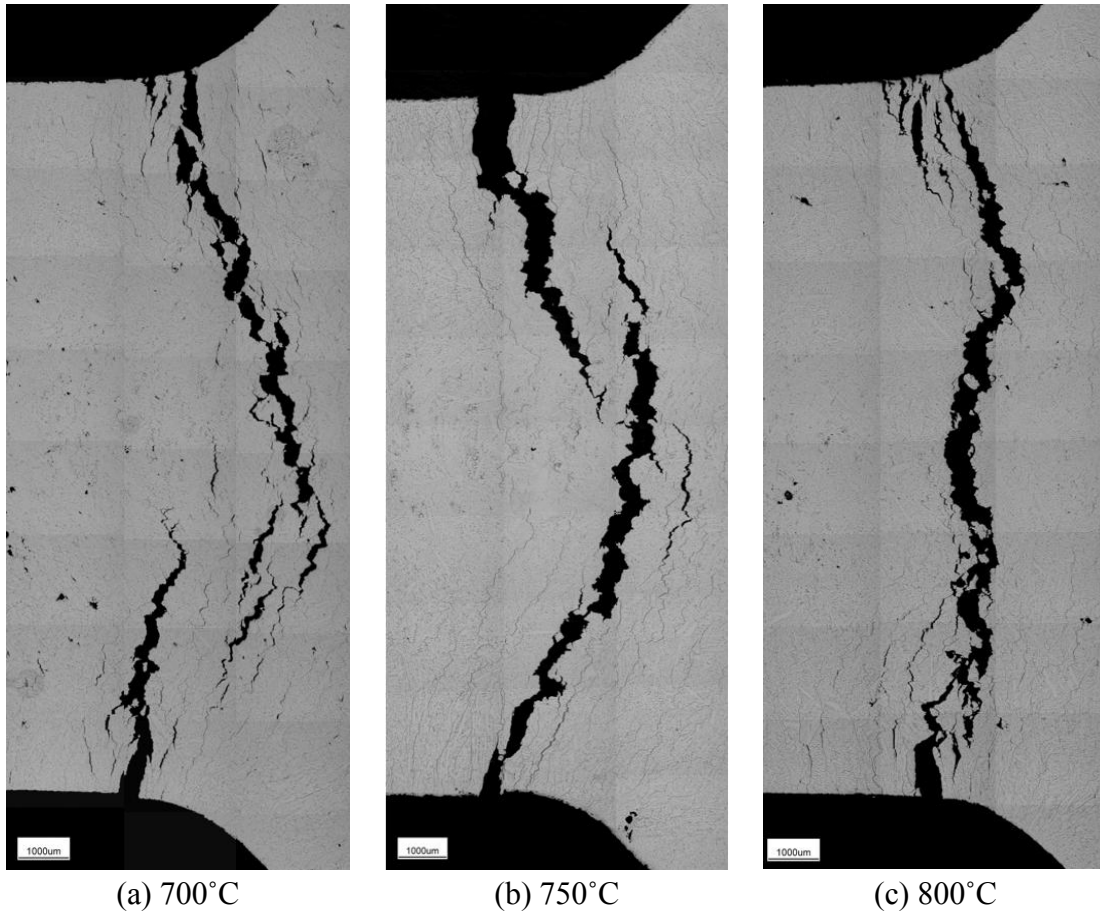


Fig. 9 - Mosaic optical micrographs showing hot tears in neck region of M206 (sample sectioned from location 1 shown in Fig. 3).

Pouring temperature: (a) 700°C, (b) 750°C, (c) 800°C, Mold temperature: 300°C.

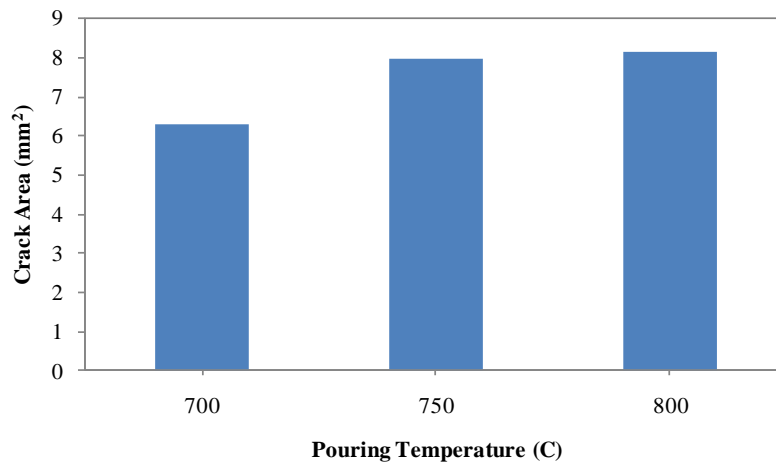


Fig 10 - Crack area at different pouring temperatures for alloy M206.

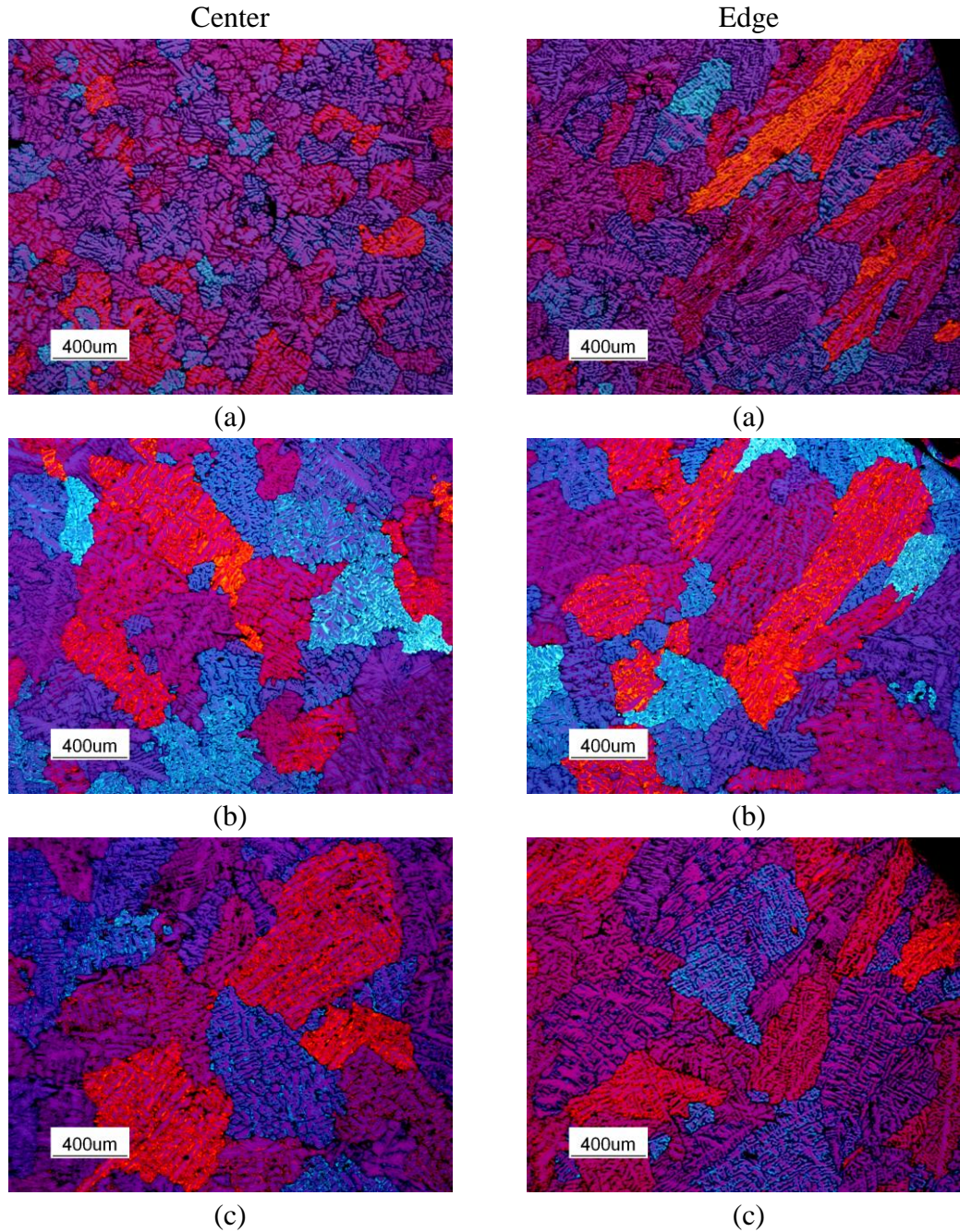


Fig. 11 - Microstructure of M206 showing grain and dendritic morphology at the center and edge of the rod (sample sectioned from location 4 shown in Figure 3)

Mold Temperature: 300°C, Pouring Temperature: (a) 700°C, (b) 750°C, (c) 800°C

The temperature and load recorded during casting of M206 at three pouring temperatures are shown in Figure 12. Table 6 summarizes the important thermal data from temperature analysis. The pouring temperature showed negligible effect on solidification range ( $\Delta T$ ). The cooling rate

decreased slightly with increasing pouring temperature. As a result, the dendrite arm spacing (SDAS) increased. However, it seems the influence of pouring temperature on grain size (equiaxed grains) is more obvious than that of mold temperature (Figure 11). Columnar structures are observed for all three cases.

Table 6: Solidification characteristics data

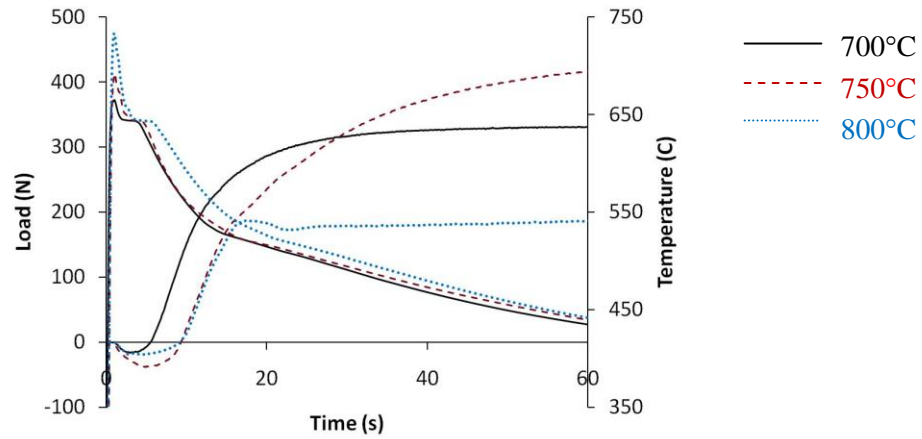
Alloy	Pouring temp. (°C)	$T_l$ (°C)	$T_{nes}$ (°C)	$\Delta T$ (°C)	Cooling rate (°C /s)	SDAS ( $\mu\text{m}$ )
M206	700	647	486	168	5.21	20.60
	750	647	485	164	5.13	22.40
	800	647	484	165	4.86	27.70

$T_l$ : liquidus,  $T_{nes}$ : non-equilibrium solidus,  $\Delta T$ : solidification range

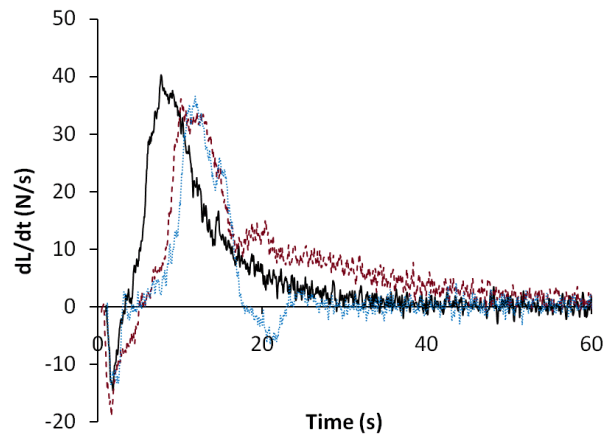
It can be determined from the load curve (Figure 12(a)) and its first derivative curve (Figure 12 (b)) that severe hot tearing occurred for all three castings. The critical information from the load measurement is given in Table 7. The load onset was delayed (higher fraction of solid) with increasing mold temperature. This trend is similar as that of the influence of mold temperature, though the effect is less obvious. This is because higher pouring temperature of melt results in higher mold temperature hence lower cooling rate when the solidification starts. The maximum loading rates and the crack initiation temperatures were not significantly influenced by pouring temperature. The maximum loading rate was slightly higher for casting cast with low superheat than casting cast with higher superheat. The fractions of solid at which the cracks initiated are very close possibly due to the small difference between the cooling rates.

It is observed from the first derivative curves, the propagation of hot tearing was more gradual (smaller serrations) for low pouring temperature case (700°C), possibly due to the smaller grain size of the casting which can better accommodate stress. However, for higher pouring temperature (800°C), the load suddenly released and the loading rate hit zero at some point, which suggests the casting bar broke at that time. This was confirmed by visual examination of cracks in the neck region of the casting (Figure 9 (c)). The external crack propagated inward and internal crack propagated outward. The casting bar broke when these two types of cracks met. There are two possible reasons which explain why the severity of hot tearing increased with

increasing pouring temperature. First, the grain size increases due to lower cooling rate. The ability of the structure to accommodate the stress buildup decreases. On the other hand, the liquid film thickness between grains increased, which tends to increase hot tearing susceptibility.



(a)



(b)

Fig. 12 - (a) Temperature and load development as a function of time for M206 at different pouring temperatures, temperature measured at centerline of the rod at the riser end ( $T_{c1}$ );  
(b) Derivative of load vs. time curves.



Table 7: Contraction force (load) measurement data

Alloy	Pouring temp. (°C)	Onset temp. (°C)/ fs	Maximum loading rate (N/s)	Cracking initiation temp. (°C) / fs	Major crack temp. (°C) / fs	Load @ T <sub>nes</sub> (N)
M206	700	634/0.50	40	584/0.851	569/0.88	320
	750	601/0.80	36	562/0.885	544/0.90	360
	800	599/0.81	36	570/0.876	547/0.90	180

*f<sub>s</sub>: fraction of solid*

#### 4. CONCLUSIONS

- The effect of mold temperature and pouring temperature were studied using a constrained rod mold which enables the simultaneous measurement of the load (contraction force)/ time/ temperature in a constrained casting or linear contraction/ time/ temperature of a relaxed casting during solidification and cooling. The experimental technique developed in this project is sensitive to investigate load development, the crack initiation and propagation.
- Important solidification characteristic data and critical hot tearing formation data are determined from these measurements.
- The crack area in the hot spot region for each condition was calculated and used as hot tearing susceptibility index.
- Alloy A356 has high resistance to hot tearing. No hot tearing forms under three different mold temperatures, while M206 shows significant hot tearing tendency under the same casting conditions.
- The load onset temperature and crack initiation temperature both decreased with increasing mold temperature.
- The severity of hot tearing and linear contraction in alloy M206 decreased significantly when the mold temperature increased. On one hand, higher mold temperature resulted in lower cooling rate, which slows down the load development thus reduces thermal stresses/strains on the solidifying metal (concentrated in the hot spot area). On the other hand the thermal gradient influences the grain morphology during solidification. Lower mold temperature results in higher thermal gradient which promotes columnar structure. The columnar

structure is detrimental when it stands tensile force vertical to the growth direction, which favors the hot tearing formation.

- The results showed that the severity of hot tearing in alloy M206 increased with increasing pouring temperature. The effect is not as significant as that of mold temperature. Two factors might contribute this increasing. First, the ability of the structure to accommodate the stress buildup due to thermal contraction decreases since the grain size becomes larger with increasing pouring temperature (a lower cooling rate). On the other hand, the liquid film thickness between grains increases, which would tend to increase hot tearing susceptibility.
- The grain morphology of the casting and loading (contraction) rate are the most important factors to hot tearing formation.

## **ACKNOWLEDGEMENTS**

The authors gratefully acknowledge the member companies of the Advanced Casting Research Center (ACRC) for their support of this work, and for their continued support of research focused on the science and technology of metal casting at Worcester Polytechnic Institute. The authors also would like to thank very much Jim Thomson, Geethe Nadugala and Stuart Amey of CANMET Material Technology Laboratory for their support during this work.

## **REFERENCES**

1. C. Monroe and C. Beckermann: *Materials Science and Engineering A*, 2005, vol. 413-414, 30-36.
2. J. Campbell: *Castings*, Oxford: Butterworth-Heinemann, 1991.
3. C. Davidson, D. Viano, L. Lu, and D. Stjohn: *International Journal of Cast Metals Research*, 2006, vol. 19, 59-65.
4. W. S. Pellini: *Foundry*, 1952, vol. 80, 125-199.
5. K. Singer and H. Benek: *Stahl and Sisen*, 1931, vol. 51, 61-65.
6. J. M. Middleton and H. T. Protheroe: *Journal of the Iron and Steel Institute*, 1951, vol. 168, 384-397.

7. W. I. Pumphrey and J. V. Lyons: *J. Inst. Met.*, 1948, vol. 118, 439-455.
8. L. Bichler, A. Elsayed, K. Lee, and C. Ravindran: *International Journal of Metalcasting*, 2008, vol. 2, 43-54.
9. A. Couture and J. O. Edwards: *AFS Trans*, 1966, vol. 74, 709-721.
10. C. W. Briggs: *The Metallurgy of Steel Castings*, McGraw-Hill, London, 1946.
11. H. F. Bishop, C. G. Ackerlind, and W. S. Pellini: *AFS Trans*, 1952, vol. 60, 818-833.
12. T. W. Clyne and G. J. Davies: *The British Foundrymen*, 1975, vol. 68, 238-244.
13. J. A. Spittle and A. A. Cushway: *Metals Technology*, 1983, vol. 10, 6-13.
14. Z. Zhen, N. Hort, O. Utke, Y. Huang, N. Petri, and K. U. Kainer: *Magnesium Technology*, 2009.
15. C. Limmaneevichitr, A. Saisiang, and S. Chanpum: *Proceedings of the 65th World Foundry Congress*, 2002.
16. S. Li, K. Sadayappan, and D. Apelian: submitted to *International Journal of Cast Metals Research*.
17. L. B äckerud, G. Chai, and J. Tamminen: *Solidification Characteristics of Aluminum Alloys*, AFS/Skanaluminum, Oslo, Norway, 1990.
18. N. L. M. Veldman, A. K. Dahle, D. H. StJohn, and L. Arnberg: *Metallurgical and Materials Transactions A*, 2001, vol. 32, 147-155.
19. D. G. Eskin and L. Katgerman: *Materials Science Forum*, 2006, vol. 519-521, 1681-1686.

# **Why Some Al Alloys Hot Tear and others do not?**

## *- The role of grain refinement*

The effects of grain refinement on hot tearing formation and contraction behavior of Al-Cu alloy 206 have been studied. The experiments were conducted using a newly developed Constrained Rod Mold, which could simultaneously measure the contraction force/time/temperature during solidification for a restrained casting, and thereby could be used in investigating hot tearing formation. Quantitative information on crack initiation, refilling, and propagation can be detected by analyzing the load measurement data. Al-Ti and Al-Ti-B grain refiner were added to the melt at various levels to obtain grain structures ranging from columnar dendritic structure to equiaxed dendritic and globular structures. Effects of grain structure and grain size on hot tearing susceptibility were investigated. Grain refinement was found to have a complex effect on load onset. The hot tearing tendency was significantly affected by both grain size and morphology.

### **1. INTRODUCTION**

Hot tearing is a common and severe defect encountered in alloy castings and perhaps the pivotal issue defining an alloy's castability. Once it occurs, the casting has to be repaired or scrapped, resulting in significant loss. Since there was published research paper in foundry area hot tearing has been one of the focus topics. Over the years many theories and models have been proposed and accordingly many tests have been developed. Unfortunately many of the tests that have been proposed are qualitative in nature; meanwhile, many of the prediction models are not satisfactory as they lack quantitative information and data. The need exists for a reliable and robust quantitative test to evaluate/characterize hot tearing in cast alloys. Based on these industry and research needs MPI teamed up with CANMET launched the hot tearing research project. In this project an apparatus with an instrumented constrained rod mold was developed. The system is designed to quantitatively evaluate and investigate hot tearing behavior through measuring the real time contraction force developed during casting solidification and cooling. Its detailed information was presented elsewhere.<sup>[1]</sup> Quantitative information obtained using this system helped reveal the details of hot tearing formation and thus the mechanism. The effects of several

major factors on hot tearing formation of aluminum casting alloys were studied using this system. This paper will address the study of the effects of the grain refinement. It will show what has been done in this area (a brief review) and why to study it in current project, introduce the study method, testing system, and alloy selection for the study, then detail the experimentation and results, and discuss the findings.

### **A review of Effects of Grain, its Size and Morphology on Hot Tearing**

Many investigations have been conducted in studying the effects of grain refinement or grain morphology and size on hot tearing.<sup>[2-7]</sup> However, the results were not consistent and even confusing.

Studying the effect of different elements on hot tearing susceptibility of synthesized alloy Al-2%Zn-2-3%Mg, Matsuda et al. found that the effects of elements were related to their grain refining effects. When large columnar grains were dominant, the crack length (hot tearing susceptibility) was likely to reach the saturated (maximum) value, and with grain becoming equiaxed and smaller the crack length reduced, which was independent of the kind and amount of added elements.<sup>[8]</sup> Among the studied 13 elements the most favorable ones were Ti+B, Ti, and Zr, and the detrimental element was Cu. In the further study they found that the same addition might have different effects in different conditions. Easton et al. studied the effect of adding Ti in alloy 6061 on hot tearing through measuring the load development in the solidifying test bar.<sup>[5,6]</sup> It was found that the load development vs. temperature was slowed down and load was lowered with addition of grain refiner. They contributed the delay of strength development to the delay of load transfer due to grain refinement. With the addition of grain refinement the mush becomes more pliable, i.e. more liquid-like, and the point, at which the mush began to behave more like a solid than a liquid, was delayed, which reduces the severity of hot tearing. It was concluded that grain refinement decreased the hot tearing susceptibility through changing the grain morphology from columnar to equiaxed and reducing the grain size. So, they proposed that fine dendritic equiaxed grain morphology had the greatest resistance to hot tearing. However, they also pointed out the possibility that if the grain size was reduced, the permeability of the mush would decrease, which might cause the hot tearing susceptibility to increase.

Clyne et al. studied the effect of grain refinement on two Al-Mg alloys, one, Al-2%Mg, with low cracking susceptibility and another, Al-1%Mg, with high cracking susceptibility.<sup>[9]</sup> Both alloys

had columnar grain structure when no grain refiner was added. It was found that the low susceptibility alloy showed an increased cracking tendency over a narrow range of Ti contents despite the grain structure was changed to finer and equiaxed. However, the high susceptibility alloy was unaffected by the Ti additions except at high level ( $>0.2\%$  Ti) even though the grain was altered from columnar to equiaxed. So, they pointed out that there was a complex interaction between impurity content, grain structure, and cracking susceptibility. Rosenberg and Flemings et al. also “surprisingly” found that the grain refining did not have any effect on hot tearing in their experiment.<sup>[10]</sup> Warrington et al. found that the alloy could still have high hot tearing susceptibility even grain refiner was added depending on the amount of addition.<sup>[7]</sup> They found that without adding grain refiner the alloys 7010 and 7050 had columnar structures and high cracking susceptibility. With moderate addition of grain refiner the alloys formed equiaxed-dendritic grains and gained resistance to cracking. However, with higher addition equiaxed-cellular grains formed and the cracking susceptibility turned to be high again.

There were some other studies on this topic and gave similar results as shown above. Some indicated grain refinement reduced hot tearing susceptibility; some showed no beneficial or even detrimental effect; and others showed the effects could be good or bad depending on the test conditions and amount of grain refiner addition. When scrutinizing these previous studies it can be found that the inconsistency or confusion may results, to some extent, from inaccuracy in the characterizing hot tearing and in measuring and monitoring the process, because of the qualitative nature of the studies and experiments. Due to the importance of grain structure in an alloy and the newly developed apparatus developed in this study provided the capability to quantitatively monitor hot tearing process and evaluate the effects of various variables, we studied the role of grain refinement in hot tearing again. The intentions of the study are to further this investigation to one step forward by providing quantitative relations between grain refinement and hot tearing characteristics in revealing the nature of hot tearing and clarifying the confusions in the literatures and provide detailed information and quantitative data for computer simulation.

## 2. EXPERIMENTATION

### 2.1 Experimental Setup

Detailed information about the test setup can be found elsewhere.<sup>[1]</sup> Figure 1 is a schematic diagram of the system for the experiments. It consists of three sections: (1) the mold of the test casting; (2) sensors and measuring and controlling systems; and (3) alloy preparation and casting system. The mold is vertically partitioned into two halves, one half fixed in the system base frame and the second half movable. A hydraulic pump is used to move the second half mold for mold opening and closing under controlled pressure. The mold has a modulus structure containing changeable inserts to use different mold materials and to fit different configurations and dimensions of the test castings. Heating plates and water-cooling channels are built in the mold for temperature control. The sensors and measuring system consists of a load cell, a LVDT (linear variable differential transformer), thermocouples and a data acquisition system. There are two controlling systems, one for mold temperature and another for mold closing pressure. Alloy preparation and casting system (not shown in the figure) consists of an induction furnace, an inert gas rotary degasser, a spectrometer, and casting devices, which provide accurate controls for alloy composition, melting and pouring temperatures, hydrogen level, and consistent casting conditions.

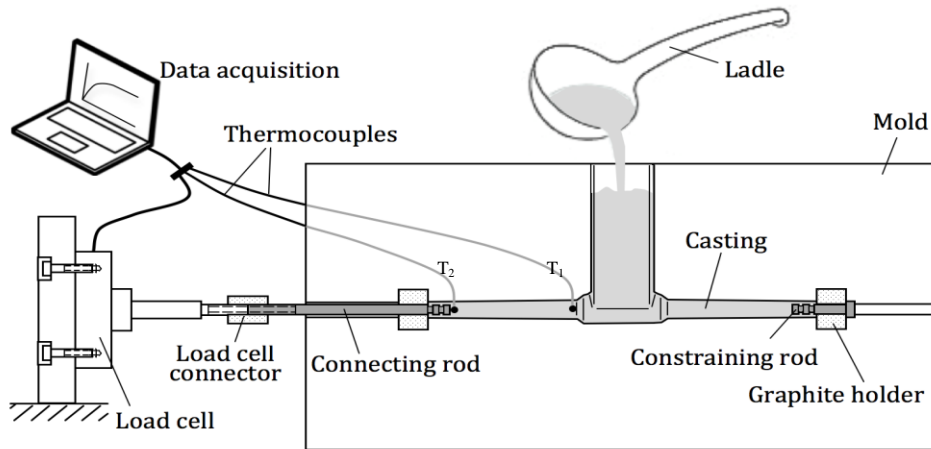


Figure 1. Schematic diagram of the apparatus setup.

In this study the mold is made of H13 and the test casting is a constrained bar as shown in Figure 2. The test piece has two arms. The arms are designed with a slight taper to reduce friction between the mold and casting. One arm (right one in the figure) is constrained at the end with a steel thread. The thread is anchored by a graphite holder and part of it is embedded in the arm end of the casting. This arm end will solidify first and fast because of the lower temperature of the embedded thread and the graphite stopper holds the arm end unmovable. This fixed end causes tension development and may induce cracking in the bar during solidification. The other arm (left one in the figure) is used for load/displacement and temperature measurements. This end is connected to a rod, which has one side embedded in the arm end of the casting and another side connected to a load cell. The load cell is connected to connecting rod firmly and restricts the contraction of the casting and may induce cracking in the casting. Two K-type thermocouples are used for the temperature measurement of the casting. One is positioned at the riser end ( $T_1$ ) and the other at the end of the rod ( $T_2$ ).

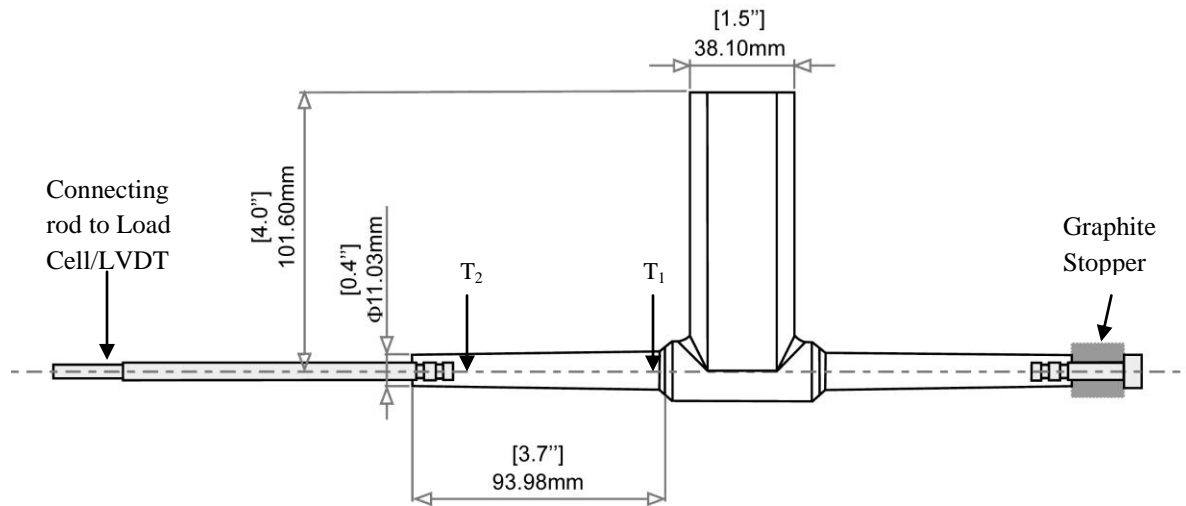


Fig. 2 – Dimensions of test casting

## 2.2 Test Alloy and Experiment Matrix

Selecting alloy for this study was based on the following considerations. It is an aluminum casting alloy and has very attractive properties for applications but have high hot tearing tendency in general condition without grain refinement. Alloy 206 was selected. This alloy has excellent mechanical properties and high temperature strength and currently is used in automotive and aerospace industries. However, it is widely recognized that this alloy is difficult to cast, mainly because of its high susceptibility to hot tearing, which limits its use. In this study



it was planned to use grain refiner, Al-6Ti% and Al-5%Ti-1%B master alloy, for refining the grain and to test the alloy from not grain refined to fully refined. So the starting alloy needs to have minimum amounts of Ti, B and other refiners.

### 2.3 Operation Procedure

The alloy was melted in an induction furnace. For each set of experiments about 35 lbs of alloy was prepared. Because the commercial 206 alloy contains some Ti and cannot be used in studying grain refinement of different levels, a lab-made alloy, tagged as M206, was prepared as base alloy. This alloy was produced using commercial pure Al, Al-50%Cu, Al-25%Mg and Al-50%Mn master alloys to keep the Ti, B and other grain refiners in minimum. To fully dissolve all the alloying elements, the melt was kept at ~780C for about 40 min after all the charging materials are added. The alloy composition was measured using a spark emission spectrometer and accordingly was adjusted. When the composition met the target the melt was degassed for 40 min at about 700C using inert gas Ar and a rotary degasser to ensure the minimum hydrogen content, thus the porosity, and inclusions in the alloy. After degassing the grain refiner, if needed, was added and the melt composition was measured. During melting the alloy the mold was prepared: the load cell was installed, connected to the connecting rod, which was placed in mold with graphite holder, thermocouples and thread with graphite holder were placed and then the mold was closed and preheated to predetermined temperature. When the mold temperature reached the desired value the melt was transferred and poured into the mold with a steel ladle. In this study the pouring temperatures was 750C and mold temperature was 300C. Right before pouring the data acquisition system was started to record the temperatures and contraction force (load) simultaneously. After the alloy solidified and cooling, in about two minutes, the mold was opened and casting was taken out.

### 2.4 Hot Tearing Measurement, Microstructure and Data Analyses

At each level of the grain refiner addition one test casting was taken for hot tearing measurement and microstructure analysis. The bar was sectioned in the way as shown in Figure 3. Three samples, #1, #2, and #3, were taken from the left arm, which was connected to load cell. The arm was sectioned longitudinally along its centerline and the longitudinal cross sections were

analyzed. One sample, #4, was taken from the right arm and its transversal cross section was examined.

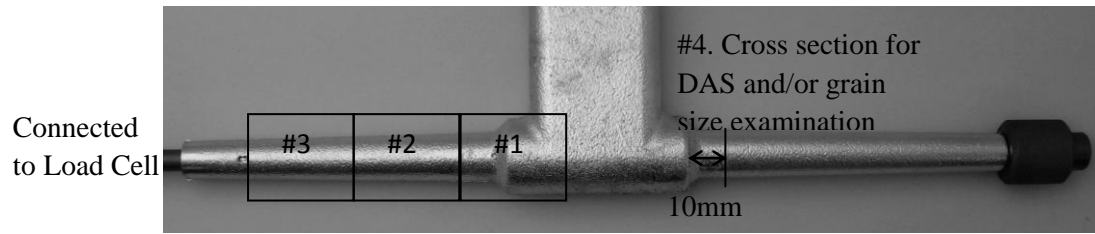


Fig. 3 - Sample locations for microstructure examination

The microstructures were analyzed using optical microscope and SEM. The total area of cracks in the center longitudinal cross sections (hot spot) was measured using an image analysis software ImageJ and was taken as the hot tearing index. ImageJ was also used in measuring DAS and grain size based on the linear intercept method.

The temperature and load data were plotted into two sets of curves. One was load and their first derivatives vs. time and another was temperature vs. time. In the first set of curves the hot tearing process, the crack initiation and propagation can be identified and related to time quantitatively. The second set of curves gave alloy solidification data, its liquidus, solidus and cooling rate, etc. Putting together and comparing these two sets of curves the quantitative relations between the hot tearing process and the alloy solidification characteristics could be established. Detailed information about the analysis method was presented in a separate paper.<sup>[1]</sup>

### 3. RESULTS AND DISCUSSIONS

#### Alloy Compositions

The chemical compositions of unrefined M206 are given in Table 1. The alloy contains a very low level of Ti (0.006%).

Table 1: Chemical Composition of unrefined M206 (wt%)

Alloy	Si	Fe	Cu	Mn	Mg	Ti	Al
M206	0.05	0.05	4.55	0.36	0.25	0.006	Bal.

Al-6%Ti and Al-5%Ti-1%B grain refiner were added to the melt at predetermined levels to obtain grain structures ranging from columnar dendritic structure to equiaxed dendritic and to

globular structures. The measured Ti and B contents in the castings for various grain refining levels are given in Table 2.

Table 2: Experimental parameters and results

Sample No.	Grain refiner levels		Grain size ( $\mu\text{m}$ )	Grain structure type	Hot tearing	
	Ti (%)	B (ppm)			Crack area ( $\text{mm}^2$ )	Comments
M206 (NGR)	0.006	0	388	C+ED	7.9614	Severe cracks (external and internal)
M206-2	0.052	18	108	ED	5.3103	Severe cracks (external and internal)
M206-3	0.099	20	57	ED	0.1102	Small cracks (external)
M206-4	0.138	22	47	ED	0.0937	Small cracks (external)
M206-5	0.052	110	62	ED to G	0.0190	Hairlike cracks (external)
M206-6	0.105	220	37	G	0	No cracks
M206-7	0.149	300	29	G	0	No cracks

*NGR: Non Grain Refined, C: Columnar structure, ED: Equiaxed Dendritic structure, G: Globular grains*

### Microstructure

In order to relate the cracking behavior to grain structure, the microstructure in the neck region (hot spot), where hot tearing occurs potentially, were examined on sample #4. Electrolytic etching method was used to reveal grain structure and micrographs were taken using polarized light. Grain size was measured and results are given in Table 2. The unrefined M206 (minimum 0.006% Ti) consisted of mainly columnar grains with few small equiaxed grains at the edge and large equiaxed grains at the center (Fig. 4). Grain transitioned to equiaxed dendritic with Ti and B additions, even at small amounts of addition (0.052% Ti and 18 ppm B in Fig. 5). When increasing Ti from 0.006 to 0.138% and at the constant level of ~20ppm B grain size was significantly reduced from 388  $\mu\text{m}$  to 47  $\mu\text{m}$ , but till 0.138% Ti the grains are still equiaxed dendritic. It implies that 20ppm B seems not functional to obtain globular structures in the test with Ti addition up to 0.15%. The structure transitioned from equiaxed dendritic to globular at 0.052% Ti and 110ppm B additions. Fine globular grains formed with further Ti and B additions. In all grain refined samples, the grains are uniformly distributed across the cross section (color

micrographs in Fig. 5). In all the cases, the DAS was about  $22\ \mu\text{m}$ . Fig. 5 also shows micrographs of the longitudinal section of hot spot where usually hot tearing occurs.

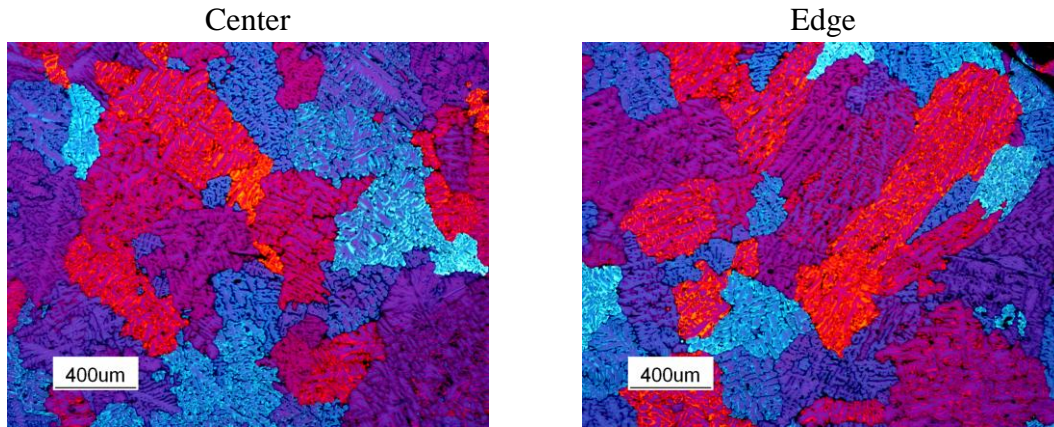
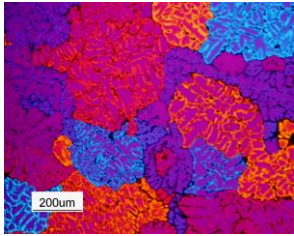


Fig. 4 - Microstructure of unrefined M206 showing grain and grain morphology at center and edge of the rod (sample sectioned from location 4 shown in Fig. 3)

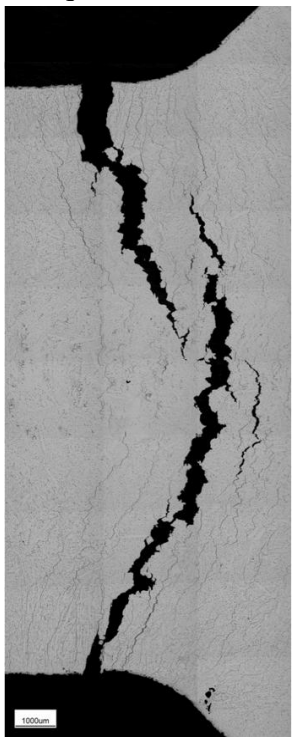
#### **Crack Area Measurements (Hot Tearing Index)**

Total area of cracks in the center longitudinal cross sections (sample #1 in Fig. 3) was measured and taken as hot tearing index. The results are given in Table 2. The results clearly demonstrate that grain refinement has significant influence on hot tearing susceptibility of alloy 206. The susceptibility decreases generally with decreasing grain size, but also depends on grain morphology. Unrefined M206 casting, with mainly columnar grains at the edge and large equiaxed dendritic grains at the center, has highest susceptibility. Hot tearing was mitigated when equiaxed grains formed. Internal cracks were eliminated when fine equiaxed dendritic or globular grains were obtained. Both external and internal cracks were eliminated in the casting with extremely fine globular grains ( $29\text{-}37\ \mu\text{m}$ ).

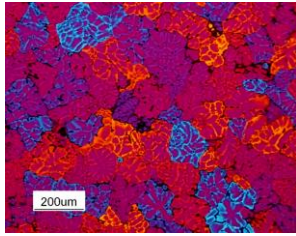
M206 NGR



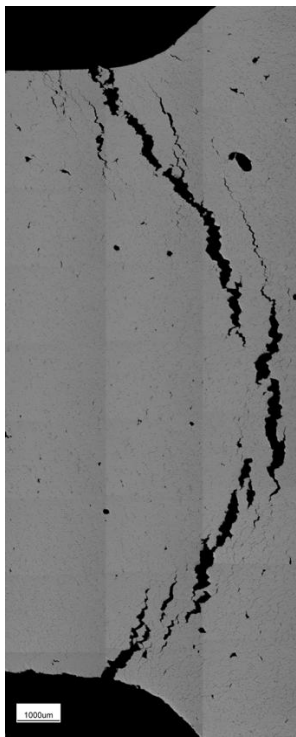
(388 µm at center)  
Columnar(Edge)  
+Equiaxed (Center)



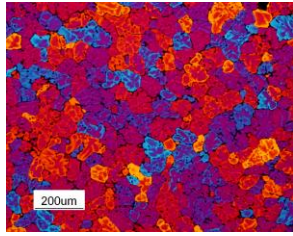
M206-2



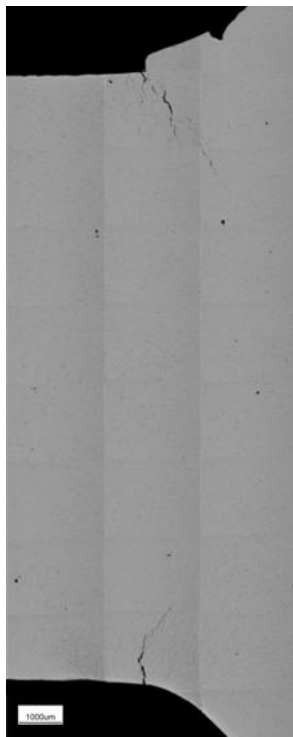
(108 µm)  
Equiaxed



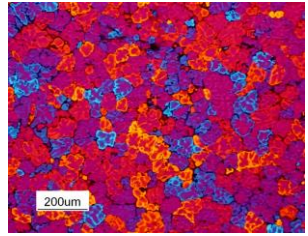
M206-3



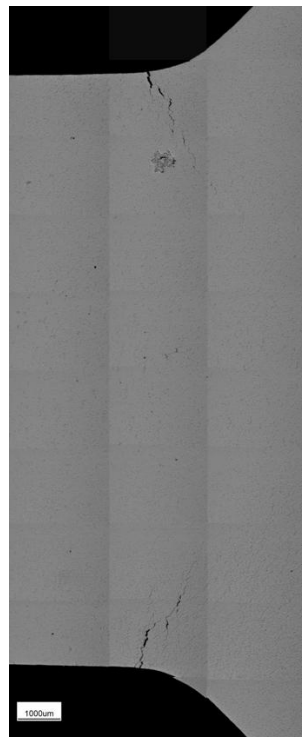
(57 µm)  
Equiaxed



M206-4



(47 µm)  
Equiaxed



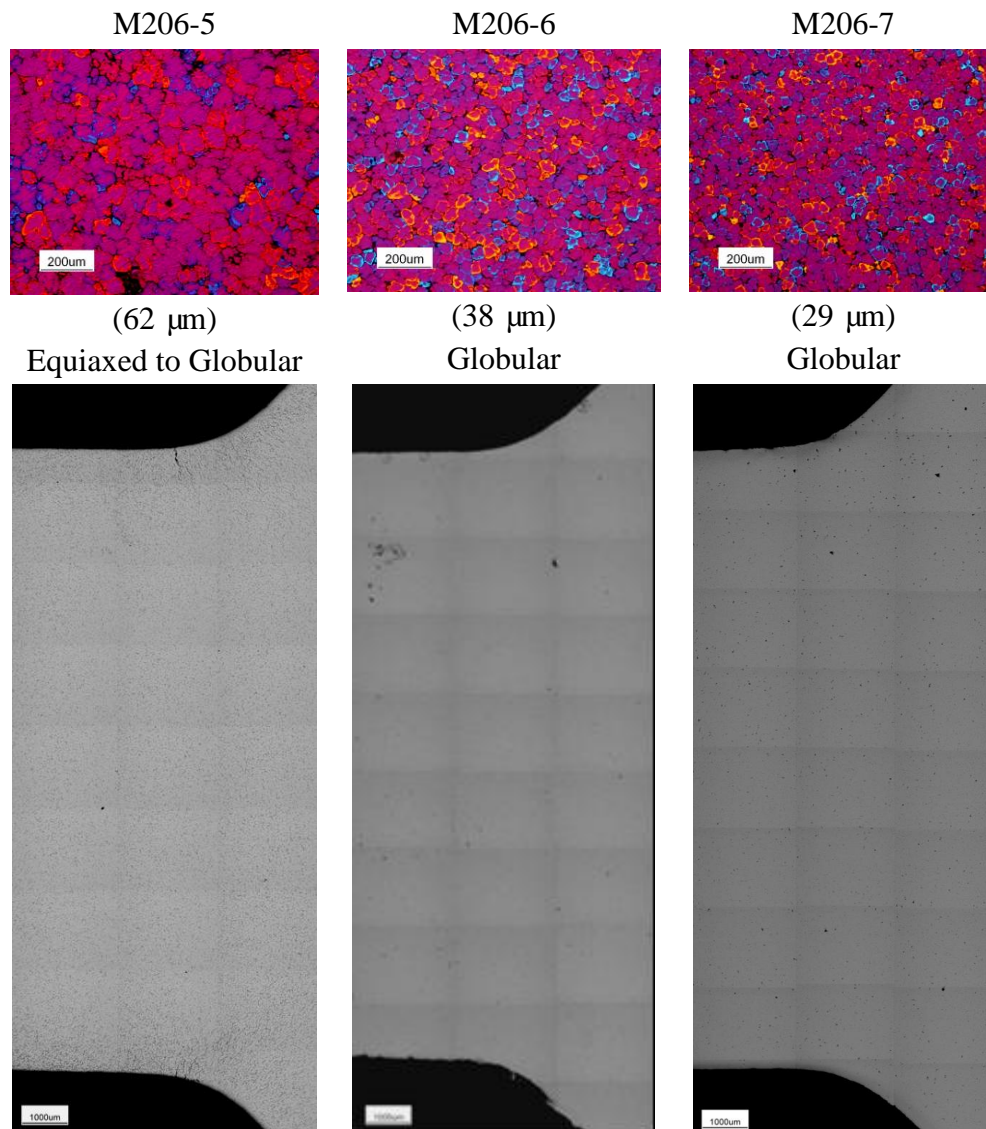


Fig. 5 - Mosaic optical micrographs showing hot tears in neck region and optical micrographs showing grain structure of M206 at different grain refinement levels.

### Temperature and Load Measurements

Load and temperature measurements were conducted for all the cases. Typical results are plotted in Fig. 6. It contains both load and temperature curves for three grain refinement conditions, unrefined M206 with columnar and equiaxed dendritic grains, M206-3 with equiaxed dendritic grains, and M206-7 with fine globular grains, for comparison.

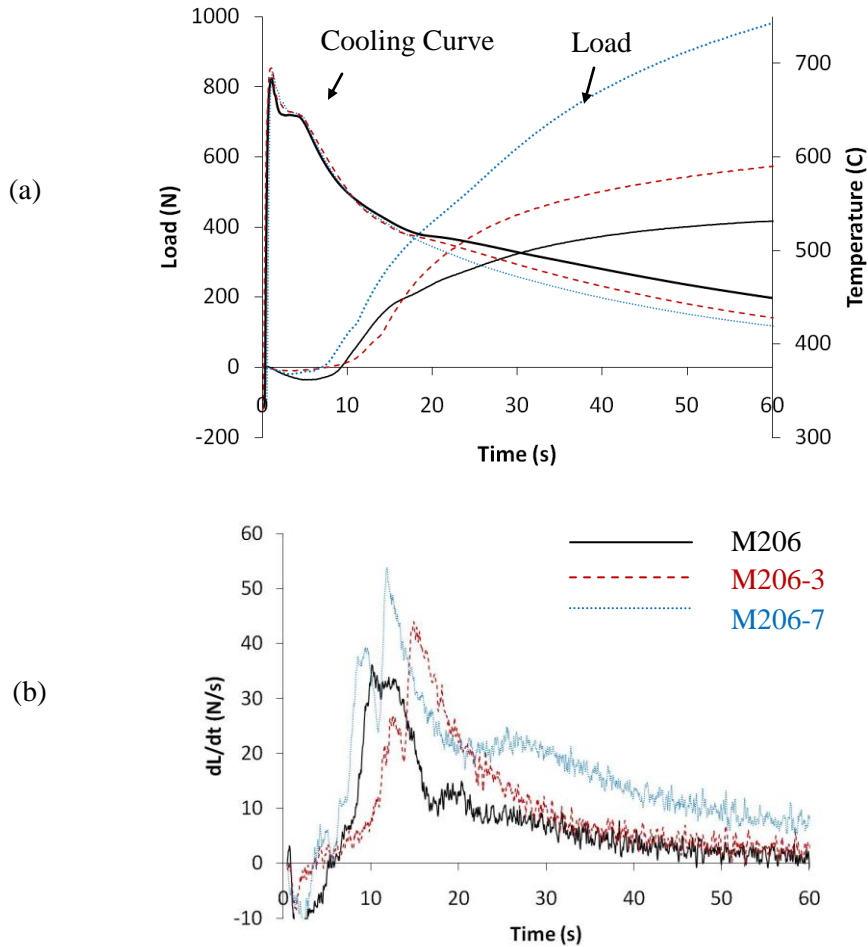


Fig. 6 - (a) Temperature and load development as a function of time for the alloys at different grain refinement levels (M206: unrefined, M206-3: 0.099% Ti and 20ppm B, M206-7: 0.149% Ti and 300ppm B), temperature measured at centerline of the rod at the riser end ( $T_{C1}$ );  
 (b) Derivative of load vs. time curves.

The load represents the tensile force developed in the rod due to solidification shrinkage and thermal contraction. Temperatures were measured at two locations  $T_1$  (riser side) and  $T_2$  (edge) at the centerline of the constrained rod as shown in Fig. 1 and 2. The temperatures at the same locations but on surface of the rod were also recorded in parallel tests. Only the temperature at centerline of the rod at location  $T_1$  was plotted in the figure. In all the curves time zero was normalized to correspond to the moment when the thermocouple 1 starts to react the increase of the temperature upon pouring. The first derivatives of load with respect to time were calculated and plotted, which represents the rate of load increase and pictorially demonstrate the variation

of load with time. In both of load and displacement measurements, slight decrease in the reading were observed shortly after pouring, possibly due to the melt pressure head.

Comparing and relating different curves, many pieces of information on hot tearing formation can be derived. The information includes the range of refilling the incipient cracks, load onset, crack (the finally shown open crack) initiation and propagation, and furthermore the remaining liquid fractions at these points. The information generated in this study is shown in Table 3. The fraction solids are determined using Pandat\* software with Scheil model. It was found from the first derivative curves that the load onset (the time at which the casting starts bearing tensile force) was delayed when equiaxed dendritic grains formed (M206-3). Then, it turned to start earlier when fine globular grains were formed (M206-7). The underlying mechanism is still not totally clear, but it should be related to both grain size and morphology of the casting, which affect the refilling of the incipient cracks at the early stage. The transition of columnar to equiaxed and refining equiaxed grains improve the uniformity of the grain structure and the intergranular liquid films. These improvements favor the feeding through interdendritic and intergranular channels and mass feeding and delay the formation of the continuous solid skeleton which can bear the tensile load. However, when the grains are getting finer, the intergranular liquid films become thinner, which would tend to facilitate the formation of the continuous solid skeleton which can bear tensile load, and thus load onset goes earlier.

Another observation as shown in Table 3 is that the load developed until non-equilibrium solidus generally increased with decreasing grain size. Since the load (contraction force) releases when hot tear forms, the load recorded would be smaller for castings more inclined to hot tear, in this case, for castings with larger grain size.

---

\* Pandat software is developed by CompuTherm LLC.



Table 3: Contraction Force (load) Measurement Data

Sample No.	Load onset: temp./ fraction solid (°C)/ $f_s$		Cracking initiation temp./ fraction solid (°C) / $f_s$		Load @ $T_{nes}$ (N)
	$T_{C1}/f_s$	$T_{SF1}/f_s$	$T_{C1}/f_s$	$T_{SF1}/f_s$	
M206 NGR	601/ 0.804	530/0.976	562/0.889	518/0.985	360
M206-2	571/ 0.887	520/0.984	553/0.899	514/0.987	337
M206-3	564/ 0.897	519/0.985	547/0.905	510/0.989	477
M206-4	597/ 0.829	529/0.978	555/0.898	516/0.986	654
M206-5	584/0.862	525/0.980	558/0.895	517/0.986	511
M206-6	598/0.830	529/0.978	*(572)/0.878	521/0.987	643
M206-7	630/0.602	536/0.961	*(580)/0.866	524/0.983	740

*NGR: Non-grain refined,  $f_s$ : fraction of solid,  $T_{nes}$ : non-equilibrium solidus,*

*$T_{C1}$ : temperature at the center of the rod,  $T_{SF1}$ : temperature at the surface of the rod.*

*\*: cracked but filled*

The results show that the effects of grain refinement on hot tearing are complex. The variations of both the grain morphology and size play important roles in hot tearing formation. The severity of hot tearing decreased significantly with grain refinement, which could be due to, first, grain refinement improves feeding; secondly, the structure can better accommodate the stress built-up in the mush with smaller grain size. On the other hand, the liquid film thickness between grains decreases, which would tend to decrease hot tearing susceptibility.

## CONCLUSIONS

- The effect of grain refinement was studied using a constrained rod mold which enables the simultaneous measurement of the load (contraction force)/ time/ temperature in a constrained casting during solidification and cooling. The experimental technique developed in this project is sensitive to investigate load development, the crack initiation and propagation.
- The crack area in the hot spot region for each grain refinement level was measured and used as hot tearing susceptibility index. The severity of hot tearing decreased significantly with grain refinement. It was affected by both grain size and morphology. Several factors might contribute to the improved resistance to hot tearing. First, grain refinement improves feeding; secondly, the structure can better accommodate the stress built-up in the mush with smaller grain size. On the other hand, the liquid film thickness between grains decreases, which would tend to decrease hot tearing susceptibility.

- Grain refinement was found to have a complex effect on load onset. This is related to both grain size and morphology of the casting, which affect the refilling of incipient cracks at early stage.

## ACKNOWLEDGEMENTS

The authors gratefully acknowledge the member companies of the Advanced Casting Research Center (ACRC) for their support of this work, and for their continued support of research focused on the science and technology of metal casting at Worcester Polytechnic Institute. The authors also would like to thank very much Jim Thomson, Geethe Nadugala and Stuart Amey of CANMET Material Technology Laboratory for their support during this work.

## REFERENCES

1. S. Li, K. Sadayappan, and D. Apelian: Characterization of hot tearing in Al cast alloys: methodology and procedures. Submitted to *Int. J. Cast Metals Res.*
2. D. G. Eskin, Suyitno, and L. Katgerman: *Progress in Materials Science*, 2004, vol. 49, 629-711.
3. W. I. Pumphrey and J. V. Lyons: *J. Inst. Met.*, 1948, vol. 118, 439-455.
4. M. Fortier, D. J. Lahaine, M. Bouchard, and J. Langlais: *Light Metals*, 2001.
5. M. Easton, J. Grandfield, D. StJohn, and B. Rinderer: *Materials Science Forum*, 2006, vol. 30, 1675-1680.
6. M. Easton, H. Wang, J. Grandfield, D. StJohn, and E. Sweet: *Materials Science Forum*, 2004, vol. 28, 224-229.
7. D. Warrington and D. G. McCartney: *Cast Metals*, 1991, vol. 3, 202-208.
8. F. Matsuda, K. Nakata, and Y. Shimokusu: *Transactions of JWRI*, 1983, vol. 12, 81-87.
9. T. W. Clyne and G. J. Davies: *The British Foundrymen*, 1975, vol. 68, 238-244.
10. R. A. Rosenberg, M. C. Flemings, and H. F. Taylor: *AFS Trans*, 1960, vol. 69, 518-528.

# Quantitative Investigation of Hot Tearing of Al-Cu Alloy (206) Cast in a Constrained Bar Permanent Mold

S. Li<sup>1</sup>, D. Apelian<sup>1</sup> and K. Sadayappan<sup>2</sup>

<sup>1</sup>Metal Processing Institute, WPI, Worcester, MA, 01609 USA

<sup>2</sup>CANMET- Materials Technology Laboratory, Ottawa, Ontario, K1A 0G1 Canada

## Abstract

The mechanisms of hot tearing are generally understood; inadequate feeding initiates the tear and further thermal deformation propagates the tear. However, a reliable experimental methodology/apparatus to quantitatively measure and characterize hot tearing is not available for the casting industry. In this study, a hot tearing apparatus with a load cell and LVDT developed at CANMET-MTL was used to measure the load and contraction in the mushy zone of an Al-Cu alloy. The onset of hot tearing can be determined from the load curve, its first derivative and cooling curve. The linear solidification contraction of the bar is measured. Alloy 206, which is an alloy that is quite prone to hot tearing was evaluated by the apparatus; results are given and discussed.

## Introduction

Hot tearing has been a perennial problem in metal casting and is prone to occur during solidification; it occurs when the alloy partitions and the multi-phases in the mushy zone have different capacity to accommodate strains. Hot tearing is alloy dependent and can be mitigated through casting design to reduce the strains. Over the years many researchers have addressed the fundamentals of hot tearing. Most notably, Pellini [1] developed a strain theory of hot tearing based on strain accumulation and the concept of liquid films. If the strain accumulated in the liquid film during solidification contraction is greater than a critical value, hot tearing occurs. Campbell [2] quantified Pellini's theory and expressed the strain ( $\epsilon$ ) in the hot spot by  $(\alpha\Delta T L) \cdot l^{-1}$  where L,  $\alpha$ ,  $\Delta T$  and  $l$  are respectively the length of the casting, coefficient of thermal expansion, length of mushy zone and length of hot spot. If the grain size is a, then the number of grains is

1/a. So the strain per grain boundary is  $(\alpha\Delta T L a).I^2$ . Clyne and Davies [3] pointed out that the strain can be accommodated during liquid and mass feeding, and will occur during the last stage of solidification. They reasoned that liquid feeding and mass feeding readily occur at liquid fractions of 0.6-0.1, and defined the time spent in this range as the stress-relaxation time,  $t_R$ . Strain accommodation during solidification may occur at liquid fractions of 0.1- 0.01. The time spent in this range is the vulnerable time ( $t_V$ ) when cracks may propagate. The Crack Susceptibility Coefficient (CSC) is the ratio of these two times; namely,  $t_V/t_R$ . Combining the CSC with the equation derived for the strain per grain boundary Campbell [2] modified and expressed it by the following:  $[(\alpha\Delta T L a).xI^2][ t_V/t_R ]$ .

In addition to the theoretical analysis and formulations, casting engineers have developed cast house tests to evaluate hot tearing tendency. Among these tests, the I-beam or dog bone type tests and ring mold tests are the classical tests [4], which do have certain limitations. The severity of hot tearing is usually measured by either the length or width of the crack; nevertheless, only a qualitative index can be obtained from such tests for assessing hot tearing tendency. The reader is referred to the excellent review by Eskin [4], which covers the various means of evaluating hot tearing tendency. Many other researchers have carried out extensive work in this arena [5-8] on a variety of systems and also in an attempt to quantify hot tearing tendency. Our colleagues at CAST have developed a quantitative method [9,10] to evaluate hot tearing particularly in direct chill castings and directional solidification.

In parallel, mathematical models for hot tearing have been pursued by many researchers [12 - 16], and these have been useful in our understanding of the complexity of the problem. However, a generic reliable hot tearing prediction model is still not available [4, 9]. The limitation of the models suggests the need for reliable quantitative input data, which are not easily available and need to be measured experimentally.

The objective of this work is to develop a simple *quantitative* test that can be used by both industry and in the research laboratory, and also to evaluate alloy and processing variables affecting hot tearing of Al based casting alloys. The team at MPI in USA and CANMET in Canada have collaborated on the development of such a foundry test that is easy to use and will yield quantitative data. The test method is similar with the one developed by Instone et al [9].

The latter was designed to simulate the DC casting process where two solidification fronts meet at the center of the casting and the load is generated at the semi-solid center, while the test method presented in this study is developed to reproduce shape casting processes. Due to the space limitations, only a description of the apparatus and analyses of results are given. The quantitative effects of processing variables on hot tearing determined by the apparatus are not given in this paper.

## **Experimental**

Instrumented Constrained Rod Mold: The constrained rod mold used in this study was developed at CANMET Materials Technology Laboratory (MTL) and designed to measure the load or shrinkage/contraction developed during solidification. Figure 1 is a schematic diagram showing the components of the apparatus. Figure 2 is an exploded view of the mold plate. Two different molds are available, one made of copper and the other made of H-13. The results presented here were carried out using the copper mold. The mold temperature is controlled precisely with heater plates. Different castings dimensions can be obtained by replacing the inserts (shown in Figure 2). The test piece has two arms. One test arm is constrained at one end with threads to keep the bar from contraction; this causes tension to be developed and hence cracking is induced during solidification. The other arm is for temperature and load/displacement measurement with one end connected to a load cell or linear variable differential transformer (LVDT). The LVDT is unrestrained and can move horizontally (Figure 4) while the load cell will offer a resistance (Figure 3) and cause cracking in the casting. The casting rod was designed with a slight taper to reduce friction between the mold and casting. Two K-type thermocouples are used for the temperature measurement of the casting. One is positioned at the riser end (T1) and the other at the end of the rod (T2) as shown in Figure 3 and 4.

After pouring the melt into the mold, temperatures and load/displacement were recorded by a PC-based NI (National Instrument) data acquisition system. The system consists of SCXI-1303 terminal block, PCI-6043E interface card and LabVIEW software (DASYLab). The data was acquired at a rate of 100HZ to 200HZ.

Melting and pouring: Al-Cu alloy 206 was slightly modified to ensure that it did not contain Ti and was tagged as M206. Approximately 25lbs of the alloy was melted in an induction furnace.

The molten metal was well degassed. Graphite lubricant spray was applied to reduce the friction between the mold wall and the casting. The constrained rod castings were poured with about  $\sim 100$  °C superheat. The mold was preheated to  $200 \pm 2$  °C before pouring.

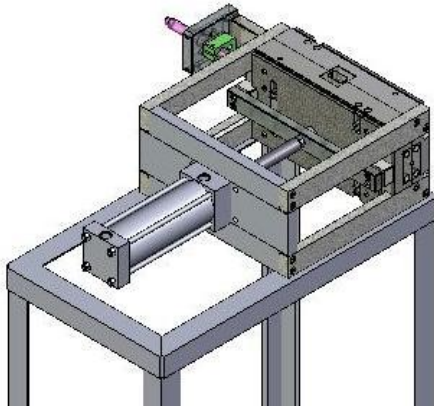


Figure 1: Copper Mold Assembly

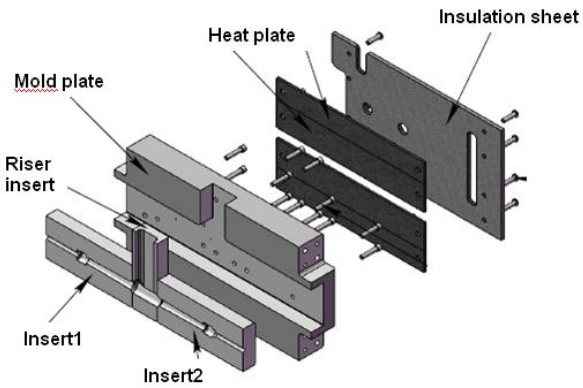


Figure 2: Mold Plate Exploded View

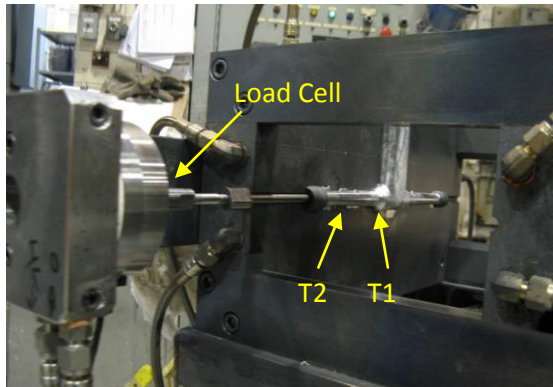


Figure 3: Load cell setup

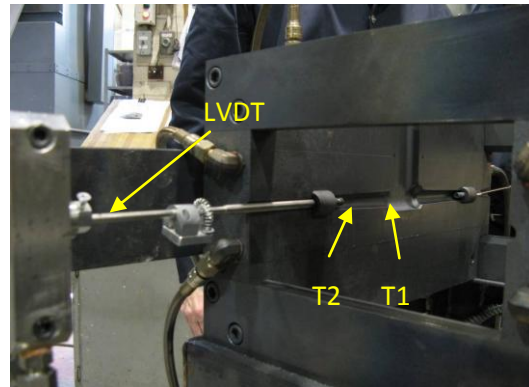


Figure 4: LVDT setup

## Results and Discussion

Figure 5(a) shows the cooling and load curves for alloy M206 tested at a mold temperature of  $200^{\circ}\text{C}$ . The two temperatures were recorded with the thermocouple tips located at T1 (riser side) and T2 (edge) shown in Figures 3 and 4, and at the centerline of the constrained rod. The temperatures at the surface of the rod can also be obtained in parallel testing. Time zero corresponds to the moment the thermocouple 1 starts to record the increase of the temperature

upon pouring. Figure 5(b) shows the derivative of load vs. time curves. The measured displacement is shown in Figure 5(c).

From Figure 5(a), the load started to develop at three seconds and increased with time but levelled off to about 20N at 5 seconds. This can also be seen in its first derivative curve. The rate changed abruptly to 0 at about 5 seconds, suggesting the occurrence of severe cracking. At three seconds, the temperature at riser side (T1) is around 616°C, in which the solid fraction is around 0.72 by Pandat Scheil simulation. Also at three seconds, the temperature near the end of the casting (T2) is ~ 520°C when the solid fraction is about 0.97. According to Beackerud et al [17], when alloy A206.2 is solidified with a cooling rate of 0.6°C, coherency is achieved around 641°C when the fraction solid is 30%. The temperatures at the surface of the casting close to the riser location and at the end are 397°C and 378°C, respectively. This indicates that a solid shell was formed very quickly after pouring; hence it is possible for the load transfer to occur early on the solidification journey. The temperature of the crack position was not measured, but it can be obtained by solidification simulation as the temperature of T1 and T2 are known. Modelling efforts are being carried out with commercial casting simulation software Magma. Photographs showing hot tearing location and severity in constrained rod casting) are shown in Figure 5(d). From Figure 5(c), we can note that shrinkage/contraction starts at around 2 seconds and increases rapidly during solidification and cooling. Because of the high cooling rate (in excess of 30°C/s in the case of mold temperature of 200°C), the end temperature of solidification is difficult to infer from the curve. The end temperature of 206 is about 491°C at a cooling rate of 4.5°C/s [17]. The end point in this test should be slightly lower than 491°C given such a high cooling rate. From the data and the curves, solidification was complete at around 8 seconds. The total linear shrinkage/contraction (displacement) of the solidification range is around 0.3mm compared to the length of the rod of 75mm. This displacement is expected to correlate to hot tearing susceptibility of the alloy.

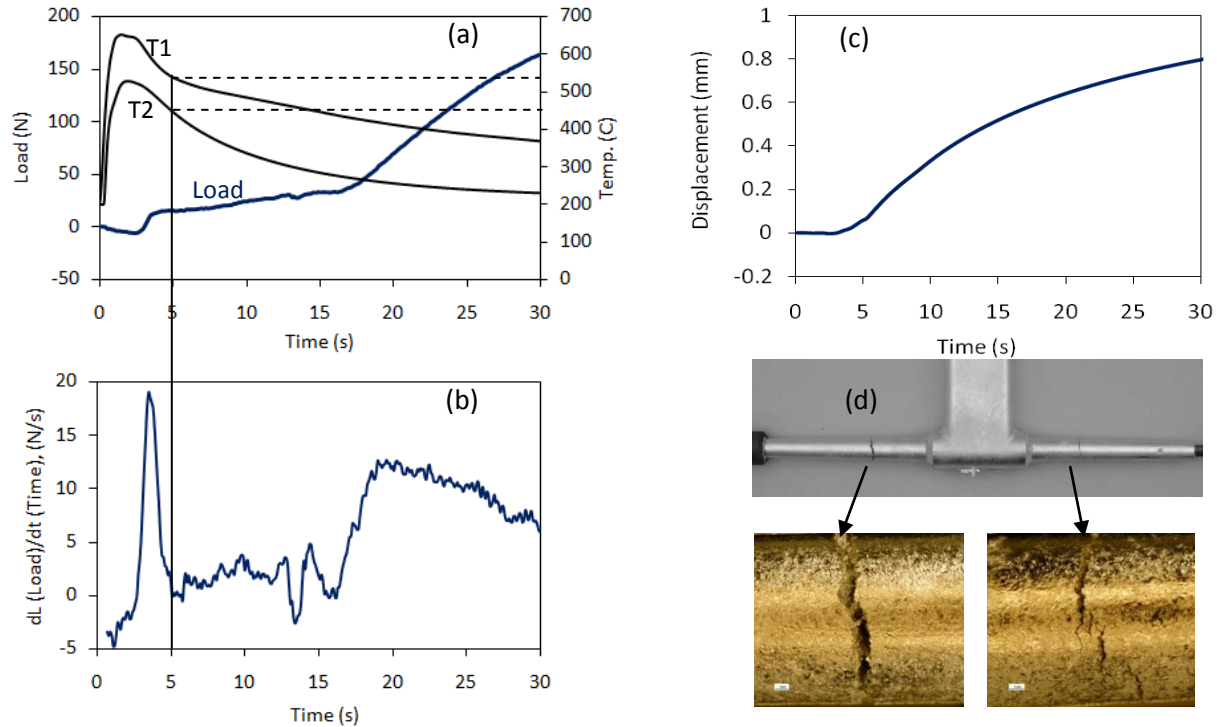


Figure 5: (a) Temperatures and load development as a function of time, T1 and T2 are thermocouples defined in Figure 3 and 4; (b) Derivative of load vs. time curves; (c) Measured displacement as a function of time; (d) Photographs of the constrained castings.

It seems that the load point does not necessarily correspond to the LVDT movement. The load starts recording only when coherency is achieved in the hot spot, but shrinkage/contraction can begin in the unrestrained rod and coherency is not required. The important contribution of this work is the development of a measurement device (as well as the process) to quantitatively evaluate hot tearing in Al alloys. Now that the measurement device has been established (verified and validated), we are carrying out a host of experiments to evaluate alloy and processing variables affecting hot tearing.

## Conclusions

1. Constrained rod mold with load cell/LVDT was used to characterize and quantify the contraction behavior of alloy 206 during solidification.
2. Onset of hot tearing can be determined from load curve, its first derivative and cooling curve. The amount of shrinkage/contraction can be quantitatively measured.



3. The load point does not correspond to the LVDT movement. The load starts recording only when coherency is achieved in the hot spot. But shrinkage/contraction can begin in the unrestrained rod and coherency is not required.
4. Work is continuing between WPI and CANMET, and we intend to have a LMT project on hot tearing bringing together with the partners of the Alliance.

### **References**

- [1] Bishop, H.F., Ackerlind, C. G. & Pellini W. S. (1952) Metallurgy and mechanics of hot tearing, AFS Trans, 60,818-833
- [2] Campbell J. (1991) Castings, Oxford: Butterworth-Heinemann
- [3] Clyne, T.W. & Davies G.J. (1975) A quantitative solidification test for castings and an evaluation of cracking in aluminium-magnesium alloys, The British Foundryman, 68, 238.
- [4] Eskin, D.G., Suyitno, & Katgerman, L. (2004) Mechanical properties in the semi-solid state and hot tearing of aluminum alloys, Progress in Materials Science 49, 629-711
- [5] Hamaker J.C. & Wood W.P. (1952) Influence of phosphorus on hot tear resistance of plain and alloy gray iron, AFS Trans, 60, 501-510
- [6] Eeghem J. V. & Sy A. D. (1965) A contribution to understanding the mechanism of hot tearing of cast steel, AFS Trans, 73, 282-291
- [7] Metz S. A. & Flemings M.C. (1970) A fundamental study of hot tearing, AFS Trans, 78, 453-460
- [8] Guven Y.F. & Hunt J.D. (1988) Hot-tearing in aluminum copper alloys, Cast Metals, 1, 104-111
- [9] Instone S., StJohn D. & Grandfield J. (2000) New apparatus for characterizing tensile strength development and hot cracking in the mushy zone, International Journal of Cast Metals Research, 12(6), 441-456
- [10] Viano D., Stjohn D., Grandfield J. & C áceres C. (2005) Hot tearing in Aluminium-Copper alloys, Light Metals, Edited by Halvor Kvande TMS (The minerals, Metals and Materials Society)
- [11] Cao G. & Kou S. (2006) Hot tearing of Ternary Mg-Al-Ca Alloy castings, Metallurgical and Materials Transactions A, 37A, 3647

- [12] Prokhorov, N.N. (1962) Resistance to hot tearing of cast metals during solidification. Russian Castings Production, 2, 172-175
- [13] Novikov, I.I. (1966) Goryachelomkost tsvetnykh metallov i splavov (Hot Shortness of Nonferrous Metals and Alloys), Nauka, Moscow,
- [14] Katgerman, L. (1982) A mathematical model for hot cracking of aluminum alloys during DC casting, J. of Metals. 34, 46-49
- [15] Rappaz, M., Drezet, J.-M. & Gremaud, M. (1999) A new hot tearing criterion, Metallurgical and Materials Transactions A, 30A, 449
- [16] Stangeland, A., Mo, A., M'Hamdi, M., Viano, D. & Davidson, C., (2006) Thermal strain in the mushy zone related to hot tearing, Metallurgical and Materials Transactions A, 37A,705
- [17] Backerud et al., Solidification Characteristic of Aluminum Alloys, Vol 2, Foundry Alloys, published by AFS

### **Acknowledgments**

The authors gratefully acknowledge the member companies of the Advanced Casting Research Center (ACRC) for their support of this work, and for their continued support of research focused on the science and technology of metal casting at Worcester Polytechnic Institute. The authors also would like to thank very much Mr. Geethe Nadugala and Stuart Amey of CANMET Material Technology Laboratory for their support to this work.

# **CASTABILITY MEASURES FOR DIECASTING ALLOYS: *FLUIDITY, HOT TEARING, AND DIE SOLDERING***

B. Dewhurst, S. Li, P. Hogan, D. Apelian

Metal Processing Institute  
WPI, 100 Institute Road  
Worcester, MA 01609 USA

## **ABSTRACT**

Tautologically, castability is a critical requirement in any casting process. Traditionally, castability in sand and permanent mold applications is thought to depend heavily on fluidity and hot tearing. Given capital investments in dies, die soldering is a critical parameter to consider for diecasting. We discuss quantitative and robust methods to insure repeatable metal casting for diecasting applications by investigating these three areas. Weight reduction initiatives call for progressively thinner sections, which in turn are dependent on reliable fluidity. Quantitative investigation of hot tearing is revealing how stress develops and yields as alloys solidify, and this has implications on part distortion even when pressure-casting methodologies preclude hot tearing failures. Understanding the underlying mechanism of die soldering presents opportunities to develop methods to avoid costly downtime and extend die life. Through an understanding of castability parameters, greater control over the diecasting process can be achieved.

**Keywords:** *Castability, Die Soldering, Fluidity, Hot Tearing, Part Distortion, Residual Stress*

## **INTRODUCTION**

Over the years, castability has been addressed through various angles and perspectives. However no matter what has been accomplished, it is fair to state that at the present there is not a single method that the community can point to as a means of defining an alloy's castability in terms of

measurable quantitative parameters. It is critical that means for controlling the casting process be developed. Without robust measures, one will not be able to control the casting process. It is the latter that is the motivating force behind this project. Hopefully, the investigative techniques being developed in this research will become standardized so that an accepted lexicon and methodology is practiced throughout the casting community.

This paper will focus on three parallel lines of research with applicability to light metals diecasting: Fluidity, Hot tearing (as it relates to stresses developing within solidifying metals as a function of chemistry and microstructure), and die soldering. Each of these three areas of research has the potential to positively benefit the HPDC industry, either directly or as an accompanying benefit to research conducted for other purposes. Vacuum fluidity testing allows for the evaluation of various alloys and process modifications in a laboratory setting under rapid solidification conditions, but suffers from a poor reputation and, as a consequence, has principally been used for qualitative experimentation. Hot tearing, a consequence of stresses developing during feeding until the casting tears itself apart, is not found in alloys used in HPDC, but the investigative techniques being applied to understand hot tearing are providing a window into how these stresses develop. Die soldering is important because, in improperly designed castings, soldering can be a significant problem that can severely inhibit productivity.

## **FLUIDITY**

Fluidity is a material's ability to flow into and fill a given cavity, as measured by the dimensions of that cavity under specified experimental conditions, and fluidity is heavily dependent on heat flow during solidification.

Investigations into the impact of foundry variables such as mold coatings, alloying additions, head pressure, and especially superheat have been investigated and correlated with mechanisms. For sand and permanent mold castings, it is abundantly clear that increasing solidification range results in decreasing fluidity (all other factors being equal). Specific investigations are often alloy or metal/mold/coating specific in scope, but very subtle influences of minor variations in alloy purity can be detected. There is some question as to whether these trends transfer over to die casting, and that question will be the focus of our discussion.

Thanks in large part to the work of Ragone in developing his vacuum testing apparatus, which Flemings et al. built upon, fluidity has seen great advances since Ragone's 1956 doctoral thesis [1-6]. Over a period of 8 years, Flemings and collaborators produced the fluidity equations and solidification mechanisms which are at work in linear castings during standard fluidity tests.

Ragone demonstrated that the influence of viscosity or a change in viscosity on (casting) fluidity was minimal, and while the equations he presented did include a viscosity term, subsequent formulations correctly dropped it as insignificant as compared with other sources of experimental error [1].

The fluidity equation from Flemings [3], for metal with some superheat  $T$  and a mold which conducts heat rapidly is given below as **Equations 1 and 2**.

$$L_f = \frac{(p^*a * V_o)(\lambda H + c' * \Delta T)}{2 * h * (\bar{T} - T_o)} \quad (1)$$

$$\lambda = \left(\frac{c'}{H}\right) * \frac{L_f}{dL_f/dT} \text{ evaluated at } T_m \quad (2)$$

Where:

$L_f$	final length, fluidity
$a$	channel radius
$k$	critical solid concentration
$c'$	specific heat of liquid metal
$T_o$	ambient environmental temperature (room temperature)
$T$	superheat
$\rho$	density of metal
$V_o$	velocity of metal flow
$H$	heat of fusion of metal
$h$	heat transfer coefficient at mold-metal interface
$\bar{T}$	the time average melt temp in the fluidity test
$T_m$	metal melting temperature
$T'$	temperature of superheated metal entering flow channel
	critical solid concentration required to stop flow in 'mushy' alloys

Flemings reports that the critical solid concentration is between 0.2 and 0.3 fraction solid, and Campbell gives 0.5-0.6 using slightly different criteria [4,7,8]. This is the fraction solid where, as will be discussed under flow stoppage mechanisms, the flow is choked off. Attempts to tie this choking off to dendrite coherency by Dahle, as explored by Backerud, were inconclusive. He did not find an unambiguous impact of dendrite coherency measurements on fluidity [9-11]. The specific fraction solid at which this takes place varies with alloy composition and solidifying phase morphology. This critical fraction solid is likely to be higher for die casting due to the increased pressure involved, but the extent of increase is likely to depend on alloy-specific morphology characteristics. Much work on the relevant solid fractions where flow is possible has been carried out in the area of SSM, both in terms of alloy rheology and thermodynamics, and this may have much to contribute in understanding how this factor changes according to the specific casting and alloy conditions [12].

Past work in the field has focused on maximizing fluidity, however we believe that decreasing the variations in fluidity is as important as determining under which conditions fluidity is maximized. There are two main aspects to variation in fluidity:

- ⇒ One is the standard deviation of test methods used in the lab to determine fluidity.
- ⇒ The other is the range over which fluidity values will vary in a real casting environment where alloy chemistry, temperature controls, etc. vary within some range.

Given the high part numbers involved in die casting, questions of repeatability are especially important. Thin sections are desirable for a variety of reasons, and can be achieved with increased mean fluidity, but if that increase is coming at the expense of increased fluidity variation, this will have the undesirable effect of increasing scrap rates. Often, the factors which can be adjusted to improve fluidity have other impacts on the casting process, and so a careful tradeoff must be achieved between insuring there is enough fluidity (and a margin of safety) without causing deleterious side-effects. Greater fluidity is often achieved by increasing melt superheat, but as will be discussed below, this has negative implications for die soldering. Mold coatings can decrease the heat transfer coefficient, and thus increase fluidity, but this may have a small negative impact on cycle time. While minor alloy additions often have little impact on fluidity, the secondary alloy components (specifically, their heat of fusion and morphology) do contribute to fluidity.

Our work to improve the laboratory testing of vacuum fluidity measurements is largely focused on improving the repeatability of measurements by controlling the various experimental parameters. After a controlled volume of melt is collected, a thermocouple is inserted into it. When the metal cools to a pre-set temperature, it is elevated such that the end of a borosilicate tube is immersed in the melt, and vacuum is applied. The measurement of that length is then made before the pyrex tube is removed from the experimental setup, as the rapid fracturing of the glass and other factors otherwise make it difficult to determine the ‘zero point.’ Through repeated measurements under controlled experimental conditions we are establishing the reliability of the test.

A continuing trend in all of engineering, including metal casting, is the application of modeling software to problems of interest. These codes, in the case of casting intended to predict filling, hot spots, etc. are no more reliable than the data upon which they are built. It is hoped that increased precision of fluidity testing will have a positive impact on these modeling codes by allowing direct comparison of simple geometries in both simulation and the laboratory. Since these codes do not include direct fluidity calculations, accurate experimental tests of fluidity would seem to be a good independent check.

## **HOT TEARING AND INTERNAL STRAIN**

Though hot tearing is a casting phenomenon that occurs in sand castings and processes where the solidification rate is slower than in die-castings, the mechanism of stress distribution during solidification is appropriate for discussion in high integrity castings. This is more so than ever now that we can measure and quantify stresses during solidification. Material behavior during solidification is what matters.

Campbell [7] defines a hot tear as a uniaxial tensile failure, which results in cracks on the surface or inside the casting. Alloys having a wide freezing range have a higher tendency to hot tear. Variables that influence hot tearing include alloy composition and processing variables [13,14].

Hot tearing susceptibility of alloys is greatly influenced by solidification behavior of molten metal in the mushy zone. Solidification can be divided into four stages [15]: (i) Mass feeding where the liquid and solid are free to move; (ii) Interdendritic feeding when the dendrites begin to contact each other, and a coherent solid network; (iii) Interdendritic separation. With increasing fraction solid, the liquid network becomes fragmented. If liquid feeding is not adequate, a cavity may form. As thermal contraction occurs, strains are developed and if the strain imposed on the network is greater than a critical value, a hot tear will form and propagate. Lastly, in stage (iv), Interdendritic bridging or solid feeding occurs. Simply stated, hot tearing occurs if the solidification shrinkage and thermal deformation of the solid cannot be compensated by liquid flow.

Measuring the development of strains and the evolution of hot tearing during solidification is not trivial. The Metal Processing Institute is a member of the Light Metals Alliance, and we have teamed up with our alliance partner CANMET to address hot tearing in aluminum alloys. The constrained bar mold used in this study was developed at CANMET Materials Technology Laboratory (MTL) and designed to measure load and temperature during solidification. **Figure 1** shows one of the mold plates and testing setup. The mold is made of cast iron and coated with insulating mold wash. The test piece has two arms. One test arm (12.5mm) is constrained at one end with heavy section (22.5mm) to keep the bar from contraction, so the tension will be developed and hence cracking could be induced during solidification. The other arm is for load and temperature measurement with one end connected to a load cell. This opened end of the mold is closed with a graphite cylinder block which can move freely in horizontal direction. The block is connected to the solidifying material on inner side with a screw and on external side with a load cell. Two K-type thermocouples are used for the temperature measurement. One is positioned at the riser end and the other at the end of the bar as shown in **Figure 1**. After pouring the melt into the mold, the temperature and load were recorded with a computer data acquisition system.



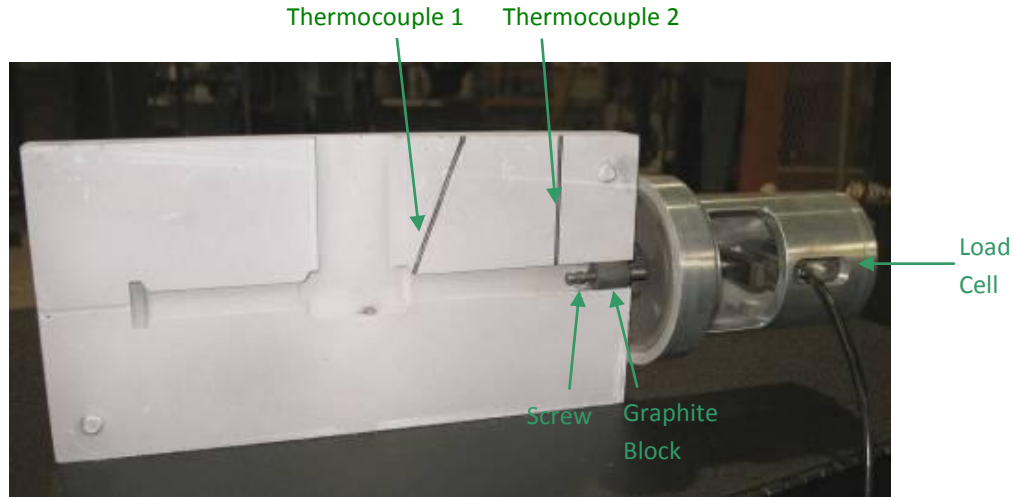


**Figure 1:** Cast Iron Mold designed to detect the onset of the hot tearing

Commercial cast alloy 713 and 518 were evaluated; the former is known to be sensitive to hot tearing, and the latter has good resistance to hot tearing. The pouring temperature was set at 60°C above the melting point of the alloy during this effort. The mold temperature was maintained around 200°C.

**Figures 2** and **3** show the measured temperatures and load recorded during casting as a function of time for alloy 713 and 518 respectively. The load represents the tension force developed in the casting during solidification. The cooling curve T1 was recorded with thermocouple tip positioned at the riser end and T2 with thermocouple tip at the end of the bar as shown in **Figure 1**. A rapid rise in temperature (both curves) was observed immediately after pouring and the temperature started falling shortly. It's noticed that negative loads (compressive forces) were developed shortly after pouring for the tests, probably due to the pressure head of the melt [16]. When the rod begins to solidify but cannot contract freely, the tension force increases. **Figure 2(b)** and **3(b)** are derivatives of load vs. time curve to determine onset of hot tearing. An obvious change in the rate suggests that cracking might occur there.

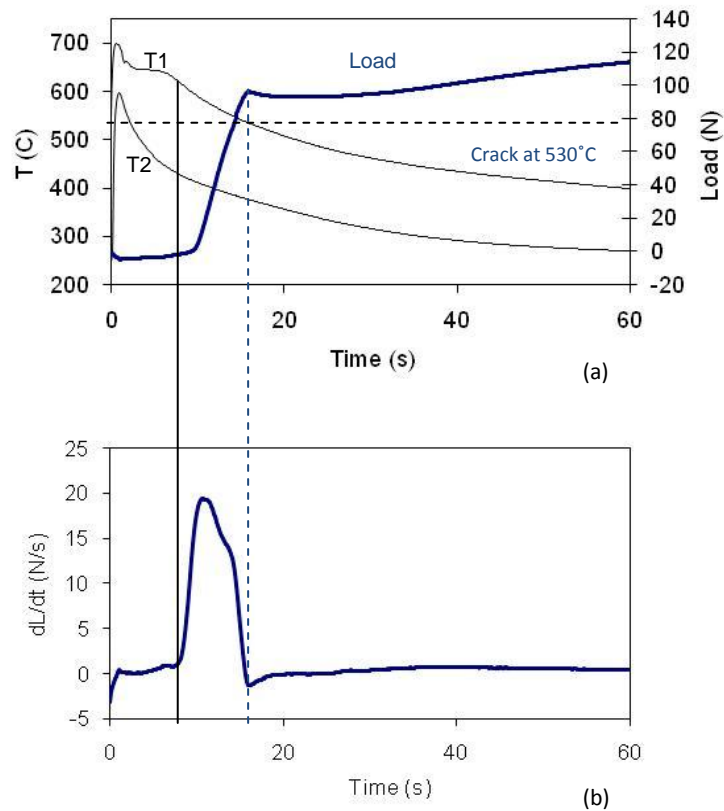


**Figure 2:** (a) Temperature-load-time curves of alloy 713;  
 (b) Derivative of Load vs. time curve.

From **Figure 2b**, load began developing at proximately 9 seconds and the solidification temperature was around 617°C (**Figure 2a**), then increased rapidly. It is shown that the rate changed abruptly to zero at 16.5 seconds, suggesting a severe tear occurred there. Hot tearing occurred at around 530°C, corresponding to 94% solid, according to Pandat Scheil solidification calculation.

The technique developed to measure hot tearing tendency is a valuable tool to differentiate between alloys and to use it to optimize alloys for high integrity castings.

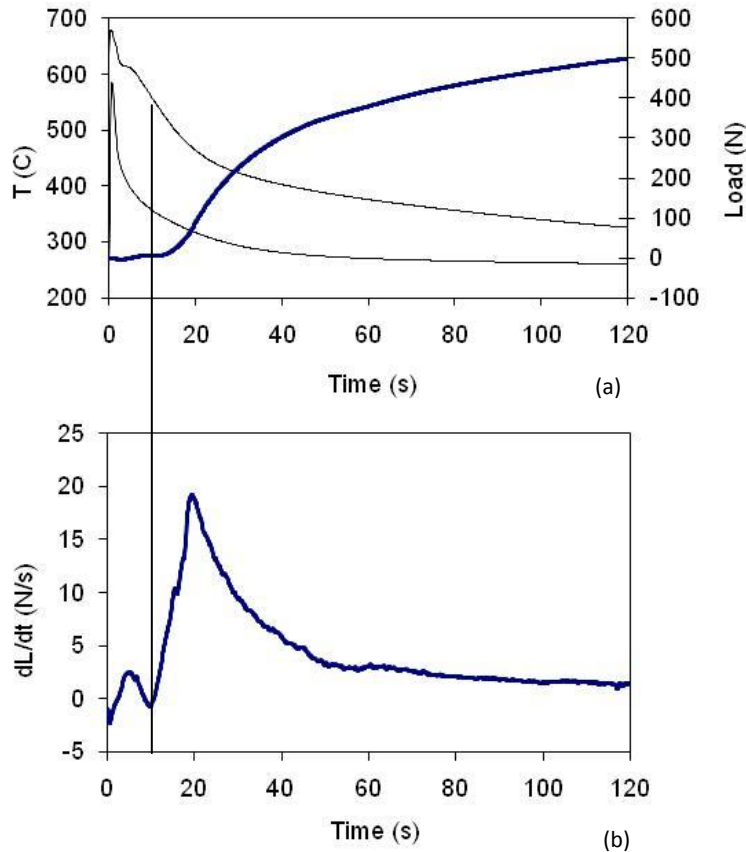


**Figure 3:** (a) Temperature-load-time curves of alloy 518;  
 (b) Derivative of Load vs. time curve.

**Figure 3:** shows the temperature-load-time curves of alloy 518. The load started to develop at 10 seconds, and then increased smoothly with time. No abrupt change of rate was observed, suggesting no crack would occur during solidification. The difference between the load curves of alloy 713 and 518 reveals different hot tearing susceptibility between the two alloys.

## DIE SOLDERING

Die soldering occurs when the cast aluminum alloy comes into contact with die steel. Due to the natural affinity of iron and aluminum, a reaction occurs at the surface which results in the formation of intermetallic phases. Over a series of shots, a significant amount of aluminum becomes stuck to these phases at the die surface, and the resulting cast part can begin to miss

critical tolerances or to lose integrity. At this point, the die must be shut down and cleaned, which is an expensive process when it occurs too frequently. It is estimated that 1 to 1.5% of variable overhead is directly attributed to die soldering in casting plants.

With such a large economic effect on the casting process, it is clear why die soldering needs to be controlled. There are several ways in which this can be achieved. These can be broken down into three groups, which will be discussed further below: *melt chemistry, process conditions and the die surface condition.*

The chemical composition of an alloy can have a dramatic effect on soldering behavior. The importance of alloy chemistry was shown at WPI's Metals Processing Institute by Sumanth Shankar [17]. In his experiments, he dipped H13 steel pins in 380 alloy and rotated them to simulate the drag force experienced at the surface of the die during injection of the metal. After dipping, the thickness of the intermetallic layers that had formed on each sample was analyzed as a measure of soldering tendency. His results showed that small additions of Sr and Ti (0.004% and 0.125%, respectively) had a much greater effect on soldering tendency than the time of dipping (30 to 75 seconds) or the temperature of the melt (1150 to 1250F).

To further expand on this discovery, Shankar performed another set of experiments to test the effects of a much wider range of alloying elements. The main effects are shown in **Figure 4**.

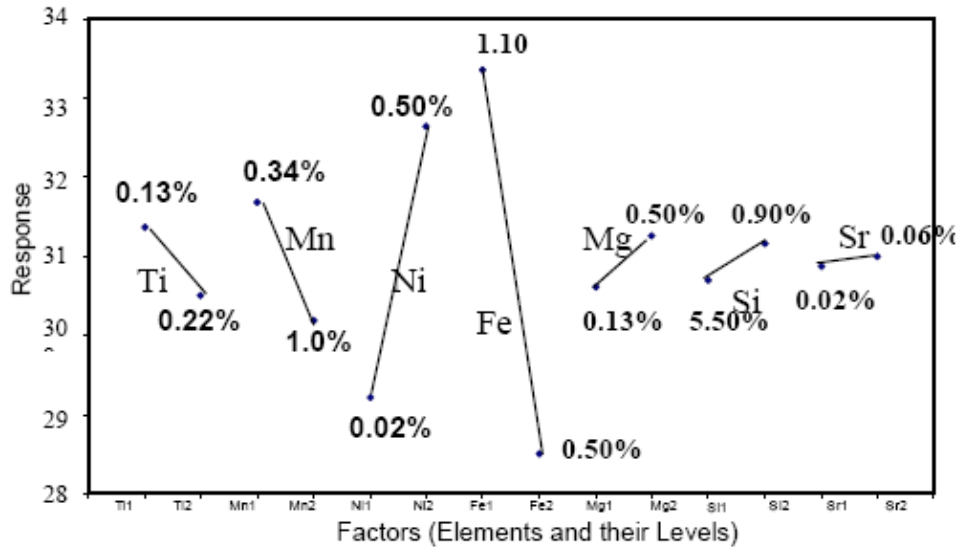


**Figure 4:** Main effects plot of the effect various alloying elements on die soldering. Iron, Manganese and Titanium show strong positive effects on reducing soldering, while Nickel promotes soldering [17].

Not surprisingly, iron had the greatest effect of any alloying element in the study on reducing die soldering. Iron has long been added to die casting alloys in order to reduce the die soldering tendency of alloys. It is well known that alloys with insufficient iron content (<0.8-0.9%) will solder readily to the die under the right conditions. A look at the phase diagram in **Figure** shows that the solubility of iron in aluminum with 10% silicon at typical casting temperatures is quite low, around 2-3%. At temperatures where the melt is likely to be in contact with the die, this solubility drops even lower. Therefore, even at low concentrations the presence of iron in the melt reduces the chemical potential gradient of iron from the steel to the melt significantly and slows the reactions that occur at the surface.

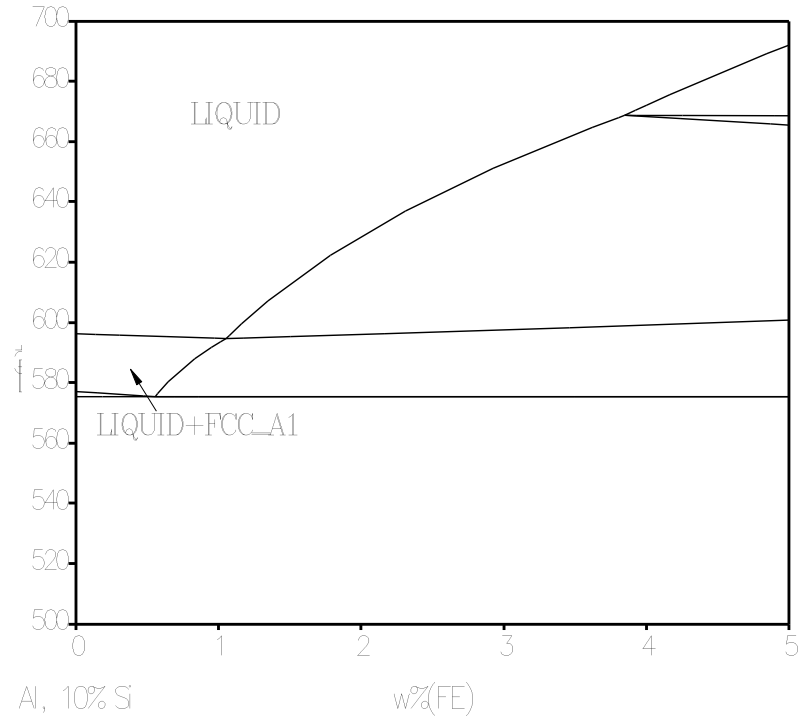


**Figure 5:** Phase diagram of Aluminum-10% Silicon and low solubility of Fe .

Of the other alloying elements, strontium also has the potential to help control die soldering, in addition to its common use as a eutectic modifier. In industrial trials a small strontium addition was shown to reduce die soldering by more than 20%. The effect is not apparent in the main effects plot above because both of the levels selected were at or above the critical concentration.

The mechanism behind this reduction has to do with the effect strontium has on the viscosity and surface tension of the alloy. As **Figure 6** shows, the addition of strontium changes the apparent viscosity and subsequently the surface energy of the alloy. This causes a reduction in the ability of the alloy to wet the die surface and reduces the contact area and the reaction between the two.

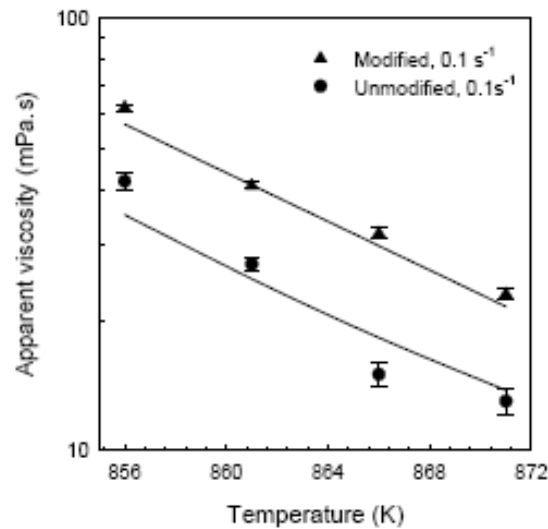


**Figure 6:** Change in viscosity of an Al-Si alloy with the addition of 230ppm Sr [18].

High temperatures and high melt velocity are process conditions which lead to soldering. Of the two, high temperature is the most important to avoid in order to prevent soldering. This can most effectively be done through careful design of the die. By configuring the part and optimizing the design of the die cooling system, the potential for soldering can be greatly reduced. It is very important to consider this during the design phase of a die because once a die is manufactured it is very difficult to reduce any hot spots. Other potential solutions include using additional spray in the high solder areas to reduce temperature or the use of inserts with high conduction coefficients

Impingement velocity is important to control as well. The die surface should be coated with lubricants and is likely oxidized from prior treatment. A high impingement velocity can wash these protective coatings off of the die surface, exposing the die steel to the aluminum alloy and begin erosion of the die surface. Both of these effects will promote the beginning of die soldering.

SSM processing can help to reduce both the temperature and velocities apparent in the casting system, and should help reduce die soldering [12].

Die coatings can be useful as a diffusion barrier between the steel in the die and the aluminum in the cast alloy. An effective coating must be able to withstand the harsh conditions at the surface of the die, however. Coatings which are sometimes used include CrN+W, CrN, (TiAl)N and CrC

[19]. Additionally, surface treatments such as nitriding and nitro-carburizing can help to strengthen the surface and prevent erosion, which accelerates the soldering process by roughening the surface and creating local temperature excursions at the peaks of the die surface which solder very quickly.

Accurate modeling of the casting process during the design phase is very important to an effective control against die soldering. All of the previously mentioned controls require additional cost during the design and manufacturing of the die, and it must be understood how badly soldering will affect the process before the costs of any of those controls can be justified.

## **CONCLUSIONS**

Though these three alloy characteristics seem tangentially related, they are factors that influence castability. In order to control these castability indices, it is necessary to develop experimental methods until robust quantitative analysis is possible. Once quantitative data can be extracted, the improvement in our understanding will occur. In the case of die soldering, multiple possible avenues to reduce the problem have been identified. Even when the initial intention was to resolve problems occurring in sand and permanent mold castings, such as hot tearing, the information gleaned about how stresses develop in liquid metal has wider applicability. Though die casting usually assures good fluidity through the use of pressure, if fluidity (and the factors which influence its variation) are well understood, it is possible to operate within tighter processing windows.

## **REFERENCES**

- 1) D.V. RAGONE, C.M. ADAMS, H.F. TAYLOR, AFS Trans. 64, (1956), p.640.
- 2) D.V. RAGONE, C.M. ADAMS, H.F. TAYLOR, AFS Trans. 64, (1956), p.653.
- 3) M.C. FLEMINGS, Brit. Foundryman 57, (1964), p.312.
- 4) M.C. FLEMINGS, Solidification Processing. McGraw-Hill, New York (1974).
- 5) M.C. FLEMINGS, E. NIYAMA, H.F. TAYLOR, AFS Trans. 69, (1961), p.625.
- 6) J.E. NIESSE, M.C. FLEMINGS, H.F. TAYLOR, AFS Trans. 67, (1959), p.685.
- 7) J. CAMPBELL, Castings. Butterworth-Heinemann, Oxford (1993).
- 8) A.K. DAHLE, L. ARNBERG, Materials Science Forum, 217-222, (1996), p.259.



- 9) A.K. DAHLE, L. ARNBERG, Materials Science Forum, 217-222, (1996), p.269.
- 10) L. BACKENRUD, E. KROL, J. TAMMINEN, Solidification Characteristics of Aluminum Alloys Volume 1: Wrought Alloys. (1986).
- 11) L. BACKENRUD, G. CHAI, J. TAMMINEN, Solidification Characteristics of Aluminum Alloys Volume 2: Foundry Alloys. (1986).
- 12) Science and Technology of Semi-Solid Metal Processing. North American Die Casting Association, (2001).
- 13) G.K. SIGWORTH, AFS Trans. 104, (1996), p.1053.
- 14) A.S. METZ, M.C. FLEMINGS, AFS Trans. 78, p.453.
- 15) D.G. ESKIN, K.L. SUYITNO, Progress in Materials Science, 49, (2004).
- 16) G. CAO, S. KOU, Met. Trans. A. 37A, (2006), p.3647.
- 17) S. SHANKAR, A Study of the Interface Reaction Mechanism Between Molten Aluminum and Ferrous Die Materials, Ph.D. Worcester Polytechnic Institute, (2000).
- 18) S. SHANKAR, M.M. MAKHLOUF, Internal ACRC Report, May 2005.
- 19) J. Wallace, A Guide to Correcting Soldering. North American Die Casting Association, (2006).